Examining the interplay between oxidative and β-adrenergic regulation of PKARIα and its impact on the mitochondrial fission protein DRP1

Doctoral Thesis

In partial fulfillment of the requirements for the degree

"Doctor of Philosopy (PhD)"

Division of Mathematics and Natural Sciences

In the Molecular Medicine Study Program

at the Georg-August University Göttingen

Submitted by

Alexander Johnston

born in Dublin, Ireland

Göttingen 2016

Members of the Thesis Committee:

Prof. Dr. Stephan E. Lehnart (Supervisor)

Email: slehnart@med.uni-goettingen.de

Phone: +49 (0) 551 39 10575

Postal Address: Institute of Cardiology and Pneumology
University Medical Center Goettingen
Georg-August University Göttingen
Robert-Koch-Str. 40
37075 Göttingen
Germany

Prof. Philip Eaton (Second Supervisor)

Email: philip.eaton@kcl.ac.uk

Phone: +44 (0) 20 7188 0969

Postal Address: The Rayne Institute
4th Floor, Lambeth Wing
St Thomas' Hospital,
SE1 7EH, London
United Kingdom

Prof. Dr. Viacheslav O. Nikolaev (Third member of thesis committee)

Email: v.nikolaev@uke.de

Phone: +49 (0) 40 7410 51391

Postal Address: Institute of Experimental Cardiovascular Research
University Medical Centre Hamburg-Eppendorf
Martinistr. 52
20246, Hamburg
Germany

Date of Disputation: November 7th 2016

AFFIDAVIT

Here I declare that my doctoral thesis entitled:

"Examining the interplay between oxidative and β-adrenergic regulation of PKARIα and its impact on the mitochondrial fission protein RP1"

has been written independently with no other sources and aids than quoted.

Alexander Johnston

Göttingen, August 27, 2016

List of publications:

Johnston, A.S., S.E. Lehnart, and J.R. Burgoyne, Ca^{2+} signaling in the myocardium by (redox) regulation of PKA/CaMKII. Front Pharmacol, 2015. **6**: p. 166

List of poster presentations:

Johnston A, Burgoyne J, Eaton P, Lehnart S (2015). Redox-modification of PKARIα as a regulator of mitochondrial fission during starvation. *IRTG annual symposium, Wernigerode, Germany*

Johnston A, Wenniger G, Korff B, Eaton P, Lehnart S (2014). Redox-regulation of SR Ca^{2+} cycling by PKARIα versus PKARII. *.BHF annual symposium, London, UK*

Johnston A, Wenniger G, Korff B, Eaton P, Lehnart S (2014). Redox-regulation of SR Ca2+ cycling by PKARIα versus PKARII. *.IRTG summer symposium, Goettingen, Germany*

Table of contents

Acknowledgements

I want to sincerely thank Prof. Dr. Stephan Lehnart and Prof. Phil Eaton for giving me the opportunity to complete my PhD under their joint supervision. In particular, Prof. Dr. Lehnart for his polite and unwavering patience and Prof. Eaton for his generous accommodation and interest throughout the extent of my project.

To my family, I'm sorry I've missed so much of your lives during my stay this past decade in the ivory tower. It's only through the confidence I've garnered from your continued support that I've made it this far. To my mother, whose dedication has been a perennial source of inspiration to my family, I can only dream of emulating a fraction of your selflessness and hope this goes some small way toward repatriating your sacrifices. To my beautiful grandmother and learned uncle, if I've any curiosity in this world it's because of you both.

To the numerous smiling faces that populated this story your charming personalities, wry humor, and often shared mental prostration added a rich emotional technicolor to the experience. A special thanks must be given to Dr. Oleksandra Prysyazhna for her saintly tolerance to my incessant inquiries, Elisa Sanchez for her continued nutritional support and Ms. Brigitte Korff for her technical and linguistic assistance.

To the wonderful Rachael Whale, not only did you persistently inquire, despite the predictable monotony, about my progress but also insisted on reading and correcting every page of this document. For this and your continued love these past six years I'm forever grateful.

Finally, I'd like to thank all the staff of the IRTG 1816 for their support throughout this process, for providing a programme rich in opportunity and especially for so generously funding my foray into their native language. With this you've given me a small piece of Germany I will take with me though out my life.

Abstract

PKA is activated by β-adrenergic signaling induced elevation in intracellular cAMP and sequestered into proximity with its substrates by scaffold A-kinase anchoring proteins (AKAPs). PKARIα is a unique isoform of PKA as in response to oxidants it forms two inter-protein disulfide bonds between its regulatory subunits, which directly flank its interaction site with AKAPs. As such, it is probable that the oxidation of PKARIα affects its localization with AKAPs, therefore serving as a regulatory mechanism by which the kinase is targeted to its substrates. This thesis examines the interplay between β-adrenergic and oxidant induced PKARIα regulation and its impact on PKA substrate phosphorylation. In particular, regulation of the mitochondrial fission protein dynamin-related protein 1 (DRP1) is assessed as this is facilitated by the PKARIα scaffold protein Dual-AKAP1 (D-AKAP1).

PKARIα formed a disulfide-dimer during *ex vivo* Langendorff perfusions with H_2O_2, which was associated with its translocation to the insoluble fraction of cardiac homogenates. This model of PKARIα oxidation was then replicated *in vivo* in the context of starvation. In heart, 24 hours starvation increased PKARIα disulfide-dimer formation and PKA-substrate phosphorylation, as detected by a pan-specific "total" PKA substrate antibody, specific phosphorylation of DRP1-S637 was unchanged. In liver, 24 hours starvation increased PKARIα disulfide-dimer formation, which co-fractionated with D-AKAP1. DRP1 also formed higher molecular weight complexes consistent with its phosphorylation by PKA. Identifying whether these changes were mediated by PKARIα phosphorylation of DRP1 was not possible as the antibody failed to produce a specific phospho-signal in immunoblots from liver. Unexpectedly, PKARIα-C17S KI mice showed increased cardiac DRP1-S637 phosphorylation after starvation and also displayed a basal elevations in both PKARIα expression and "total" PKA-substrate phosphorylation

Langendorff perfusion experiments revealed that Na-pyruvate attenuates H_2O_2 induced cysteine oxidation. Physiologically this was evidenced by abolished responses in left ventricular end diastolic pressure (LVEDP) and coronary flow rate (CFR) in response to H_2O_2 in the presence of Na-pyruvate. PKARIα disulfide-dimer formation in response to H_2O_2 was not affected by elevating cAMP with the β-adrenergic agonist isoprenaline. H_2O_2 attenuated isoprenaline-induced elevations in "total" PKA-substrate phosphorylation which physiologically was reflected by blunted CFR, LVEDP and left ventricular end systolic pressure (LVSP) responsiveness to isoprenaline. However, using the PKARIα-C17S KI mouse these changes were seen to occur independently of PKARIα disulfide-dimer formation.

Taken together, the above findings indicate that PKARIα is modulated by both its oxidation to a disulfide-dimer and cAMP binding. However, the interplay between these two factors remains unclear as evidenced by a failure of cellular models to translate to *ex vivo* and *in vivo* scenarios. In the heart, starvation induced disulfide PKARIα does not appear to regulate DRP1. However in the context of liver, promising results indicate that starvation induced disulfide PKARIα may contribute to the protective effects of reduced mitochondrial fission through inhibition of DRP1.

Abbreviations

2-AHA-cAMP	2-(6-aminohexylamino)-adenosine- 3', 5'- cyclic monophosphate
DNP	2, 4 dinitrophenol
CM-H2DCFDA	2',7'-dichlorodihydrofluorescein diacetate
DCF-DA	2',7'-dichlorofluorescin diacetate
AC	adenylate cyclase
AKAPs	A-kinase anchoring proteins
BS3	bis-sulfosuccinimidyl-suberate
CICR	Ca^{2+} induced Ca^{2+} release"
CaMKIα	calmodulin-dependent kinase I
CFR	coronary flow rate
cAMP	cyclic adenosine monophosphate
cGMP	cyclic guanosine monophosphate
CNBA and CNBB	cyclic nucleotide binding domains
CDK1	cyclin-dependent kinase 1
S^-	deprotonated 'reactive' thiolate anion
DHE	dihydroethidum
N_2O_3	dinitrogen trioxide
DSG	disuccinimidyl glutarate
D/D	docking/dimerization domain
D-AKAPs	dual specific AKAPs
DRP1	dynamin related protein 1
EGS	ethylene glycol bis-succinimidyl succinate
ECC	excitation-contraction coupling
GPCR	G protein-coupled adrenergic receptors
GSH	glutathione
H_2O_2	hydrogen peroxide
HO•	hydroxyl radical
HIF-1 α	hypoxia-inducible factor 1α
IP	intraperitoneally
I/R	ischaemia reperfusion

ISO	isoprenaline
JPH2	junctophilin 2
LVEDP	left ventricular end diastolic pressure
LVSP	left ventricular systolic pressure
LTCC/Cav1.2	L-type Ca^{2+} channels
LC3-I	microtubule-associated protein 1A/1B-light chain 3
MFF	mitochondria fission factor
Mdivi-1	mitochondrial division inhibitor 1
MID49/51	mitochondrial dynamic proteins 49 and 51
MPTP	mitochondrial permeability transition pore
BRP44	mitochondrial pyruvate carrier 2
MFN1	mitofusion protein 1
MFN2	mitofusion protein 2
NOX	nicotinamide adenine dinucleotide phosphate-oxidase
NO	nitric oxide
NOS	nitric oxide synthases
NO^+	nitrosonium cation
OMM	outer mitochondrial membrane
GSSG	oxidized glutathione
$ONOO^-$	peroxynitrite
PDE	phosphodiesterase
PKARIα	protein kinase RIα
PKA-cat	catalytic subunit of PKA
PCR	polymerase chain reaction
PKA	protein kinase A
PKG1α	protein kinase G 1α
RNS	reactive nitrogen species
ROS	reactive oxygen species
R	regulatory
RyR2	ryanodine receptors
SR	sarcoplasmic reticulum
SERCA	sarcoplasmic reticulum ATPase

SUMO	small ubiquitin-like modifier
SNO	s-nitrosylation
SOH	sulfenic acid
SO_2H	sulfinic
SO_3H	sulfonic acid
O_2^-	superoxide anion
SOD	superoxide dismutase
TRX	thioredoxin

Introduction

1.1 Reactive oxygen species

The sequential reduction of molecular oxygen leads to the formation of biological forms of reactive oxygen species (ROS) comprising of the superoxide anion (O_2^-), hydrogen peroxide (H_2O_2) and hydroxyl radical (HO•).These forms of ROS are capable of altering cellular signaling by modifying susceptible proteins. Initially thought to contribute solely to cellular damage it has become clear that ROS signaling pathways are in fact a highly organized and compartmentalized network critical for homeostatic biological function [1, 2]. For example ROS produced by nicotinamide adenine dinucleotide phosphate-oxidase (NOX) enzymes modulate cardiac transcription factors, cell migration, vascular tone and cardiac contraction [3-5]. However, their excessive production, both transiently and chronically, is now implicated in numerous cardiovascular pathologies such as inflammation, arrhythmias, diabetes, hypertension, atherosclerosis, reperfusion injury, fibrosis and diastolic dysfunction [6-14].

1.1.1 Sources of ROS

Mitochondria are a major source of intracellular ROS generation due to leakage of electrons from the electron transport chain that react with molecular oxygen to generate superoxide. Once generated, the superoxide is readily converted to more stable H_2O_2 by the enzyme superoxide dismutase (SOD). Importantly, as mitochondrial complexes are abundant in heme groups and iron sulfur clusters H_2O_2 can also be converted to highly reactive hydroxyl radicals [15, 16]. In addition to ROS generated by electron transport chain leakage, enzymatic networks such as NOX, xanthine oxidase and uncoupled nitric oxide synthase (NOS) contribute to endogenous ROS production [17]. Homeostatic balance of this system is maintained through both enzymatic (SOD, catalase, glutathione peroxidase) and non-enzymatic (vitamins, thioredoxin (TRX), flavonoids) scavenging systems. Under normal homeostatic conditions this system is tightly balanced such that moderate increases in ROS can act as secondary messengers by reversibly modifying protein function. However, during disease states when ROS are excessively produced or when exogenously applied to mimic excess production, the innate anti-oxidant scavenging system becomes overwhelmed. The impact of this imbalance

on the cellular environment is a shift to a state of excessive ROS levels termed “oxidative stress”.

1.2 Oxidative modification of cysteine thiols

The ability of ROS to act as secondary messengers is attributed to their ability to oxidize susceptible cysteine thiols on select proteins. The alteration of cysteine residues by oxidation generates a conjugated moiety with a different shape and charge characteristic, which can induce structure rearrangement to alter enzymatic activity. Protein oxidation is considered a physiological signaling modality as it can specifically and transiently regulate protein function. The selectivity of protein oxidation is provided by the limited reactivity of cysteine thiols. This is due to the majority of cysteines being buried within proteins and thus not accessible to an oxidant. In addition the pKa of an accessible cysteine thiol is an important determinant of its reactivity. For a cysteine thiol to be sensitive to oxidation it needs to be in a deprotonated 'reactive' thiolate anion form (S^-) and thus have a low pKa. The pKa of a cysteine thiol is determined by its local tertiary environment, which is lowered by close proximity to basic amino acids lysine, arginine or histidine.

H_2O_2 is a major form of ROS responsible for oxidant-dependent signaling and is formed enzymatically through the dismutation of superoxide. Once generated, H_2O_2 readily reacts with cysteine thiols to form a sulfenic acid (SOH) intermediate, which is then rapidly resolved by an adjacent cysteine on the same protein or neighboring protein to form an intra- or inter-molecular disulfide respectively (Figure 1.1). Alternatively a sulfenic acid can react with the highly replete cellular thiol containing tri-peptide glutathione (GSH), leading to protein glutathiolation.

Once oxidized a cysteine thiol can be reduced by the replete cellular reducing system. The rate of reduction and hence stability of an oxidative modification is determined by its type, accessibility and the quantity of oxidant present. Formation of an inter- or intra- molecular disulfide within a target protein can be reduced by TRX through a disulfide exchange reaction [18]. This leads to reduction of the target protein and oxidation of TRX, which is then recycled back to its reduced form by TRX reductase and electrons provided by NADPH. The formation of a glutathione adduct on a protein is also readily reversible and is enzymatically reduced by

glutaredoxin. However in contrast to TRX, glutaredoxin does not have an oxidoreductase and instead uses free GSH to reduce its target, which leads to the formation of oxidized glutathione (GSSG). Under conditions of excessive oxidant production cysteines can transition to an irreversibly oxidized state known as hyperoxidation which is associated with disease. A cysteine sulfenic acid can be further oxidized to a sulfinic (SO_2H) and then to sulfonic acid (SO_3H). The formation of a sulfonic acid is irreversible, whereas a sulfinic acid is only reversible on peroxiredoxin at the expense of ATP and driven by the enzyme sulfiredoxin [19].

In addition to H_2O_2 reactive nitrogen species (RNS) also contribute to thiol-dependent redox signaling by forming protein nitric oxide (NO) adducts termed S-nitrosylation (SNO). NO generated from L-arginine by the nitric oxide synthases while remaining in its native form is unable to directly modify cysteine thiols. However the formation of the nitrosonium cation (NO^+) or dinitrogen trioxide (N_2O_3) can induce direct thiol oxidation ($N_2O_3 + RSH \rightarrow RSNO + HNO_2$), whereas small thiol containing compounds such as S-nitrosoglutathione (GSNO) can induce protein S-nitrosylation through an exchange reaction termed trans-nitrosylation ($GSNO + RSH \rightarrow RSNO + GSH$) [20]. A protein nitrosothiol is relatively unstable and can therefore act as an intermediate in the formation of a more stable disulfide in a similar manner to a sulfenic acid. In situations where there is localized formation of both nitric oxide and superoxide this can lead to formation of the highly reactive species peroxynitrite ($ONOO^-$). Peroxynitrite can induce S-nitrosylation but also irreversible tyrosine nitration that is often associated with disease.

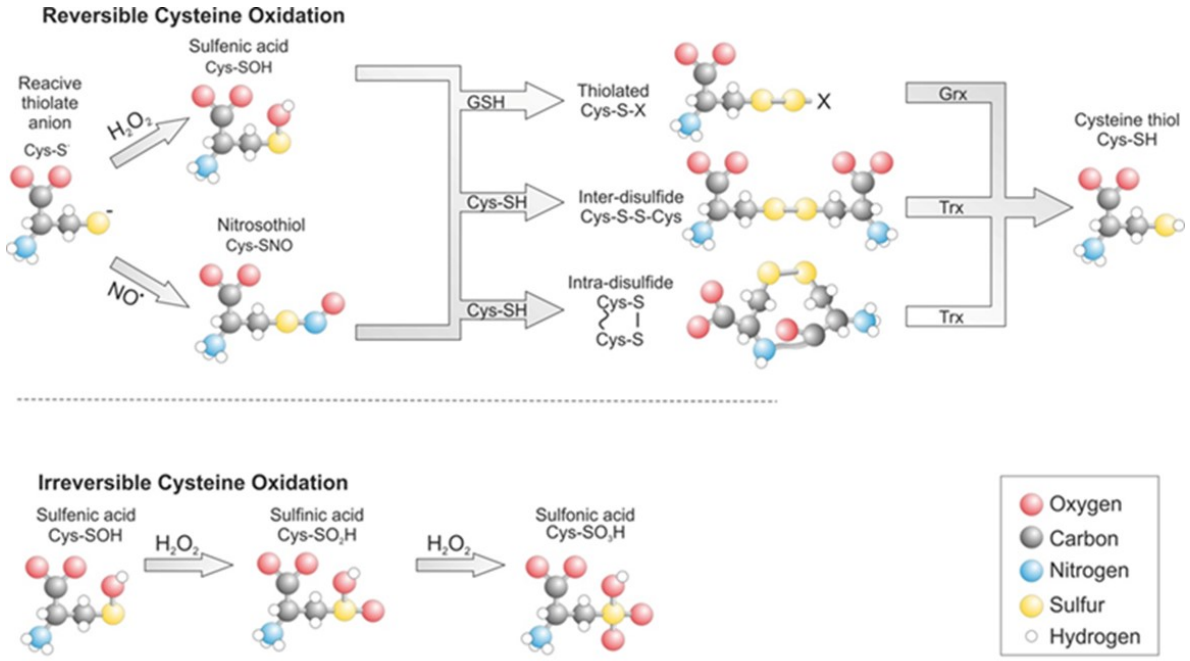

Figure 1.1 Reversible and irreversible post translation oxidative modification of cysteine residues. Cysteine thiols are oxidised by H_2O_2 to a sulfenic acid (SOH) intermediate that is quickly resolved by another cysteine on either the same or an adjacent protein to form an intra- or –inter-molecular disulfide respectively. Alternatively, sulfenic acid can be glutathiolated by glutathione (GSH). Gluthathiolation is reduced by Glutaredoxin (Grx) and disulfides by thioredoxin (Trx). During excessive oxidant production cysteine thiols can be irreversibly oxidised to sulfonic acid. Figure adapted from Johnston et al. [21].

Protein Kinase A (PKA) is a heterotetrameric threonine/serine kinase replete in the cardiovascular systems and a critical mediator of cardiac function under both physiological and pathophysiological conditions. The RIα isoform of PKA (PKARIα) is distinct from other isoforms as it is one such protein that is subject to reversible cysteine oxidation. This leads to the formation of two inter-protein disulfide bonds between its regulatory subunits which are seen to catalyse PKARIα activity leading to phosphorylation of its substrates. This topic is considered in more detail below.

1.3 Classical activation of PKA

PKA is composed of two regulatory (R) and two catalytic subunits (PKA-cat). The regulatory subunits of PKA exist in two isoforms RI and RII, the presence of either identifies its isozyme nomenclature as PKARI or PKARII. PKA activation is modulated through the sympathetic nervous system (Figure 1.2). Upon binding of epinephrine or norepinephrine to G protein-coupled adrenergic receptors (GPCR), adenylyl cyclase (AC) is activated producing a rapid increase in intracellular cyclic adenosine monophosphate (cAMP) which binds to the B domain of the regulatory subunit of PKA inducing a conformational change permitting cAMP to also access the A binding domain. Once both domains are bound with cAMP the kinase fully dissociates freeing the catalytic subunits to phosphorylate serine and threonine substrate residues [22]. PKA signaling is terminated by phosphatases that remove the phosphate groups and phosphodiesterases (PDEs) which hydrolyze cAMP [23].

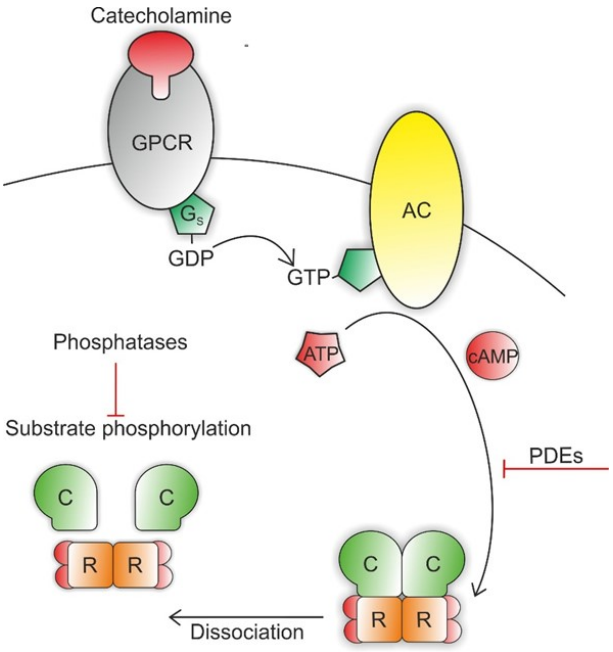

Figure 1.2 Classical activation of PKA. Catecholamine binding to G protein coupled β-adrenoreceptors (GPCR) activates the hydrolysis of GDP to GTP by stimulative regulative G-protein (Gs). GTP then activates adenylate cyclase (AC) to convert ATP to cAMP, which binds to the regulatory subunits of the kinase inducing a conformation shift that dissociates both catalytic subunits, which then phosphorylate serine and threonine substrate residues. Phosphorylation is inhibited by phosphatases and cAMP signalling terminated through its hydrolysis by phospodiesterases (PDEs).

1.3.1 Excitation-contraction coupling

Cardiac contraction is modulated through the coupling of an electrical stimulus to a contractile output in a process known as excitation-contraction coupling (ECC) [21]. An action potential depolarizes the cell membrane activating voltage sensitive L-type Ca^{2+} channels (LTCC/Cav1.2) and allowing Ca^{2+} to flow into the cell, where it binds to cardiac ryanodine receptors (RyR2) on the adjacent sarcoplasmic reticulum (SR)[23]. This binding precipitates cell-wide Ca^{2+} release from the sarcoplasmic reticulum (SR) store termed "Ca^{2+} induced Ca^{2+} release" (CICR), giving rise to a synchronous cardiac contraction necessary for cardiac output [21]. For the myocardium to relax it is necessary that cytoplasmic Ca^{2+} levels are returned to diastolic levels allowing Ca^{2+} to dissociate from the myofilaments [21]. This is accomplished through inactivation of extracellular Ca^{2+} entering through LTCC and Ca^{2+} extrusion from the cytoplasm via the sarcoplasmic reticulum ATPase (SERCA), Na/Ca^{2+} exchanger, sarcolemmal Ca^{2+}ATPase and mitochondrial uniporter [21, 23].

1.3.2 PKA mediated changes in cardiac function

PKA mediates several proteins critical for cardiac function (Figure 1.3). PKA may phosphorylate the LTCC to increase Ca^{2+} flux into the myoplasm [24]. However, the proposed LTCC phosphorylation sites are under debate [21, 25]. LTCC phosphorylation is an accepted mechanism to potentiate the release of Ca^{2+} from the SR through CICR to positively impact inotropy through augmented CICR. In addition, phosphorylation of troponin I by activated PKA increases the rate of Ca^{2+} dissociation from the myofilaments resulting in accelerated relaxation (lusitropy) [21, 26]. In addition to facilitating SR Ca^{2+} release PKA also augments Ca^{2+} sequestration into the SR by negatively regulating the inhibitory effect of PLB on SERCA [21, 27]. This increased Ca^{2+} flux to the SR has the net effect of increasing SR Ca^{2+} content, SR Ca^{2+} release and SR Ca^{2+} re-uptake thus, PKA facilitates cardiac contraction, relaxation and heart rate when activated [21, 23]. PKA has been shown to critically mediate RyR2 function via its specific S2808 phosphorylation site [21, 28, 29]. Transgenic mice harboring a S2808A mutation show blunted inotropic and chronotropic response to catecholamines [21, 30], while phosphomimetic mutation of the receptor leads to age-dependent cardiomyopathy and arrhythmias [21, 31].

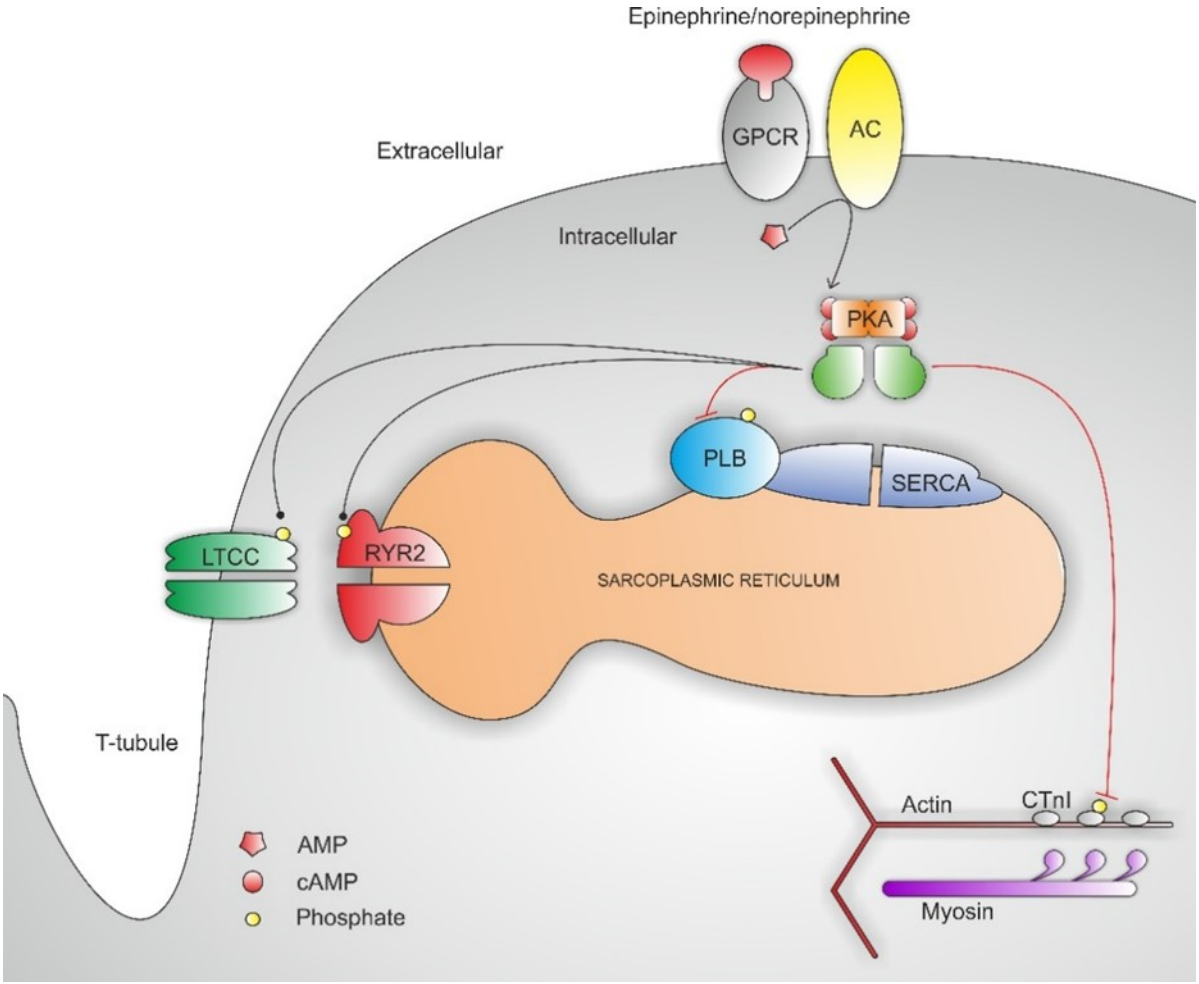

Figure 1.3. Key contractile proteins mediated by PKA phosphorylation. Under conditions of increased cardiac demand epinephrine or norepinephrine binds to g protein coupled receptors (GPCR) to increase cAMP via adenylate cyclases to activate PKA. PKA may phosphorylate the L-type Ca2+ channel (LTCC) increasing Ca2+ flux to the cytosol to increase inotropy. Phosphorylation of cardiac troponin I (CTnI) enhances lusitropy by dissociating Ca2+ from myofilaments. Phosphorylation of the sarcoplasmic reticulum ATPase (SERCA) inhibitory protein phospholamban (PLB) enhances Ca2+ re-uptake into the sarcoplasmic reticulum (SR), facilitating lusitropy and SR Ca2+ store thus also facilitating inotropy. PKA mediated phosphorylation of RYR2 reduces the stability of the receptor resulting in diastolic Ca2+ leak. Black circles indicate protein activation and red lines-inhibition.

1.4 Oxidative modification of PKARIα

PKARIα is unique from other PKA isoforms as its activation can be induced independently of cAMP by ROS. The regulatory subunits of PKARIα are composed of two cyclic nucleotide binding domains (CNBA and CNBB), an inhibitor site and a docking/dimerization domain (D/D) (Figure 1.4A).The N-terminal (D/D) dictates PKARIα's localization via its interaction with A-kinase anchoring proteins (AKAPs), thus providing an additional mechanism for compartmentalization and specificity of PKA signaling. The D/D of each regulatory subunit contains cysteines at position 17 and 38 (human and mouse) which, in the kinase's tertiary structure, lie anti-parallel to those on its opposing regulatory subunit. These cysteines were first identified following a proteomic screen and in the presence of oxidants, such as H_2O_2, lead to the formation of an anti-parallel dimer joined by disulfides between the opposing cysteines [32-35]. This bond was initially thought to be a constitutive modification due to the high concentration of reducing agent required to break it [36]. In later studies the presence of disulfides within PKARIα was evaluated by Langendorff perfusing isolated rat hearts with increasing concentrations of H_2O_2. These hearts were then homogenized in the presence of the alkylating agent maleimide to prevent artificial oxidation and PKARIα resolved using SDS-PAGE in the absence of reducing agent. By using this approach a dose dependent increase in the percentage of disulfide bound PKARIα could be observed in response to H_2O_2, which was entirely abolished in the presence of reducing agent [32]. Disulfide dimer formation was associated with translocation of the kinase to the myofilaments and phosphorylation of its targets troponin I and myosin binding protein C [32]. This resulted in enhanced myocyte contractility independent of β-adrenergic stimulation or elevations in cAMP and was inhibited, although not entirely, by the PKA inhibitor H89 [32]. In addition disulfide PKARIα was recently identified as playing a crucial role in angiogenesis. *Burgoyne et al.* showed that pro-angiogenic interventions couple NOX dependent oxidant generation to disulfide PKARIα formation inducing ERK signalling critical for angiogenesis [37]. In line with this "redox dead" PKARIα C17S KI displayed deficient angiogenesis in response to hind limb ischaemia and tumour-implant growth [37].

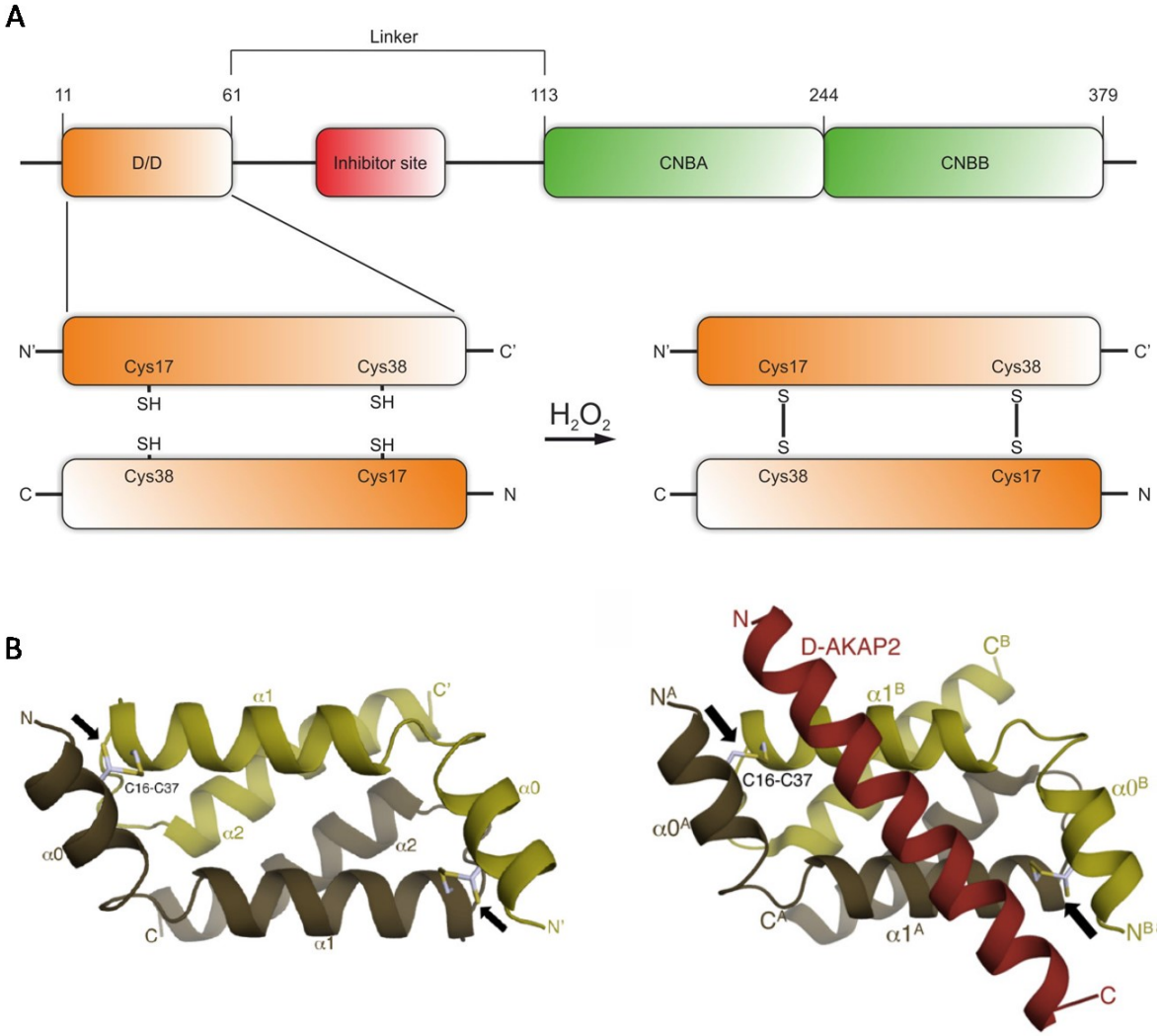

Figure 1.4. Structure of PKARIα interacting with D-AKAP2. (A) Top. Schematic of PKARIα domain structure showing docking dimerization domain (D/D), inhibitor site and cyclic nucleotide binding domains A and B (CNBA/B). Bottom. Schematic of PKARIα D/D showing antiparallel cysteine thiols which form a disulfide in response to H_2O_2. (B) Crystal structure of PKARIα D/D bound to the α-helix of D-AKAP2in showing. Cys16 and 37 (bovine residues, in mouse and human Cys17 and Cys 38). Mutation of Cys16 or Cys37 reduce affinity between RIα and D-AKAP[38]. Figure adapted from Sarma et al. [33].

1.5 AKAPs

Binding of cAMP to the regulatory subunits of PKA initiates the release of its catalytic subunits, which then phosphorylate serine and threonine residues. In addition to their interaction with cAMP, the regulatory subunits also target PKA to specific areas of the cell to localise their signalling. This is achieved through their interaction with scaffold AKAPs. AKAPs are signalling hubs containing not just PKA, but also its substrates and the proteins necessary for fine tuning of its regulation such as PDEs, phosphatases, adenylate cyclases and GPCRs [39, 40]. AKAPs are expressed in all tissue and identified by the presence of an amphipathic helix, which directly interacts with the D/D of R subunits. If the AKAP interacts with PKARI and PKARII it is denoted as a dual specific AKAPs (D-AKAPs). The majority of identified AKAPs are RII specific or bind it with a higher affinity than RI [41].

Structural discrepancies in the D/D domain of RI and RII account for their differential binding to specific AKAPs (Figure 1.5). The RIIα D/D forms a non-polar shallow cleft complimenting the diagonal hydrophobic AKAP helix. In contrast the D/D of RIα forms a deep cleft lined with more basic and acidic residues that contact the AKAP helix. In place of isoleucine 17 RIα contains glutamine 26, this exchange of a non-polar for polar amino acid would result in a more hydrophilic groove less suitable for the hydrophobic AKAP helix [42]. Additionally, the N-terminal of RIIα contains a β-strand with two isoleucine residues that stabilize the interaction between the D/D and AKAP helix. This feature is lost in RIα as the isoleucine residues are instead contained within an N-terminal helix [33, 41]. The most abundant and well characterised D-AKAP is D-AKAP1, also known as AKAP1, AKAP121, AKAP149, or S-AKAP84. D-AKAP1 localises PKA to the outer mitochondrial membrane [43].

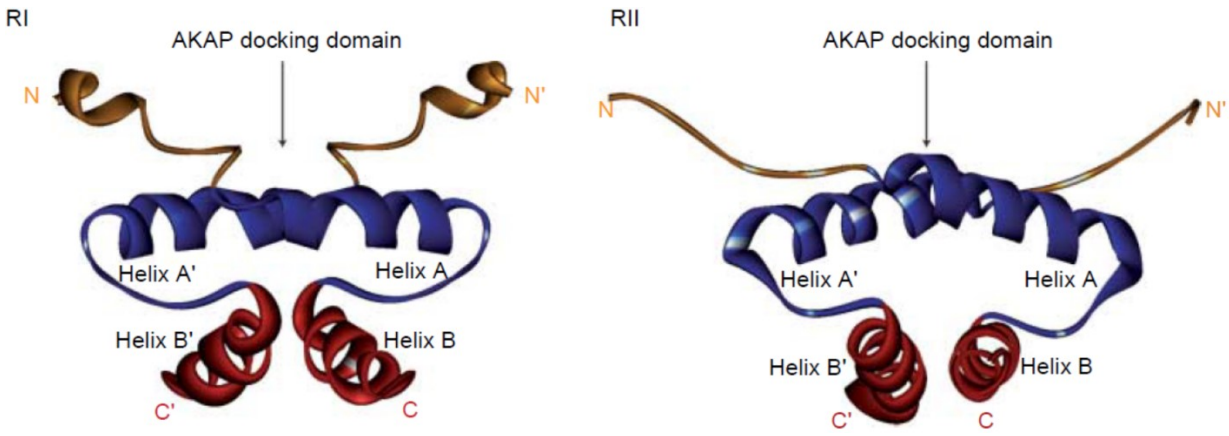

Figure 1.5. Structural discrepancies in the D/D domain of PKARIα and PKARIIα account AKAP specificity. The D/D of RIα forms a deep cleft lined with basic and acid residues resulting in a hydrophilic groove. In contrast the D/D of RIIα forms a shallow cleft that is complimented by the diagonal hydrophobic AKAP helix.

1.6 Disulfide-dependent changes in PKARIα affinity for D-AKAPs

The translocation of disulfide bound PKARIα to alternate subcellular locations may be explained by redox mediated changes in its affinity for AKAPs (Figure 1.6). D-AKAPs associate with both PKARI and PKARII. Crystal structure analysis of the D/D of bovine PKARIα shows the disulfide forming cysteines to lie antiparallel to one another flanking the area responsible for AKAP α-helix binding (Figure 1.4B) [33]. Based on this proximity, *Sarma et al.* hypothesized that PKARIα disulfide formation may impact the kinase's affinity for D-AKAPs [33]. Indeed, utilizing bovine RIα with Cys17Ala or Cys37Ala mutations to prevent disulfide formation a 3 fold and 16 fold reduction, respectively, in nanomolar affinity for D-AKAP2 in comparison to wild-type RIα was observed.[33]. Disulfide formation was reported to facilitate PKARIα-D-AKAP2 interaction by reducing regulatory subunit flexibility allowing the formation of both an AKAP binding pocket and increasing the proximity of stabilizing residues [33]. Similarly, mutation of both cysteine residues to alanine has been shown to preclude a PKARIα interaction with both D-AKAP1 and D-AKAP2 [44, 45]. *Banky et al.* also showed that Cys38 mutagenesis to histidine had a greater impact on D-AKAP1 affinity than mutagenesis of Cys17 [44]. Taken together the above work strongly suggests the disulfide dimer formation of PKARIα is an important mechanism for targeting it to its scaffold D-AKAP proteins.

1.7 Substrate-induced dissociation of PKARIα

Substrate-induced dissociation is an additional characteristic that uniquely distinguishes PKARIα from other PKA isoforms (Figure 1.6). The axiomatic view that PKA is only activated after full dissociation of its catalytic and regulatory subunits was first challenged by *Yang et al.* who demonstrated that cAMP can induce kinase activity independent of subunit dissociation [46]. Disparate responses between PKARIα and PKARII to cAMP have since been described by several groups. Dissociation PKARIα in the presence of cAMP has been reported only to occur with the addition of substrate [47]. Similarly, small angle X-ray scattering showed that PKARIα, and not PKARII, is only partially dissociated by cAMP and that the addition of both substrate and cAMP was necessary for full dissociation [48]. Additionally, the presence of substrate is also seen to sensitize PKARIα, but not PKARII, to low levels of cAMP. Using size exclusion chromatography *Viste et al.* observed that substrate enhanced the dissociation of PKARIα's regulatory and catalytic subunits but had no effect on PKARIIα [49]. Furthermore, the presence of substrate significantly attenuated the rate of PKARIα subunit re-association relative to PKARII [49]. This suggests an intricate model in which PKARIα, but not PKARII, is only partially dissociated by cAMP binding but fully dissociated in the tandem presence of both nucleotide and substrate. Such sensitization may also reconcile the apparent paradox that PKA substrate phosphorylation is seen to increase in response to H_2O_2 despite unchanged intracellular cAMP concentrations [35].

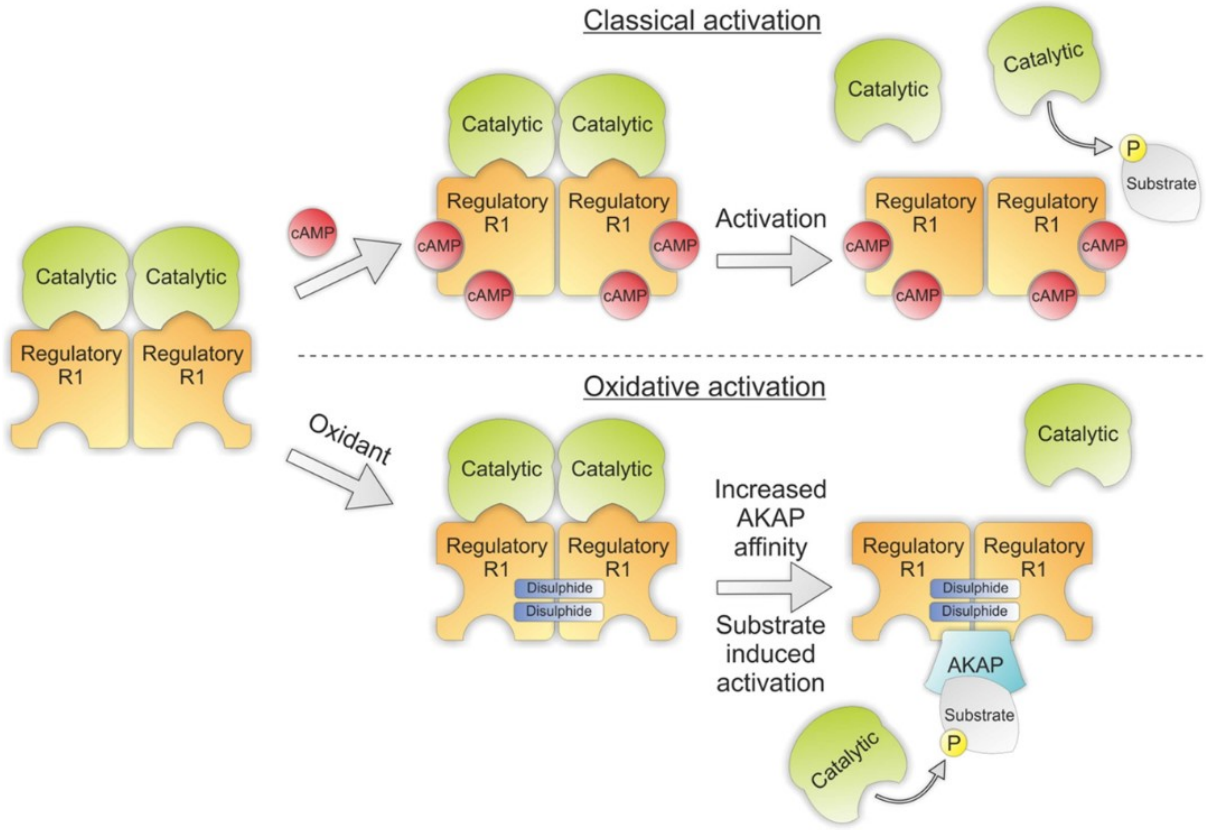

Figure 1.6. Schematic of PKA showing classical and oxidative activation. Classical activation involves the binding of cAMP to the regulatory subunits of PKA which induces dissociation of the holoenzyme resulting in substrate phosphorylation. Oxidative activation does not involve cAMP binding. Instead cysteines located in the D/D of the regulatory subunits are oxidized to form two intermolecular disulfides which increase the kinase's affinity for its AKAP scaffold proteins. This brings PKARIα into proximity with its substrate leading to substrate induced activation. Figure from *Johnston et al.* [21].

1.8 cAMP modulation of PKARIα disulfide formation

Cyclic guanosine monophosphate (cGMP) dependent protein kinase 1α (PKG1α) is another adenylyl cyclase that forms a disulfide dimer in response to ROS [5, 50]. Binding of its nucleotide cGMP prevents its formation of an inter-protein disulfide bond [5]. Though it is yet to be confirmed, as a crystal structure of the complete holoenzyme is unavailable, this is presumably through induction of a conformational change that reduces the proximity of its redox sensitive thiols to one another [5]. If cAMP binding induces an analogous change in PKARIα preventing disulfide formation this would also likely impact oxidant mediated PKARIα substrate phosphorylation.

1.9 Hypothesized model of PKARIα activation

The above models are of particular interest as they are both specific to PKARIα, the only PKA isoform capable of forming disulfide bonds. Taking both mechanisms together it is hypothesized that PKARIα disulfide formation increases the holoenzyme's affinity for D-AKAPs, bringing the kinase into proximity with its substrate which through substrate-induced dissociation results in augmented phosphorylation which is maximal in the presence of elevated cAMP via β-adrenergic stimulation (Figure 1.7).

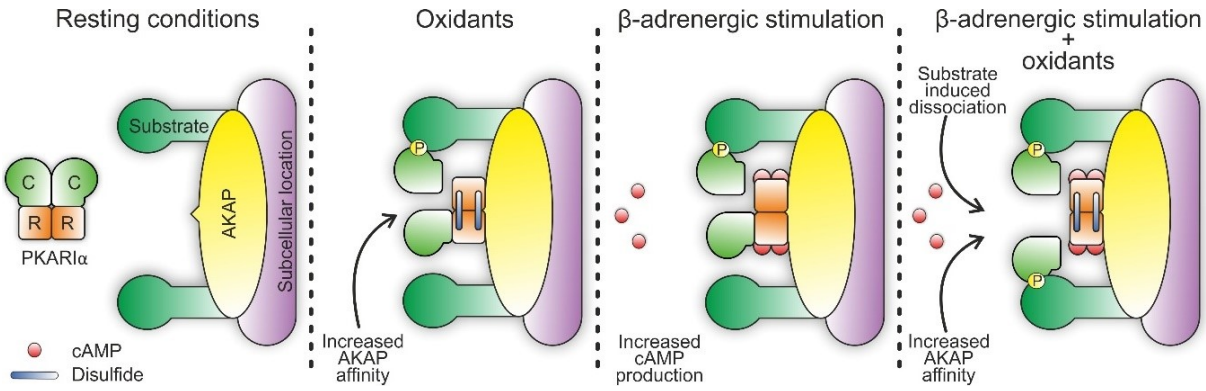

Figure 1.7. Hypothesized mechanism of PKARIα activation in the presence of oxidants and β-adrenergic stimulation. Under resting conditions PKARIα is localized in the cytosol. PKARIα is activated by oxidants, which increase its affinity for A kinase anchoring protein (AKAP) leading to substrate phosphorylation. PKARIα is also activated by β-adrenergic stimulation through increased cAMP production causing partial dissociation of the kinase and thus substrate phosphorylation. It is hypothesized that in the presence of oxidants and cAMP, PKARIα will be fully dissociated through increased AKAP affinity, substrate induced dissociation and cAMP elevation leading to maximal substrate phosphorylation.

1.10 D-AKAP1 facilitates PKA dependent DRP1 modification

D-AKAP1 localises PKARIα to the outer mitochondrial membrane (OMM) through its N-terminal targeting sequence which also contains its PKA binding helix [51]. At the OMM D-AKAP1 acts as a critical point of convergence between PKA and dynamin related protein 1 (DRP1) to modulate mitochondrial fission. Fission is one half of the continual process of mitochondrial division and fusion, which is critical for maintenance of healthy efficient pools of mitochondria. Fusion involves the preservation and expansion of mitochondrial networks by joining adjacent organelles. Fission, in contrast, refers to the process of selective mitochondrial degradation. DRP1 is considered the principal arbitrator of mitochondrial fission and is

negatively regulated by PKA [52]. The role of DRP1 in mitochondrial fission and particularly in the context of cardiac function is considered in more detail below.

1.10.1 Post translational modification of DRP1

DRP1 is an 80 kDa member of the dynamin superfamily of proteins, consisting of an amino-terminal GTPase, a middle and variable domain and carboxyl terminal GTPase effector domain (Figure 1.8). DRP1 is almost exclusively (~ 97%) localized to the cytoplasm, therefore its recruitment to the OMM is necessary to induce fission. Upon translocation to the OMM, DRP1 assembles into spirals encircling the mitochondria, which then constrict in a GTPase dependent mechanism to sever the inner mitochondrial membrane and OMM (Figure 1.8). A number of post-translation modifications have been identified that affect DRP1's activity with mitochondria. These include SUMOlyation[53], S-nitrosylation[54], phosphorylation [55-58], O-GlcNAcylation [59] and ubiquitination [60].

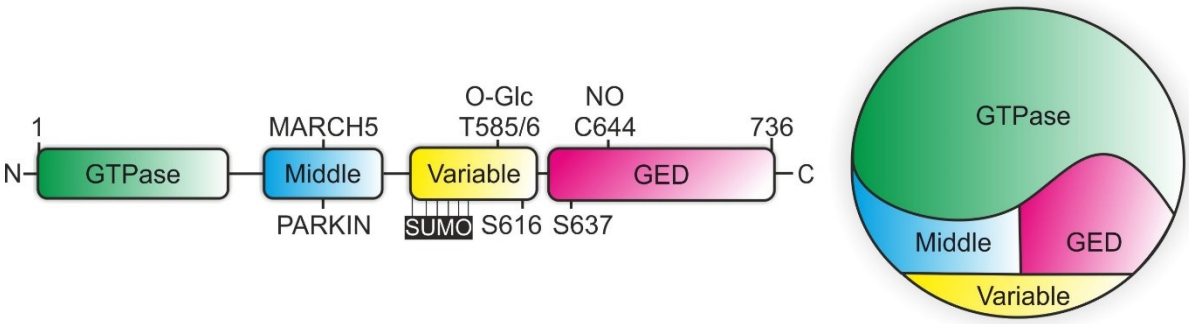

Figure 1.8. DRP1 domain structure and sites of known post-translational modification. DRP1 is composed of a GTPase, middle, variable and GTPase effector domain. P (phosphorylation), NO (S-nitrosylation), SUMO (SUMOylation), O-Glc (O-GlycNacylation). MARCH5 and PARKIN (ubiquitation).

Both Parkin and Membrane-associated RING-CH, an OMM transmembrane protein associated with mitochondrial fusion protein 2 (MFN2), have been shown to promote DRP1 ubiquitination and influence mitochondrial morphology [60, 61]. Cyclin-dependent kinase 1 (CDK1) phosphorylation of S616 drives mitochondrial division during mitosis, while phosphorylation at this same site by ERK2 promotes both tumour growth and is important for reprogramming during pluripotency [62, 63]. Calmodulin-dependent kinase I (CaMKIα) phosphorylates DRP1 at S637 and is associated with an increase in its translocation to mitochondria and affinity for

FIS1 suggesting a link between Ca^{2+} signalling and mitochondrial dynamics [58]. S-nitrosylation of DRP1 has been associated with Alzheimer's disease and neurodegeneration. Beta-amyloid, a critical orchestrator of Alzheimer's disease, resulted in NO production and S-nitrosylation of DRP1. This was associated with mitochondrial fission, neuronal dysfunction and synaptic damage which were prevented by DRP1 cysteine mutation [54]. Though not observed to modify mitochondrial recruitment small ubiquitin-like modifier (SUMO) proteins SUMO E3 ligase MAPL and SUMO protease SENP5 directly target DRP1 [53]. In cardiomyocytes O-GlcNAcylated DRP1 reduces S637 phosphorylation relocating the dynamin to mitochondria resulting in fission and decreased mitochondrial membrane potential [59]
.

1.10.2 PKA dependent DRP1 modification

Though phosphorylated at several sites, DRP1 phosphorylation at S637 by PKA is the first and best characterized mechanism of the dynamin's inhibition. This was independently described by two groups in 2007, both of which reported it to inhibit DRP1 fission activity through reduced GTP hydrolysis resulting in more reticulated and less fragmented mitochondria [55, 56]. Using a combination of fluorescence recovery after photobleaching (FRAP), fluorescent particle tracking, subcellular fractionations and intact cell crosslinking *Merrill et al.* expanded our understanding of PKA's inhibition of DRP1 [64]. The authors showed that under resting conditions DRP1 rapidly cycles between the mitochondria and cytosol, but upon S637 becomes trapped at the OMM unable to hydrolyse GTP and instead forms large oligomeric complexes incompatible with membrane fission [64]. Conversely, dephosphorylation at this same site by calcineurin enhances DRP1 fission by facilitating its hydrolysis of GTP [65, 66]. D-AKAP1 promotes this inhibition by increasing localisation of OMM PKA [67]. Knockdown of D-AKAP1 reduces PKA-DRP1 interaction resulting in increased mitochondrial fission and apoptosis while over-expression of D-AKAP1 confers protection which is abolished by mutation of its PKA binding site [56, 64]. *Ex vivo* cardiac ischaemia reperfusion (I/R) was shown to result in S637 dephosphorylation and mitochondrial DRP1 accumulation and associated with contractile dysfunction, ROS production and mitochondrial swelling [68]. This dysfunction, and importantly S637 dephosphorylation, was prevented by pre-treatment with Mdivi-1, FK506 mediated calcineurin inhibition or induced hypothermia [68]. Similar results were reported in an *in vivo* model of cardiac arrest whereby S637 dephosphorylation was associated with mitochondrial and contractile dysfunction and prevented by Mdivi-1 treatment

during cardiopulmonary resuscitation [69]. Finally, DRP1-S637 phosphorylation can also be initiated through exercise induced PKA activation [56]. In summary, the evidence suggests that DRP1 S637 phosphorylation is protective against ischaemic reperfusion injury through prevention of DRP1 fission activity. In addition to these modifications the recruitment of DRP1 to the OMM is critically dependent upon the presence of facilitation proteins resident at the mitochondria.

1.10.3 Mitochondrial DRP1 accessory proteins

Association proteins are necessary for DRP1's recruitment to the OMM as the protein itself contains no hydrophobic transmembrane domain (Figure 1.9). Mitochondria fission factor (MFF) is the best described accessory protein that localises DRP1 to the OMM. MFF co-localises with DRP1 at the OMM, which is disrupted by RNAi knockdown resulting in elongated mitochondria [70]. Conversely, MFF overexpression increases DRP1 OMM recruitment and fission. Adding further credence to this model is the observation that MFF over expression results in a fragmented mitochondrial phenotype. Mitochondrial dynamic proteins 49 and 51 (MID49/51) also localise DRP1 to the OMM though there are conflicting reports as to the impact of this on fission [71, 72]. Emerging work suggests DRP1 may interact with the critical mitochondrial fusion proteins mitofusion protein 1 (MFN1) and mitofusion protein 2 (MFN2) shifting them from a fusion-incompetent to a fusion-competent configuration [73].

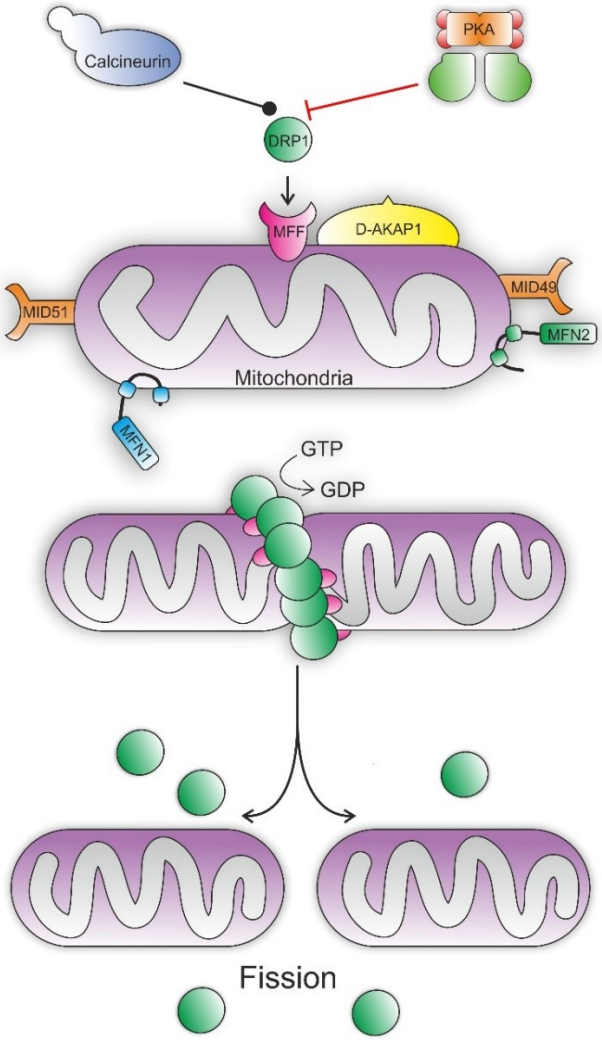

Figure 1.9. DRP1 mediates mitochondrial fission. Dephosphorylation of DRP1-S637 by calcineurin results in its recruitment to the outer mitochondrial membrane (OMM) where it associates with its accessory protein mitochondria fission factor (MFF). Mitochondrial dynamic proteins 49 and 51 (MID49/51) also recruit DRP1 to the OMM though their impact on fission is unresolved. DRP1 self assembles into spirals at the site of fission and hydrolyses GTP to mechanically constrict and sever the mitochondria. PKA phosphorylation of S637 is facilitated by D-AKAP1 and prevents GTP hydrolysis re-localising DRP1 from the OMM and preventing mitochondrial fission.

1.11 DRP1 in the myocardium

As DRP1 is the principal mediator of fission and fragmented mitochondrial networks are typically observed prior to and during apoptosis DRP1 has been implicated in programmed cell death. By exposing cells to the pro-apoptotic treatments staurosporine, etoposide or γ irradiation Frank et al. showed DRP1 was recruited to mitochondria prior to apoptosis and associated with a fragmented mitochondrial phenotype [74]. The authors then showed that this, as well as cytochrome c release, inner mitochondrial membrane depolarization and cell death

were entirely inhibited by over expression of a DRP1 dominant negative mutant [74]. Similarly, the DRP1 inhibitor mitochondrial division inhibitor 1 (Mdivi-1) is seen to prevent apoptosis through attenuated mitochondrial membrane permeabilisation and Bax/Bak-dependent cytochrome c release [75]. However, other have reported DRP1 inhibition not to prevent the release of pro-apoptotic stimuli or conversely to prevent apoptosis [76, 77].

The potential for DRP1 mutations to impact cardiac function was established following an N-ethyl-N-nitrosourea mutagenesis screen, which identified the DRP1 c452f "Python" mouse. Python mice develop dilated cardiomyopathy, a reduction in mitochondrial respiratory complexes and ATP depletion [78]. Using *DRP1* floxed allele mice, cardiomyocyte-specific DRP1 ablated mice were generated by three independent groups. In all cases knockout of DRP1 was lethal at both perinatal and adult stages. All mice harboured enlarged mitochondria due to unopposed fission and the resultant mitochondria were deficient in both bioenergetics and mitochondrial autophagy [79-81]. Following conditional knockout of DRP1, *Ikeda et al.* reported critical development of cardiac fibrosis, hypertrophy, reduced fractional shortening and diastolic dysfunction as well as higher susceptibility to I/R injury [79]. Unconditional knockout of DRP1 is postnatally lethal between days 9 and 10 and associated with severe reduction in ventricular performance [81]. *Song et al.* found that cardiac specific deletion of DRP1 led to lethal dilated cardiomyopathy, cardiomyocyte necrosis and enlarged mitochondria, the quantity of which progressively declined and was matched by a concurrent increase in mitochondrial autophagy biomarkers [80]. Caution must be exhibited however when comparing ablation of a protein, as in the above studies, and mutation of a discrete facet of its mechanism as DRP1 mediates not just fission of mitochondria, but also fission of peroxisomes. Indeed, adenovirus expression of DRP1 dominant-negative mutants showed attenuated DRP1-GTPase activity to confer protection against I/R and cardiac hypertrophy [82, 83].

Pharmacological inhibitors of DRP1 have also shed light on its essential role in the myocardium. Mitochondrial division inhibitor is a selective small molecule cell permeable inhibitor of DRP1 that blocks its hydrolysis of GTP preventing its polymerisation [75]. Pre-treatment of cells or animals with Midivi-1 appears to be cardio-protective in a number of settings. HL-1 cells pre-treated with Midivi-1 increased cell survival and reduced mitochondrial permeability transition pore (MPTP) opening during simulated I/R. In

accordance with this is also seen to reduce infarct size after I/R [84]. Similarly, mice pre-treated with Midivi-1 show improved contractile function and reduced fibrosis in pressure overload induced heart failure [85] . P110, is a selective synthetic peptide that disrupts DRP1 binding to its mitochondrial scaffold protein FIS1 preventing fission [86] and was found to confer cardio-protection to primary cardiomyocytes and *ex vivo* and *in vivo* models of I/R [87]. The factors mediating DRP1's fission activity are summarized below in Figure 1.10.

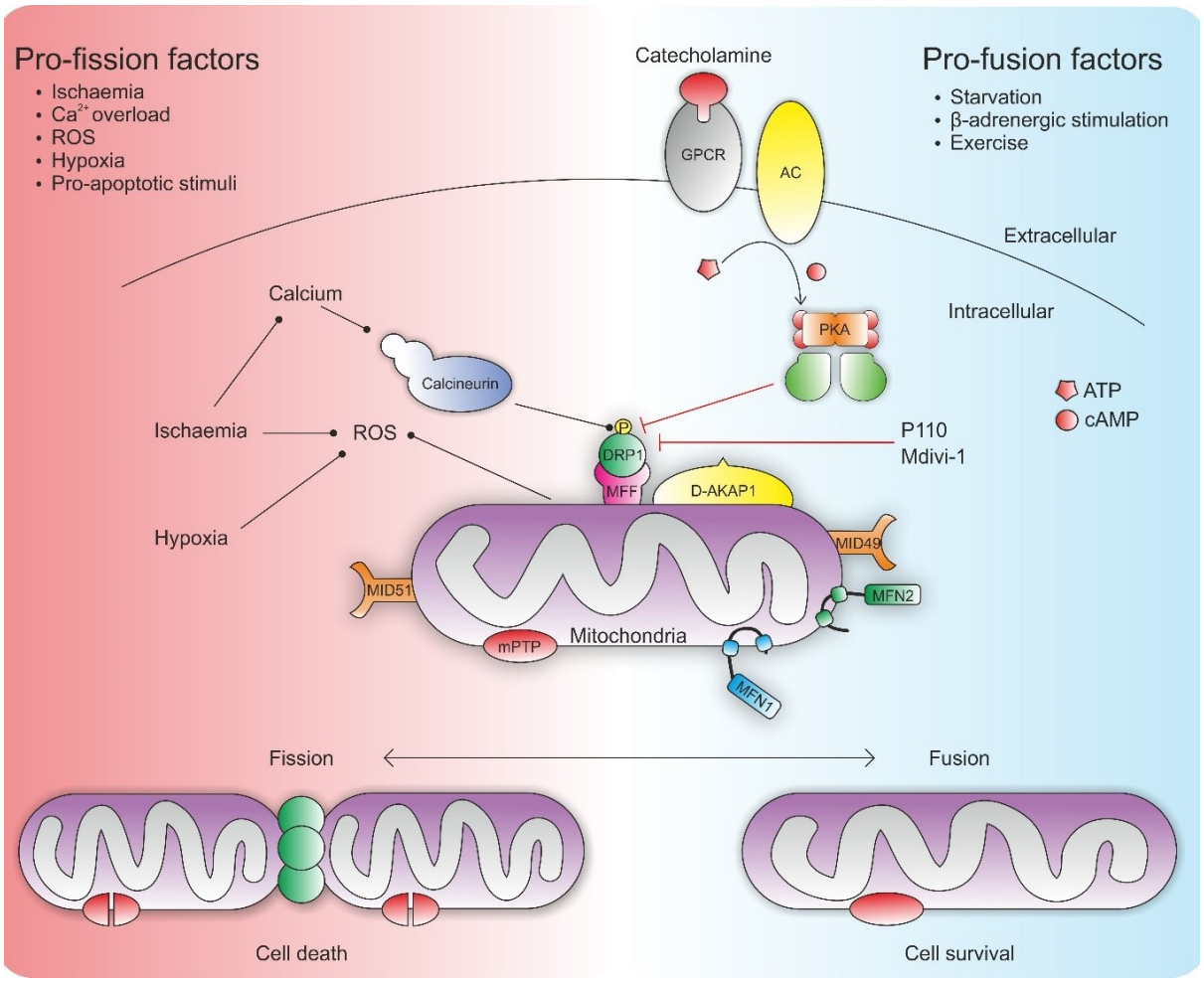

Figure 1.10. Schematic of primary factors impacting mitochondrial fusion and fission. Factors promoting mitochondrial fission are indicated on the left and those favouring fusion on the right. DRP1 is the key arbitrator of fission and is modulated by phosphorylation of its S637 site. Phosphorylation by PKA inhibits DRP1's activity promoting fusion while calcineurin dephosphorylation activates the dynamic facilitating fission [56]. Elevated cytosolic Ca^{2+}, as during ischaemia, activates calcineurin leading to mitochondrial fission [88]. Pro-apoptotic stimuli recruit DRP1 to mitochondria, leading to mitochondrial permeability transition pore (mPTP) opening (symbolised by open red oval) predisposing tissue to cell death [74]. DRP1 mediated mPTP opening during ischaemia pre-disposes the myocardium to cell death at reperfusion [84]. PKA phosphorylation of DRP1 during starvation promotes cell survival and mitochondrial fusion and can also be triggered via β-adrenergic stimulation through isoprenaline and exercise [56, 57]. DRP1 is localised to the outer mitochondrial membrane by mitochondrial fission factor (MFF) and mitochondrial dynamic proteins 49 and 51 (MID49/51) [73]. Mitochondrial fusion proteins 1 and 2 (MFN1/2) are essential for initiating fusion and may interact with DRP1 [73]. PKA phosphorylates DRP1 at the outer mitochondrial membrane (OMM) via its scaffold protein D-AKAP1 [89]. Small molecule DRP1 inhibitors mitochondrial division inhibitor 1 (Mdivi-1) and P110 prevent fission by inhibiting DRP1-GTPase activity and MFF docking respectively [75, 87]. Fragmented mitochondria, ischaemic conditions and hypoxia lead to aberrant ROS production further destabilizing mitochondria and promoting cell death [90-92]. Figure adapted from *Ong et al. [93]*

1.12 PKA mediates DRP1 during starvation

Starvation results in a state of mitochondrial dysfunction and cell wide autophagy. Autophagy is the selective engulfment of cellular macromolecules and organelles in multilamellar vesicles, which fuse with lysosomes. This leads to their digestion and the retrieval of amino acids for gluconeogenesis. A long standing, but not mechanistically understood, observation of starvation induced autophagy was that despite a replete increase in cellular autophagy, mitochondria actually increase in size [94, 95] . This paradox was resolved by *Gomes et al.* who starved cultured cells and mice to induce autophagy and mitochondrial elongation [57]. This increase in organelle size was attributed to PKA mediated inhibitory phosphorylation of DR1-S637. Using a genetically encoded cAMP FRET reporter probe EPAC, *Gomes et al.* showed that treatment of mouse embryonic fibroblasts with nutrient poor medium induces rapid elevations in cAMP [57]. This activates PKA facilitating DRP1-S637 phosphorylation inhibiting DRP1 mediated mitochondrial fission. Both pharmacological inhibition of PKA and site directed mutagenesis (DRP1-S637A) abrogated this observation resulting in fragmented mitochondria. Importantly, it was shown that elongated mitochondria more efficiently produced energy attributable to increased cristae density and mitochondrial ATP synthase dimerization. Indicating that PKA mediated DRP1-S637 phosphorylation is an adaptive mechanism to starvation [57].

1.12.1 Starvation elevates cAMP

Starvation leads to elevations in circulating glucagon, epinephrine and norepinephrine, all three of which elevate cAMP through GPCR binding [96-98]. Epinephrine initiates lipolysis from fat stores by phosphorylating hormone sensitive lipase and perilipin [99]. While glucagon produced by pancreatic alpha cells stimulates liver glycogenolysis and gluconeogenesis by elevating cAMP activated PKA [100, 101]. The pathway by which this is achieved in well characterised and described below in Figure 1.11 [100, 102].

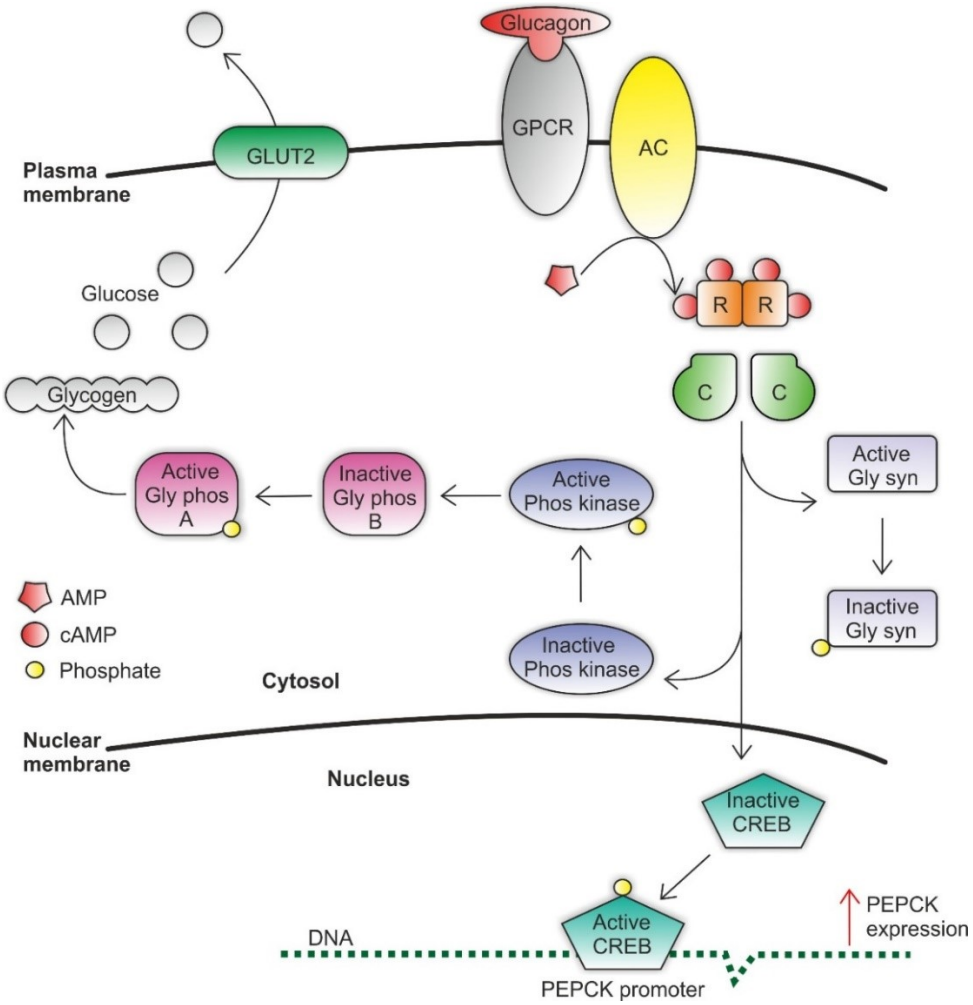

Figure 1.11. Glucagon promotes cAMP elevation activating. Glucagon binds to plasma membrane G protein-coupled receptors (GPCR) leading to the activation of the cAMP producing enzyme adenylate cyclase (AC) which activates PKA [100]. PKA induces glycogen degradation by inhibiting glycogen synthase (Gly syn) and phosphorylating phosphorylase kinase (Phos kinase) [100]. Phosphorylase kinase activates glycogen phosphorylase B (Gly phos B): converting it to its active "A" (Gly phos A) conformation which liberates glucose-1-phosphate from glycogen polymers and is transported from hepatic cells to the blood via the glucose transporter 2 (GLUT2) [100]. Active PKA also enters the nucleus to phosphorylate and activate cAMP-responsive element binding protein (CREB) [103]. CREB associates with the promoter of the phosphoenolpyruvate carboxykinase (PEPCK) promoter increasing transcription of PEPCK and other gluconeogenic enzymes, therefore elevating gluconeogenesis [103]. Figure adapted from *Bradshaw et al.* [103].

1.12.2 Starvation elevates ROS

In addition to increased cAMP production during starvation, it is widely accepted that nutrient scarcity elicits a rapid elevation in ROS production [104]. The principal source of oxidant generation during nutrient deprivation appears to be via mitochondrial electron transport leak [105-107]. The hypothesis for this, as opposed to membrane bound NOX oxidant generation for example, is that nutrient scarcity produces an energetic deficit that is compensated for by increased mitochondrial ATP production, resulting also in electron transport chain leak and ROS generation [105]. Indeed, using dihydroethidum (DHE), a fluorescent probe that reacts to peroxides, *Scherz-Shouval et al.* showed that CHO and HeLa cells serum starved for 3 or 13 hours accumulated peroxides [108]. In particular, H_2O_2 accumulation was confirmed using 2',7'-dichlorofluorescin diacetate (DCF-DA), a fluorescent probe that primarily reacts with H_2O_2 [108]. In line with this incubation of cells with catalase, which decomposes H_2O_2, abrogated starvation induced DCF-DA fluorescence [108]. The authors noted a strong colocalisation between DCF-DA and MitoTracker Red, a mitochondrial marker, fluorescence suggesting the organelle was responsible for the ROS production [108]. In accordance with, this mitochondrial electron transport chain disruptors, rotenone and TTFA as well as H_2O_2 all induce complete autophagy signalling cascades [109]. Additionally, during autophagy catalase is selectively degraded promoting H_2O_2 accumulation [110]. By contrast *Chen et al.* posit that O_2^- is the principal ROS generated during starvation induced autophagy [111]. Flow cytometric analysis of ROS using DHE and the chloromethyl derivative of 2',7'-dichlorodihydrofluorescein diacetate (CM-H2DCFDA) as indicators of O_2^- and H_2O_2 respectively. The authors showed that autophagy induced by starvation, mitochondrial electron transport chain inhibitors and exogenous H_2O_2 application all correlated with increased O_2^- and reduced H_2O_2 levels [111]. Although the relative production of both O_2^- and H_2O_2 during starvation may be uncertain the literature is consensual that nutrient deprivation is accompanied by a general increase in ROS.

1.13 Hypothesized model of starvation induced PKARIα activation

Taken together the above evidence suggests that: during starvation cAMP is elevated which activates and recruits PKA to the mitochondria via D-AKAP1, once localised PKA phosphorylates DRP1 at its S637 residue preventing fission activity of the dynamin to preserve mitochondrial function, and that these events take place against a background of aberrant ROS production. Therefore, during starvation cAMP is elevated in addition to a concomitant rise in ROS production, such scenarios are of particular relevance to this thesis as it is concerned with the integration of both nucleotide and oxidant signalling by PKARIα [80, 112]. It is therefore hypothesized that PKA's inhibitory phosphorylation of DRP1-S637 during starvation is mediated by disulfide activated PKARIα via D-AKAP1 (Figure 1.11)

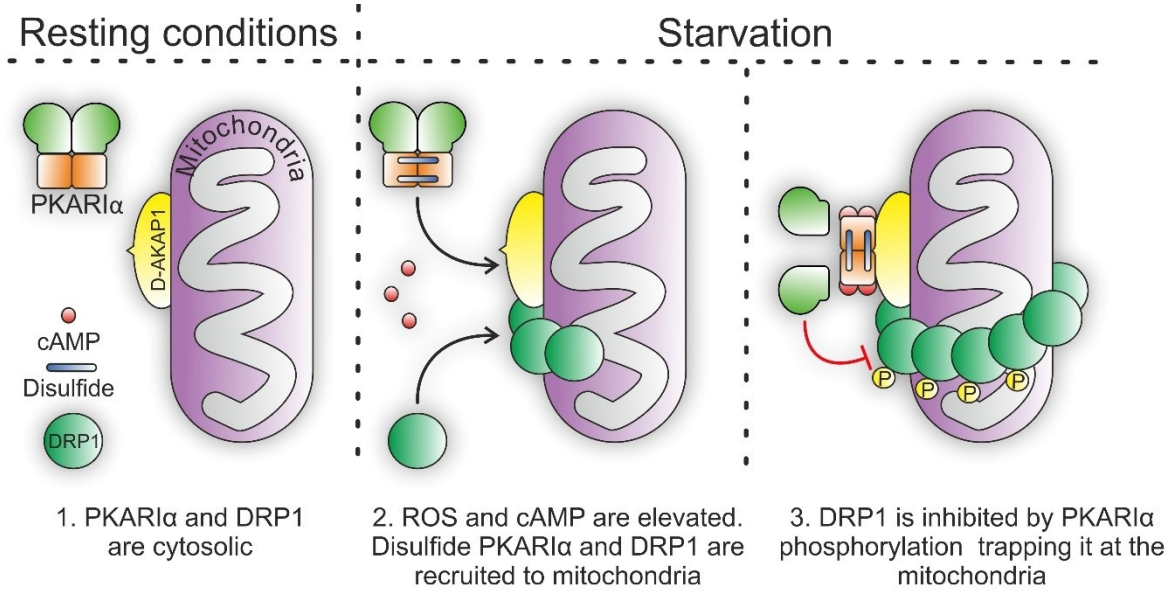

Figure 1.11. Hypothesized model of PKARIα modulation of DRP1 during starvation. (1) Under resting conditions PKARIα and DRP1 are primarily cytosolic. **(2)** During starvation ROS and cAMP are elevated as byproducts of metabolism and glucagon. PKARIα becomes oxidized forming disulfides increasing its affinity for D-AKAP1, similarly DRP1 is recruited to the mitochondria where it self assembles into oligomers. **(3)** In the presence of DRP1, PKARIα is sensitized to elevated cAMP, leading to its full dissociation and phosphorylation of DRP1-S637. This inhibits DRP1's GTPase activity trapping it at the mitochondria in large in-active oligomeric complexes.

1.14 Aim of thesis

The aim of this thesis was to investigate the ramifications of redox modified PKARIα on both total substrate, and specifically DRP1-S637, phosphorylation. A number of *in vivo* interventions involving elevated ROS and cAMP production, as well as metabolically challenging mitochondria, were investigated as this was anticipated to invoke a PKARIα-D-AKAP1-DRP1 signalling axis. Starvation was principally utilized as PKA, DRP1 and D-AKAP-1 have been shown to critically modulate the cells adaptive response nutrient deprivation. In addition, during starvation these events takes place amid an environment replete in both oxidants and cAMP. Factors that are the principal mechanisms by which PKARIα is activated. It was anticipated that starvation would result in aberrant ROS production oxidising the kinase to form inter-regulatory subunit disulfide bonds increasing its affinity for D-AKAP1 at the mitochondria where it would negatively regulate DRP1 via S636 phosphorylation (Figure 1.11). To further investigate disulfide PKARIα activity, Langendorff perfusion experiments using the oxidant H_2O_2 and β-adrenergic agonist isoprenaline were also undertaken. This permitted tight regulation of both agents in the myocardium and was used to assess the impact of their presence on PKARIα mediated substrate phosphorylation, disulfide formation and cardiac function. It was hypothesized that disulfide PKARIα mediated substrate phosphorylation would be exacerbated by isoprenaline through increased cAMP production (Figure 1.7).

Material and Methods

1.15 Mice

All animal protocols were carried out in the UK in accordance with the Home Office Guidance on the Operation of the Animals (Scientific Procedures) Act 1986 and approved by King's College London's Animal Welfare and Ethical Review Body. Unless otherwise stated all mice were 6 week old C57BL/6J (Charles River, UK); weighing between 20-22 grams.

1.15.1 PKARIα C17S knock-in mice

C57bl/6 mice were used to generate constitutively expressing PKARIα C17S knock in (KI) mice by TactonicArtemis as described previously [37]. Briefly, a targeting vector was constructed for murine Prkar1a by polymerase chain reaction (PCR) amplification of the murine Prkar1a region, introducing the Cys17Ser mutation to exon 1 by site-directed mutagenesis, and inserting an FRT-flanked neomycin selection marker (permitting identification of transfected embryonic stem cells) in proximity to the mutation favouring homologous recombination. Homologous recombination occurrence was confirmed by Southern blot screening; followed by validation of positive clones. Embryonic stem cells were then transfected permitting chimera generation. Chimeras were subsequently bred with an Flp deletor for *in vivo* selection marker deletion. Chimeras were bred directly to deletors for embryonic stem cells to go germline therefore obtaining germline transmission and selection marker deletion concurrently. Mice were bred from 6-7 weeks of age as heterozygous pairs producing wild-type (WT) or KI progeny (Figure 2.1). Sequence comparison of human and mouse PKARIα show high sequence homology suggesting experiments in mice should be applicable to humans (Table 1).

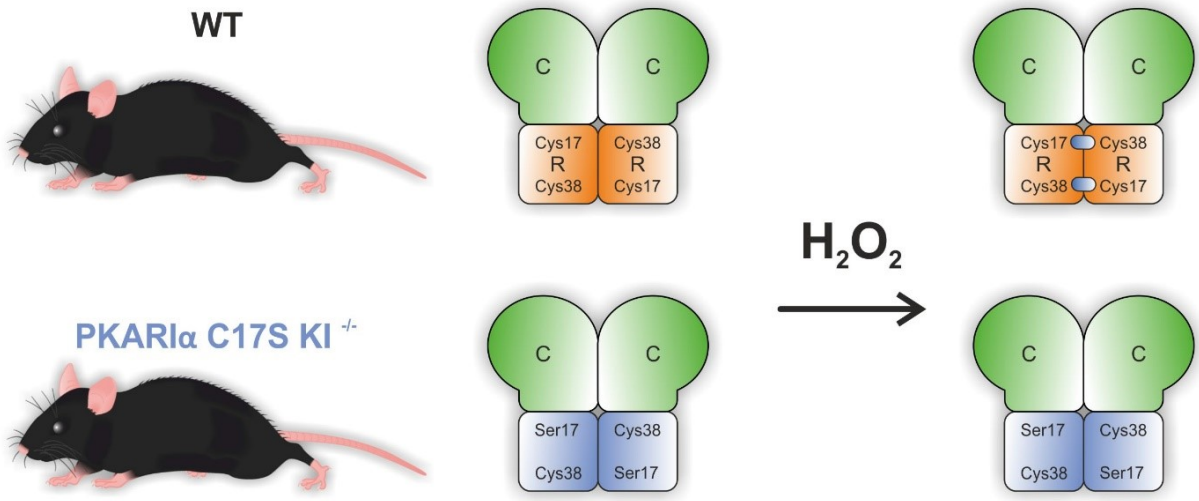

Figure 2.1. The "redox-dead" PKARIα C17S KI mouse. Two disulfide bonds are formed between cysteines 17 and 38 on adjacent regulatory subunits of PKARIα in response to oxidants such as H_2O_2. This response is precluded in PKARIα C17S KI mice through mutation of cysteine 17 serine.

Table 1. Sequence alignment of human and mouse PKARIα. Disulfide forming cysteines of interest highlighter in red, * identical, : similar

```
HUMAN MESGSTAASEEARSLRECELYVQKHNIQALLKDSIVQLCTARPERPMAFLREYFERLEKE 60
MOUSE MASGSMATSEEERSLRECELYVQKHNIQALLKDSIVQLCTTRPERPMAFLREYFERLEKE 60
      * *** *:*** **************************:******************
HUMAN EAKQIQNLQKAGTRTDSREDEISPPPPNPVVKGRRRRGAISAEVYTEEDAASYVRKVIPK 120
MOUSE EARQIQCLQKTGIRTDSREDEISPPPPNPVVKGRRRRGAISAEVYTEEDAASYVRKVIPK 120
      **:*** ***:* ********************************************
HUMAN DYKTMAALAKAIEKNVLFSHLDDNERSDIFDAMFSVSFIAGETVIQQGDEGDNFYVIDQG 180
MOUSE DYKTMAALAKAIEKNVLFSHLDDNERSDIFDAMFPVSFIAGETVIQQGDEGDNFYVIDQG 180
      ********************************* ************************
HUMAN ETDVYVNNEWATSVGEGGSFGELALIYGTPRAATVKAKTNVKLWGIDRDSYRRILMGSTL 240
MOUSE EMDVYVNNEWATSVGEGGSFGELALIYGTPRAATVKAKTNVKLWGIDRDSYRRILMGSTL 240
      * ************************************************************
HUMAN RKRKMYEEFLSKVSILESLDKWERLTVADALEPVQFEDGQKIVVQGEPGDEFFIILEGSA 300
MOUSE RKRKMYEEFLSKVSILESLDKWERLTVADALEPVQFEDGQKIVVQGEPGDEFFIILEGTA 300
      ************************************************************:*
HUMAN AVLQRRSENEEFVEVGRLGPSDYFGEIALLMNRPRAATVVARGPLKCVKLDRPRFERVLG 360
MOUSE AVLQRRSENEEFVEVGRLGPSDYFGEIALLMNRPRAATVVARGPLKCVKLDRPRFERVLG 360
      ************************************************************
HUMAN PCSDILKRNIQQYNSFVSLSV 381
MOUSE PCSDILKRNIQQYNSFVSLSV 381
       *********************
```

1.16 Langendorff perfusion of mouse hearts

1.16.1 Langendorff perfusion set-up

Mice were sacrificed with a lethal dose of intraperitoneally injected sodium pentobarbital (45 mg/kg) containing heparin (1000 IU/kg). Hearts were rapidly excised into ice-cooled Krebs-Henseleit bicarbonate buffer (K-HB), cannulated and then perfused under constant perfusion pressure (80 mmHg) at 37 °C with carbogen gassed (95 % O_2, 5 % CO_2) K-HB (Figure 2.2). Unless otherwise stated K-HB contained (118 mmol/L NaCl, 4.75 mmol/L KCl, 1.18 mmol/L KH_2PO_4, 25 mmol/L $NaHCO_3$, 1.19 mmol/L $MgSO_4$, 2 mM Na-pyruvate and 11 mmol/L glucose). Experiments in which Na-pyruvate was removed are indicated in the results description and figure legends. Prior to all experiments Deltran disposable pressure transducers (Utah Medical Products Inc, USA) were calibrated using a mercury sphygmomanometer and flow rates calibrated by collecting effluent over a one minute period. The perfusion rig was cleaned with boiling water prior to and following all experiments. Perfusion pressure was maintained by a computer-driver peristaltic pump controller and recorded using a pressure transducer. Changes in maximal left ventricular end systolic pressure (LVSP) and left ventricular end diastolic pressure (LVEDP) were assessed via a pressure transducer-connected left ventricular inserted balloon. As hearts were perfused at constant pressure changes, in flow rate were dependent on changes in the vascular resistance of the myocardium and not pump speed. Therefore, flow rate to the heart was used as a proxy measurement of coronary flow rate (CFR). Heart rate (540 bpm) was maintained by a pulse generator attached to both perfusion cannula and bath. A stabilisation period of 20 minutes preceded all interventions. All variables were monitored using LabChart 7 (AD Instruments). Inclusion criteria were CFR between 1-5 ml/min, LVEDP below 10 mmHg and LVSP above 60 mmHg. Upon cessation of all protocols, ventricular tissue was removed from hearts, placed into a cryovial, snap-frozen in liquid nitrogen and stored at -80 °C.

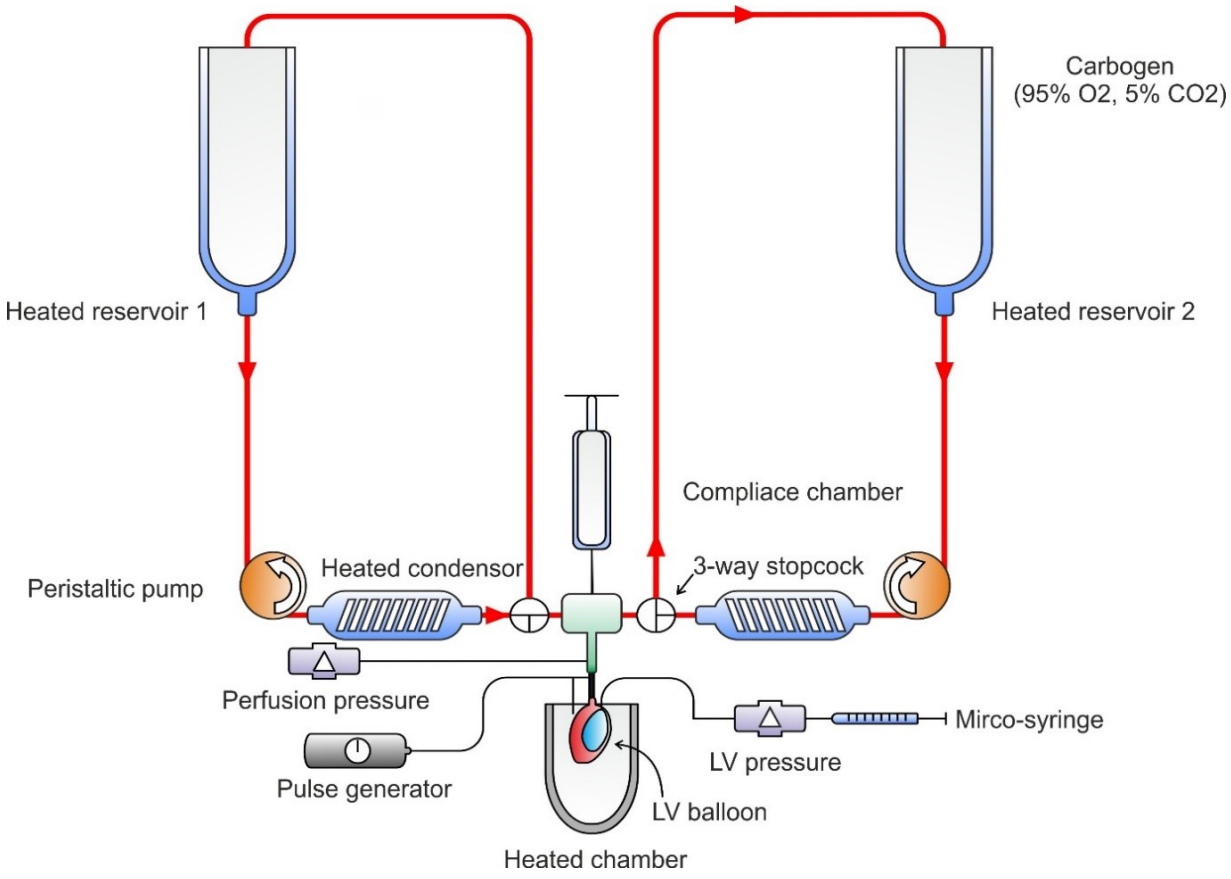

Figure 2.2. Schematic of Langendorff perfusion system. Hearts were rapidly excised into ice-cooled K-HB, cannulated and perfused from reservoir 1 at constant pressure (80 mmHg) with carbogen bubbled K-HB heated to 37 °C. The left atrium was removed, a saran wrap balloon connected to a pressure transducer inserted and inflated with a micro-syringe to record changes in LVP. Hearts were paced at 540 bpm by a pulse generator and perfusion pressure monitored by a pressure transducer connected above the cannula. A compliance chamber above the heart also functioned as a bubble trap.

1.16.2 Na-pyruvate addition to K-HB

During perfusions hearts sometimes underwent repeated cyclic fluctuations of varying periods in LVSP and LVEDP making a valid comparison of contractile function between conditions difficult. Cyclic fluctuations in contractile stability have previously been reported by other groups and attributed to metabolic substrate deficiency [113, 114]. *Wang et al.* reported that supplementation of K-HB with Na-pyruvate, as additional metabolic substrate, abolished these fluctuations [113]. Therefore, in experiments monitoring contractile function Na-pyruvate (2 mM) was added to K-HB (Figure 2.3). The presence or absence of Na-pyruvate in Langendorff experiments is indicated in figure legends.

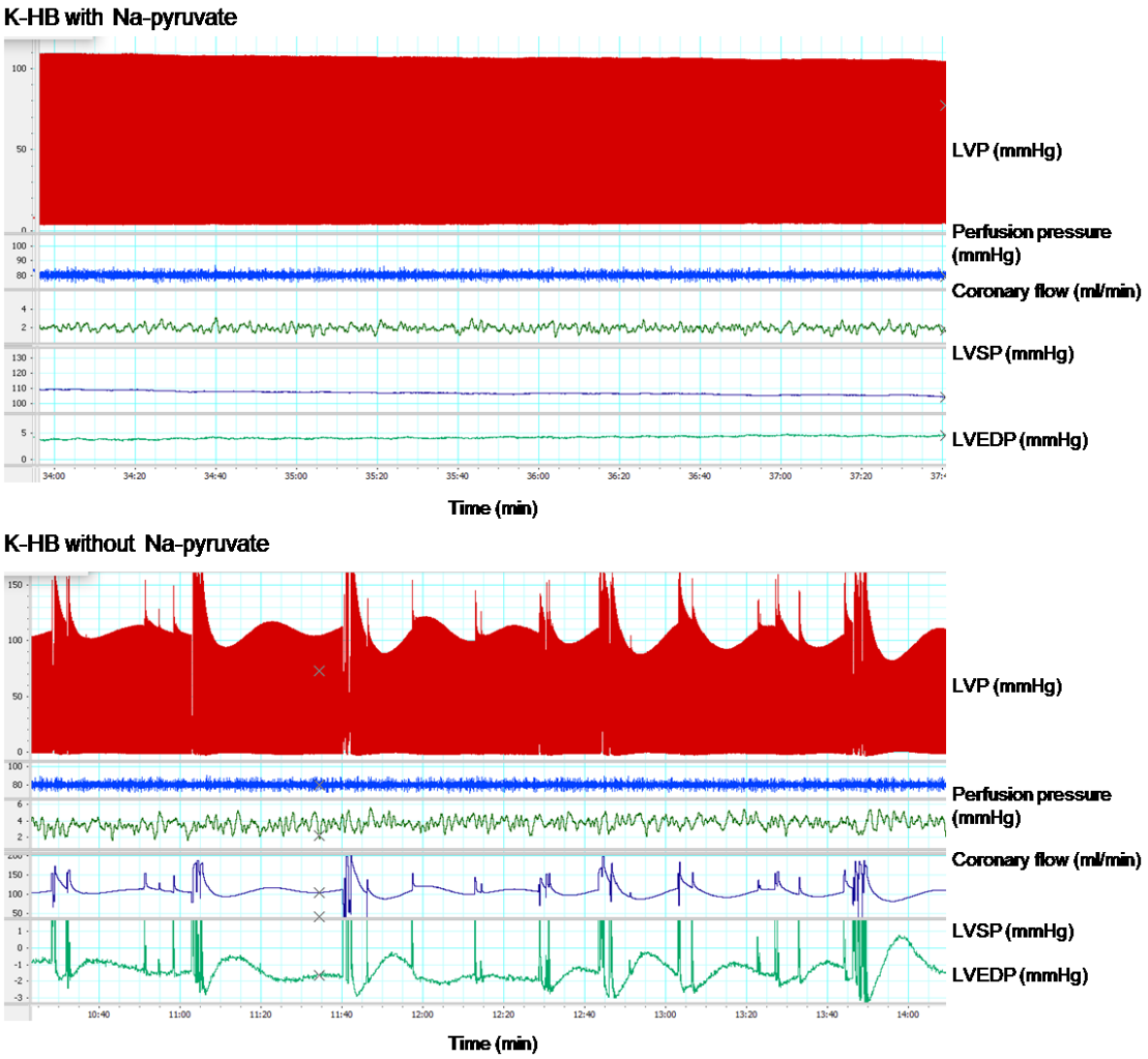

Figure 2.3. Example traces of contractile fluctuations in Langendorff perfused mouse hearts during a four minute period of recording. Regular cyclic fluctuations in LVSP and LVEDP were observed during perfusions without the presence of Na-pyruvate.

1.16.3 Selection of isoprenaline dose

Isoprenaline is a widely used and potent agonist of PKA substrate phosphorylation. Prior to examining the effects of concurrent Langendorff perfusion with isoprenaline and H_2O_2 it was necessary to identify a concentration that induced sub-maximal changes in PKA substrate phosphorylation. By using this sub-maximal dose in combination with H_2O_2, subtle changes in the phospho-status of PKA substrates may be identified indicating an influence of the oxidant on phosphorylation which may otherwise be masked by higher concentration of isoprenaline. Phosphorylation of PKA-substrate was investigated using an antibody that detects the PKA phosphorylation consensus motif Arg-Arg-X-pSer/pThr (RRXS*/T*) allowing changes in

"total" PKA substrate phosphorylation to be immunoblotted [32, 115]. In all experiments "total" PKA-substrate phosphorylation was quantified as the total signal in each lane from RRXS*/T* immunoblots normalized to GAPDH. A small pilot study using titrated doses of isoprenaline in perfused hearts and mouse intraperitoneally injected (IP) with the agonist as a positive control was undertaken. 100 nM isoprenaline led to large changes in DRP1-S637 phosphorylation and "total" PKA-substrate phosphorylation which were unchanged by 1 nM leading to our selection of 10 nM for experiments (Figure 2.4).

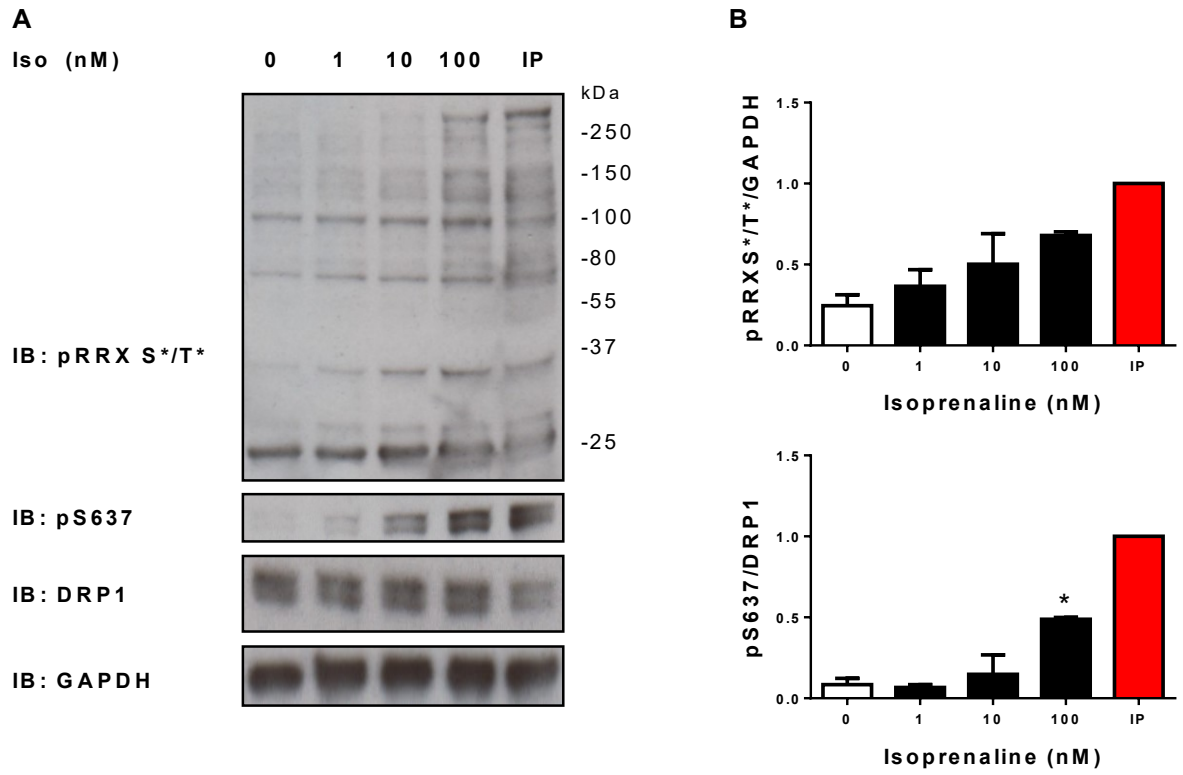

Figure 2.4. Identification of 10 nM isoprenaline as submaximal phosphorylation dose in Langendorff perfused hearts. Heart were stabilized for 20 minutes before perfusion with 0, 1, 10 and 100 nM isoprenaline for five minutes. Intraperitoneal injection (IP) of isoprenaline (1 mg/kg) was used as a positive control. Immunoblot of pDRP1-s637 and pPKAsubstrate. Analysis, One-way ANOVA with Tukey poc hoc test (n=2, ±SEM, $p<0.05$). K-HB with Na-pyruvate.

1.16.4 Perfusion of hearts with H_2O_2 and isoprenaline

Hearts were stabilised with K-HB for 20 minutes from reservoir 1. Freshly prepared H_2O_2 and isoprenaline (shielded from light) were kept at 4 °C. H_2O_2 and/or isoprenaline were added to reservoir 2, 5 minutes prior to their use. Upon treatment 3-way stopcocks were used to switch from reservoir 1 to reservoir 2. Hearts were perfused for 5 minutes with 100 µM H_2O_2 and/or

10 nM isoprenaline unless otherwise stated, control hearts were time matched and perfused exclusively from reservoir 1 (Figure 2.5).

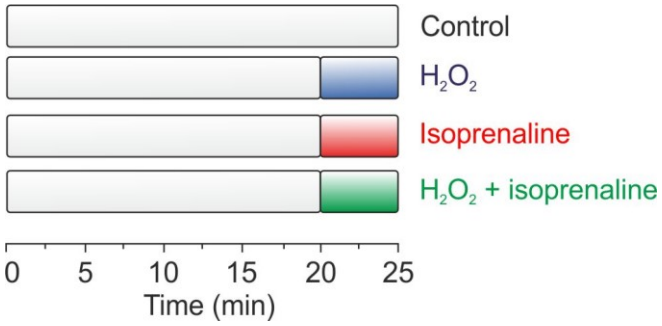

Figure 2.5. Schematic of Langendorff perfusion experiments with H_2O_2 and isoprenaline. Heart were stabilised for 20 minutes with K-HB prior to all interventions. Hearts were then perfused for 5 minutes with either H_2O_2 (100 μM), isoprenaline (10 nM) or both agents. Controls were time-matched perfused hearts with K-HB. Upon experimental cessation hearts were immediately snap-frozen in liquid nitrogen.

1.17 *Ex vivo* ischaemia-reperfusion

Reperfusion injury is the paradoxical dysfunction that ensues re-oxygenation of ischaemic tissue in an effort to quell damage caused by oxygen deficiency. The role of oxygen derived free-radicals has been implicated, and extensively examined, in the context of I/R [91]. Although it is well established that I/R is associated with aberrant ROS production, their discrete sources, forms and relative contribution to injury continue to be deeply studied [91]. So far 6 sources of ROS have been implicated in I/R including xanthine oxidase [116, 117], NOX enzymes [118], mitochondria [119-121], NOS [122], cytochrome P450 [123] and monoamine oxidase [124]. PKA is implicated in the protective effects of ischaemic preconditioning through endothelial NOS regulation [125] and proteasome assembly [126]. It has also been implicated in the protective effects of both temperature and morphine preconditioning to I/R injury [127, 128]. PKA's activation during reperfusion through is seen to reduce infarct size through Akt activation. [129]. Additionally, PDE-3B $^{-/-}$ mice, which are deficient in cAMP degradation, show reduced infarct size following coronary artery ligation and I/R [130]. In line with this, treatment with the PDE3 inhibitor milrinone prior to ischaemia elevates PKA activity and reduces myocardial infarct size after I/R [131].

PKA is also seen to confer cardio-protection during I/R injury through activation of heat-shock protein 20 a small molecular weight chaperone that assists in the maintenance of protein conformation [132]. PKA mediated mitochondrial Ca^{2+} activated K^{+} channel opening was also identified as the mechanism by which adrenomedullin, a peptide hormone, reduces infarct size following ischaemic injury [133]. Finally, while complete ablation of DRP1 provokes cardiomyopathy and mitochondrial dysfunction [79, 134] acute inhibition of the GTPase is consistently seen as protective against I/R [88]. *In vivo* experiments using selective DRP1 inhibitors mdivi-1 and P110, the non-competitive dynamin GTPase inhibitor Dynasore as well animals expressing inactive DRP1, have all been shown to confer cardioprotection through preserved contractile function or reduced infarct size during and following I/R [68, 83, 84, 87, 135, 136]. The protective effects of DRP1 inhibition during I/R have been attributed to preserved mitochondrial morphology, reduced ROS production, improved mitochondrial O_2 consumption, increased inotropy and lusitropy and both reduced infarct size and long term cardiac dysfunction [68, 83, 84, 87, 135, 136].

Taken together this suggests that I/R results in the aberrant productions of oxidants and that PKA and inhibition of DRP1 protect against ischaemic injury. Interestingly, PKA endogenously inhibits DRP1 by phosphorylating its S637 residue and PKARIα has been shown to be activated by oxidants resulting in phosphorylation of its targets [32, 55, 137]. Whether PKARIα forms a disulfide in response to oxidants produced during I/R and if this modulates DRP1 phosphorylation is unknown and was therefore investigated.

Hearts were prepared as in 2.2.1. Following a 20 minute stabilisation period hearts were subject to global ischaemia followed by reperfusion. Various time-courses of both interventions as well as pre-conditioning involving brief (1 minute) periods of ischaemia and reperfusion were used to assess if disulfide PKARIα was formed and whether this was time-dependent (Figure 2.6). During ischaemia K-HB perfusion to the myocardium was entirely ceased and the perfusate re-routed to reservoir 1, reperfusion was achieved through re-establishment of flow to the heart. Phosphorylation of DRP1-S637 was unchanged by I/R (Figure S2) and no change in disulfide PKARIα was seen in response to any of the 15 different I/R conditions tested (Figure S1). As no alteration in either the oxidative status of PKARIα or the phosphorylation state of DRP1, the proteins on which this thesis is primarily concerned, was observed these experiments were discontinued.

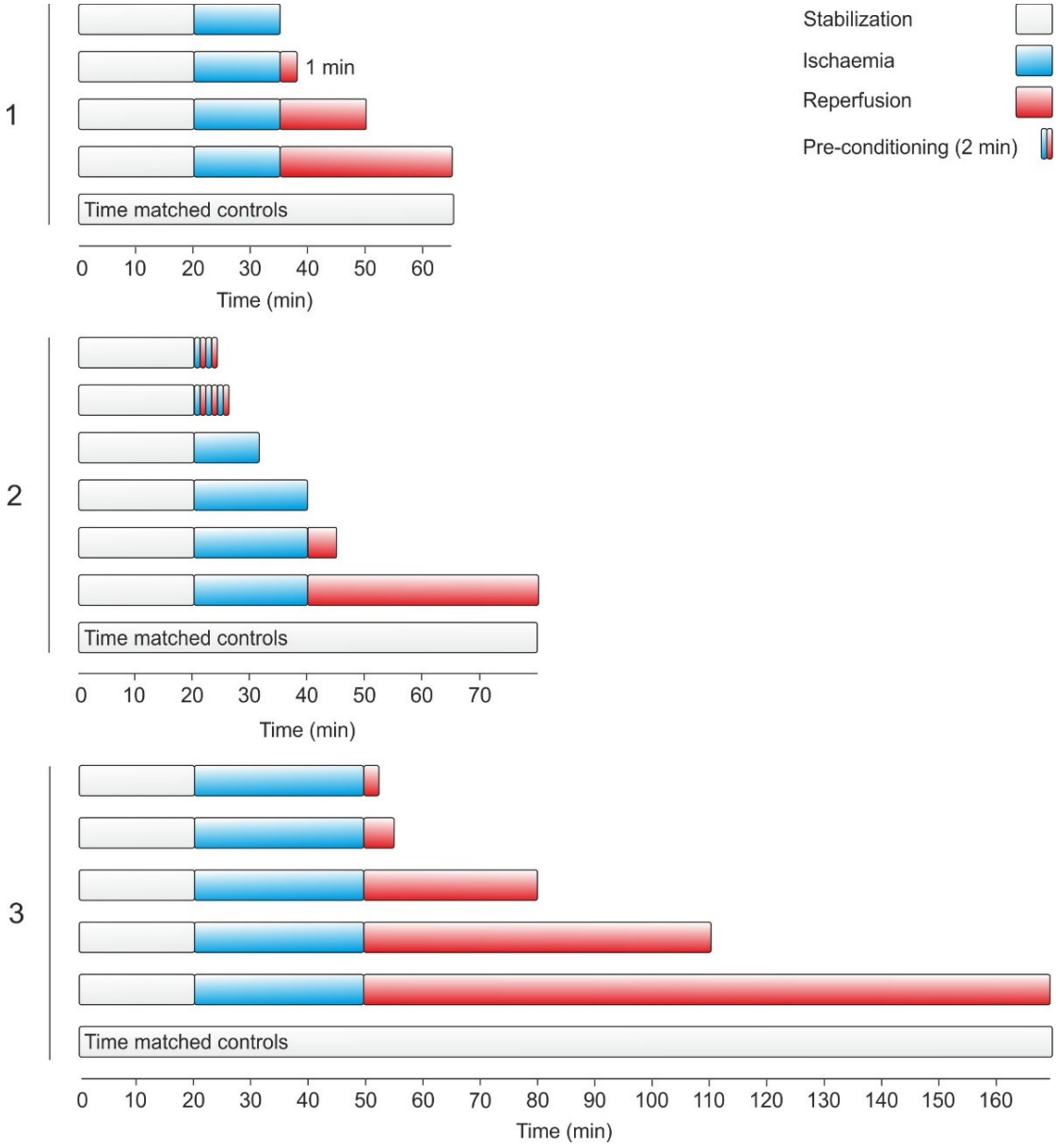

Figure 2.6. Schematic of *ex vivo* ischaemia-reperfusion experiments. 3 separate experiments were undertaken using various periods of I/R and pre-conditioning to ascertain at which point PKARIα may be oxidised. All interventions were preceded by a 20 minute stabilisation period. Experiment 1 involved 15 minutes of ischaemia followed by either 1, 15 or 30 minutes of reperfusion. Experiment 2 involved 2 and 3 bouts of pre-conditioning (1 minute ischaemia followed by 1 minute of reperfusion), 10 or 20 minutes of ischaemia, and 5 or 40 minutes of reperfusion following 20 minutes of ischaemia. Experiment 3 involved 30 minutes of ischaemia followed by 2.5, 5, 30, 60 or 120 minutes of reperfusion. Controls were time matched to the longest condition for all experiments. Upon cessation of each intervention hearts were immediately snap-frozen in liquid nitrogen. K-HB without Na-pyruvate.

Interesting, a small initial pilot study showed that levels of junctophilin 2 (JPH2), a protein linking the plasma and sarcoplasmic reticulum membranes, appeared to be reduced in a time dependent manner during reperfusion (Figure 2.7A). Experiments using larger samples sizes showed that after 60 minutes of reperfusion JPH2 levels were indeed reduced ($P<0.05$). Calpain is a Ca^{2+} dependent cysteine protease which targets both talin and spectrin for degradation when activated yielding lower molecular weight cleavage products [138, 139]. Degradation of both talin and spectrin, as well as an increase in their cleavage products ($p<0.05$), was also observed after 60 minutes of reperfusion (Figure 2.7B). It was therefore anticipated that calpain may be degrading JPH2 during reperfusion. However, the homogenisation buffer used in the above experiments contained 2 mM $CaCl^{2+}$. Although it also contained 1 mM EGTA, which sequesters Ca^{2+}, and a protease inhibitor cocktail tablet. As we were investigating a Ca^{2+} dependent protease it was thought prudent to repeat the experiments using a Ca^{2+} free homogenisation buffer (Appendix S2, Tissue homogenisation buffer). These experiments failed to show a reduction in JPH2 following I/R suggesting the previous observations were a methodological artefact (Figure 2.7C). Interestingly, shortly after these experiments *Guo et al.* showed that JPH2 was downregulated after I/R and using both computational analysis and *in vitro* calpain proteolysis reactions, identified four putative JPH2 calpain cleavage sites [140].

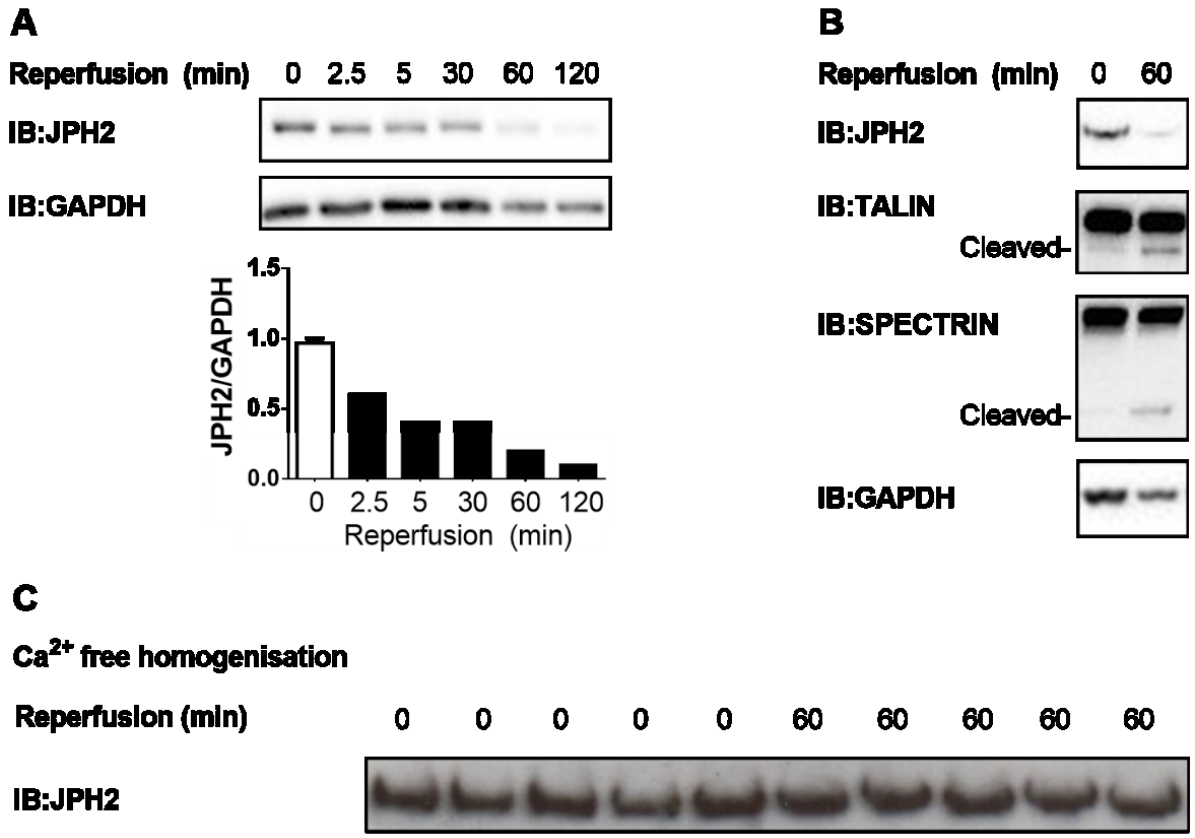

Figure 2.7. Reduction in JPH2 levels following I/R is a methodological artefact. Hearts were stabilized for 20 minutes prior to 30 minutes of global ischaemia. Reperfusion of varying durations was then commenced. "0" indicates untreated time matched controls. Upon cessation of experiments hearts were immediately snap-frozen in liquid nitrogen. **(A)** Top, immunoblots of JPH2 and GAPDH from hearts subject to 30 minutes of ischaemia followed by 2.5, 5, 30, 60 and 120 minutes reperfusion (0 n = 2, all others n = 1). Bottom, Densitometry of immunoblots. **(B)** Immunoblots of JPH2, Talin, Spectrin and GAPDH indicating cleavage products following 60 minutes of reperfusion after 30 minutes ischaemia (0 n = 4, 60 n = 5). **(C)** Immunoblot of JPH2 following 60 minutes of reperfusion after 30 minutes ischaemia homogenised in Ca^{2+} free buffer (n = 5). K-HB without Na-pyruvate.

1.18 *In vivo* interventions

1.18.1 Starvation

Mice were deprived of animal chow for 12 and 24 hours and allowed continuous access to water (Figure 2.8). Control groups were allowed ab libitum access to chow and water. In both durations of starvation food was removed at 8pm and the animals sacrificed after 12 or 24 hours. Prior to sacrifice blood glucose measurements were taken from the tip of mice tails using the Accu-Chek Aviva Blood Glucose Monitor System (Roche, USA).

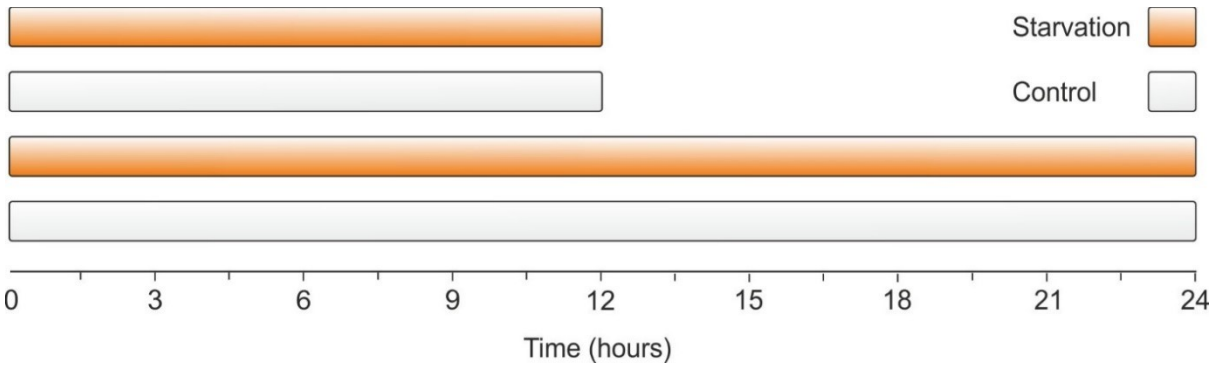

Figure 2.8. Schematic of starvation experiments. Animal chow was removed from mice for 12 or 24 hours and water was available at all times. Control animals had ab libitum access to both chow and water. Upon cessation of the experiment hearts were extracted and immediately snap-frozen in liquid nitrogen.

1.18.2 Intraperitoneal injection with isoprenaline

Mice were intraperitoneally (IP) injected with freshly prepared isoprenaline (1 mg/kg) mixed in 0.9 % NaCl or with NaCl alone as controls. 5 minutes after injection animals were sacrificed, hearts rapidly excised into ice-cooled K-HB, rinsed, snap-frozen in liquid nitrogen and stored at -80 °C.

1.18.3 Intraperitoneal injection with 2, 4 dinitrophenol

2, 4 dinitrophenol (DNP) is a potent proton ionophore that uncouples mitochondrial oxidative phosphorylation. DNP destabilises the proton gradient across mitochondria by transporting H^+ cations across its IMM independently of ATP synthase activity [141, 142]. Upon entering the mitochondrial matrix DNP is depronated, shuttled back across the inner mitochondrial membrane and its cycle repeated. Collapse of this proton motive force causes mitochondria to continuously consume oxygen in order to generate the energy needed to shuttle protons back across the IMM in an attempt to re-establish the proton gradient [143]. Thus, oxygen consumption is uncoupled from ATP production which is instead lost as heat [141, 142]. DNP treatment was therefore used to metabolically stress mitochondria and assess whether this involved recruitment of disulfide PKARIα and pDRP1-S637.

Mice were IP injected with 30 mg/kg of DNP as this dose has previously been shown in rats to decrease body weight, and increase resting and skinned muscle oxygen consumption [144]. Tissues were then harvested 0.5, 2, 4, and 8 hours post injection, placed in a cryovial, snap frozen in liquid nitrogen and stored at -80 °C. Controls received an equal volume IP of 0.9 % NaCl and were time matched (Figure 2.9). No change in disulfide PKARIα or pDRP1-S637 were observed at any time point post IP therefore mitochondrial uncoupling experiments were discontinued (Figure S3).

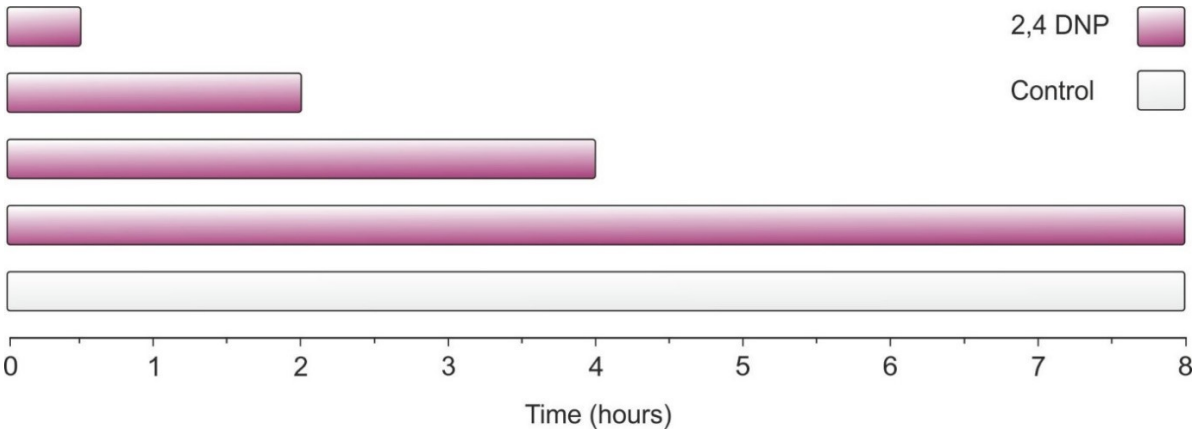

Figure 2.9. Schematic of 2,4 DNP experiments. Mice were intraperitoneally injected with 2, 4 DNP (30 mg/kg) and hearts harvested 2, 4, and 8 hours post injection. Control mice received an equal volume of 0.9% NaCl and were harvested 8 hours post IP. Hearts were immediately snap-frozen in liquid nitrogen (n = 2).

1.18.4 Intraperitoneal injection of glucagon

As previously described in Figure 1.9, the peptide hormone glucagon raises intracellular cAMP concentration by binding to GPCRs which initiates a signalling cascade resulting in glucose liberation from glycogen stores [145, 146]. As also previously discussed in chapter 1.13 nutrient deprivation is also associated with aberrant ROS production [147-149]. Therefore, we hypothesized that nutrient deprevation in combination with glucagon treatment may be an effective means to induce disulfide PKARIα formation in the presence of elevated cAMP.

Animals were fasted for 6 hours before IP injection of glucagon (1 mg/kg). Prior to and 10, 20 and 60 minutes post injection, tail vein blood glucose levels were measured using the Accu-Chek Aviva Blood Glucose Monitor System. Control mice had access to animal chow at all times and were sham injected with 0.9 % NaCl (Figure 2.10). Glucagon IP injection resulted

in elevated blood glucose levels 10, 20 and 60 minutes post injection but no difference in disulfide PKARIα or pDRP1-S637 were seen (Figure S4). These experiments were therefore discontinued.

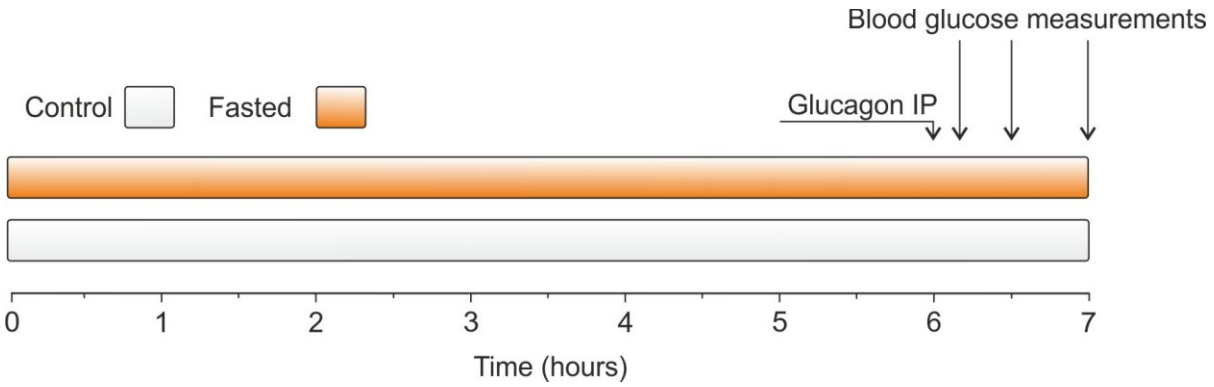

Figure 2.10. Schematic of glucagon intraperitoneal injection experiments. Mice were fasted for 6 hours prior to glucagon (1 mg/kg) IP injection. Blood glucose measurements then taken 10, 30 and 60 minutes post-IP and assessed with an Akku Chek blood glucose monitor. Control animals had ab libitum chow access at all times. Hearts were harvested after the final blood glucose measurement and immediately snap-frozen in liquid nitrogen (n = 3).

1.18.5 Hypoxic chamber exposure

An interplay between hypoxia, mitochondrial dysfunction and DRP1 has been described in several contexts. *Wu et al.* recently described a novel pathway in which FUN14 Domain containing 1 protein recruits DRP1 to mitochondria under hypoxic conditions to induce fission [150]. Rats maintained under hypoxic conditions are also been seen to upregulate DRP1 in pulmonary arterial smooth muscle cells [151]. In addition, using a combination of hemodynamic analysis and morphometric assays *Shen et al.* demonstrated that DRP1 mediates increases in right ventricular systemic pressure and hypertrophy as well as pulmonary angiogenesis in response to hypoxia by promoting the proliferation and migration of pulmonary arterial endothelial cells [152]. *Kim et al.* showed that mitochondria undergo fission in response to hypoxia which is mediated by AKAP149 availability [67]. Accordingly, under hypoxic conditions the ubiquitin ligase Siah2 was seen to degrade AKAP149 preventing PKA mediated inhibition of DRP1 mitochondrial fission [67]. AKAP149 levels were elevated in Siah2 $^{-/-}$ cardiomyocytes which showed decreased apoptosis in response to simulated ischaemia [67]. Similarly, Siah2 $^{-/-}$ mice displayed reduced infarct size and cell death in response to myocardial infarction [67].

In tandem with affecting DRP1, hypoxic conditions are a well-established stimulus of ROS production. Under normoxic conditions hypoxia-inducible factor 1α (HIF-1 α) is quickly prolyl hydroxylated resulting in its ubiquitination by the E3 ligase von Hippel-Lindau protein and subsequent degradation by the proteasome [92]. Under hypoxic conditions HIF-1 α in not hydroxylated and instead forms heterodimers with aryl hydrocarbon nuclear translocase resulting in transcriptional changes to genes regulating adaptation to hypoxia including those responsible for ROS production [92]. For example, HIF-1 α regulates the transcription of both inducible and endothelial NOS thus increasing NO bio-availability [92, 153]. Taken together this data suggest that DRP1 is responsive to hypoxic stimuli and that hypoxic conditions initiate ROS production. Therefore, we hypothesized that hypoxic conditions represented a potential environment in which to assess the role of disulfide PKARIα in DRP1 regulation.

Hypoxic experiments were conducted by Dr. Olena Rudyk. Mice were subjected to 10 % oxygen for 2 and 3 days using the Proox P360 (BioSpherix, USA) hypobaric chamber. Control mice were housed in the same room as those exposed to hypobaric conditions (Figure 2.11). Upon cessation of experiments animals were sacrificed, hearts rapidly excised, snap-frozen in liquid nitrogen and stored at -80 °C. No difference in disulfide PKARIα or pDRP1-S637 in response to 2 or 3 days hypoxic exposure was observed and so these experiments were discontinued **(**Figure S5).

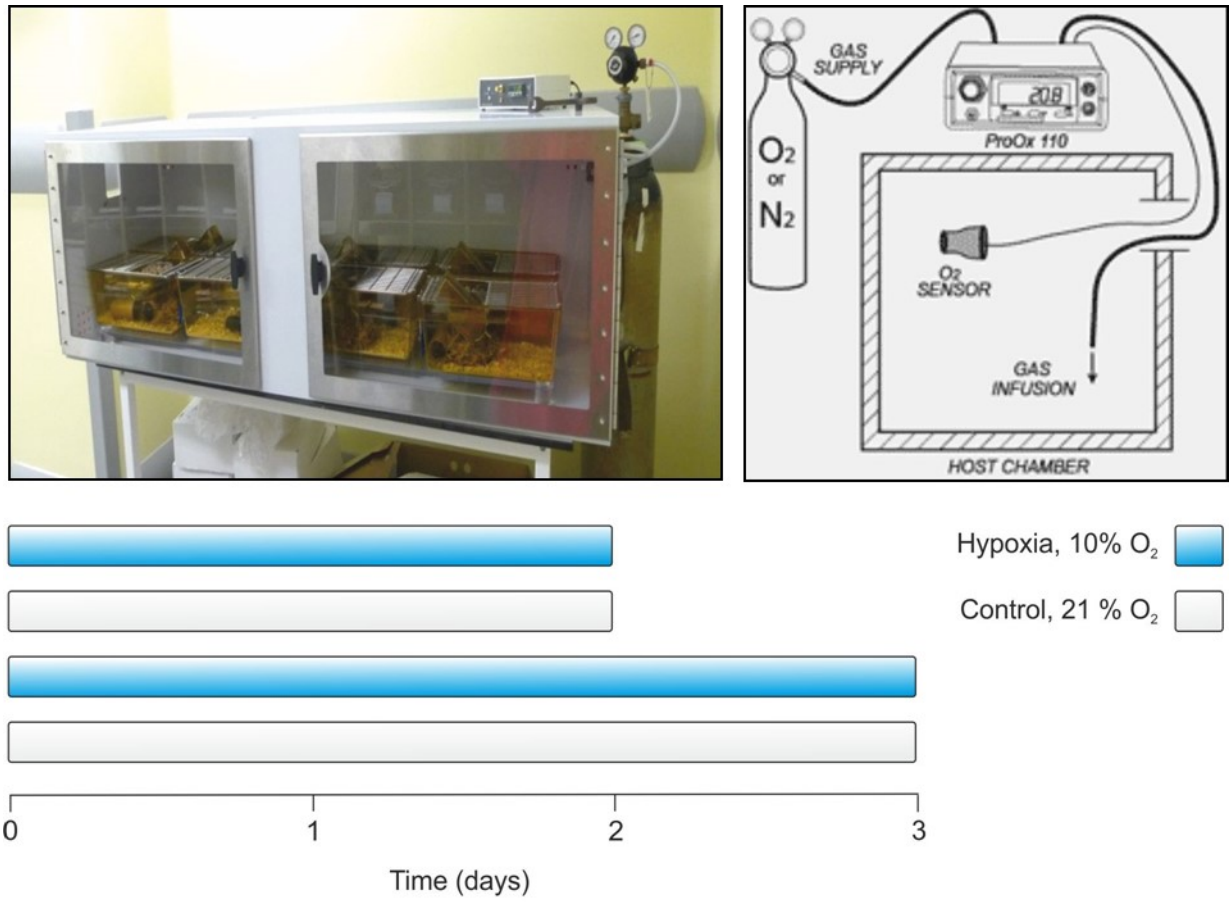

Figure 2.11. Schematic of2 and 3 day hypoxic chamber experiments. Hypoxic animals were housed in the Proox P360 hypobaric chamber containing 10 % O_2 for 2 or 3 days. O_2 levels were monitored throughout the experiment with an in-chamber O_2 sensor. Control mice were concurrently kept in the same room and exposed to ambient room O_2 (21%). Upon cessation of the experiment hearts were excised and immediately snap-frozen in liquid nitrogen. **(Top)** Left, image of hypoxic chambers housing mice cages. Right, schematic of hypoxic chamber set-up. **(Bottom)** Schematic of experiments protocol with each row representing a different experimental group (n = 4).

1.19 Isolation and treatment of mouse ventricular cardiomyocytes

1.19.1 Isolation of ventricular cardiomyocytes

C57bl/6N mice (Charles River, Sulzfeld, Germany) were anesthetized with 3% isoflurane, their cervical vertebrae dislocated, hearts rapidly extracted, cannulated with a 21 gauge blunted syringe and attached to a modified Langendorff system. Perfusion was maintained at 4 ml/min and 37 °C. Hearts were perfused with Ca^{2+} free isolation buffer for 4 minutes prior to digestion with perfusion buffer containing 40 µM $CaCl_2$ and 2 mg/ml collagenase type II (~300 units/mg) for 9 minutes. Ventricles were then removed, minced in digestion buffer with a scissors to approximately 1 mm^3 pieces, then gently agitated with a 10 ml pipette. Digestion was seized with perfusion buffer containing 10 % BCS and 12.5 µM $CaCl_2$. Cells were then sedimented

twice in an upright 15 ml falcons for 8 minutes, the supernatant discarded and the pellet re-suspended in perfusion buffer containing 10 % BCS and 12.5 µM $CaCl_2$.

1.19.2 Treatment of cardiomyocytes with H_2O_2

Freshly isolated cardiomyocytes were lightly centrifuged (1000 g, 1 min), re-suspended in MEM medium, distributed into 6 well plates and left for 1 hour to settle and stabilize. Cells were then treated for 10 minutes with H_2O_2 (100 µM, or as indicated), the thiol selective oxidant diamide (500 µM) as a positive control for disulfide dimer formation or left untreated as controls**.** In cardiomyocytes treated with 0, 10 and 100 µM H_2O_2 there was no clear dose-response in disulfide PKARIα formation, the extent of dimer formation varied substantially within conditions and no band was detected at the monomeric weight of the protein **(**Figure S6A). Similar results were seen in an additional experiment in which cardiomyocytes were treated with 100 µM H_2O_2 and diamide **(**Figure S6B**).** This rendered correct quantification of disulfide PKARIα formation impossible as it could not be expressed as a percentage of the total protein. For these reasons additional experiments were carried out in whole-heart models as these reliably showed changes in both the monomeric and dimeric form of the kinase.

1.20 Immunofluorescence

Following isolation, cardiomyocytes were settled on laminin (2 mg/ml) coated glass coverslips (Ø 18 mm) in isolation buffer for 30 minutes at room temperature. Cells were then fixed with paraformaldehyde (4 %) in Ca^{2+} and Mg^{2+} free PBS for 5 minutes. Following this cells were washed twice with PBS prior to permeabilisation with 0.2 % Triton X-100 in PBS containing 10 % BCS. Primary antibodies were then added and cells incubated over night at 4 °C. Cells were subsequently washed 3 times with PBS containing BCS and incubated with secondary antibody in the dark for 90 minutes at room temperature. Cells were then washed 3 times with PBS, embedded in mounting medium and set overnight for imaging the following day.

1.20.1 Confocal microscopy

A LSM 710 confocal laser scanning microscope (Carl Zeiss, Jena, Germany) with a 63x 1.4 NA oil objective was used to image fluorescent secondary antibodies. Transmitted light mode was used to ascertain cell viability prior to imaging. Data was recorded using the manufacturer's software (ZEN 2009). Secondary antibodies were excited at 2 % laser power, AlexaFluor 514 and AlexaFluor 633 were excited at 514 nm and 613 nm and their emissions detected between 520 – 620 nm and 640 – 740 nm respectively. Imaging pixel size was 80 nm x 80 nm.

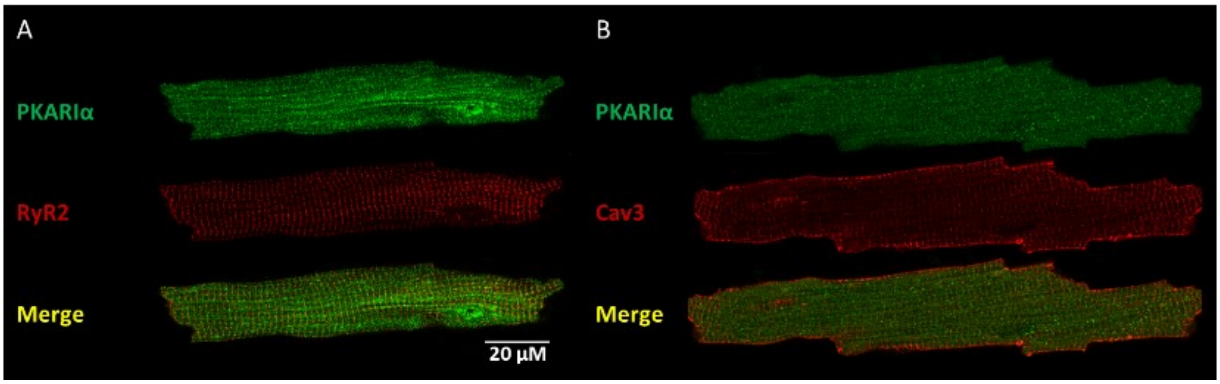

Figure 2.12. Representative confocal images of PKARIα co-stains of RyR2 and Caveolin 3. Co-staining freshly isolated mouse cardiomyocytes with immunofluorescent indicators of major structural and Ca^{2+} handling proteins. **(A)** Representative image of cardiomyocytes stained with PKARIα and RyR2 **(B)** Representative image of cardiomyocytes stained for PKARIα and the junctional protein Caveolin 3 (Cav3).

In the initial work showing that perfusion of rat hearts with H_2O_2 led to the translocation of disulfide bound PKARIα to myofilament and nuclear fractions this result was further supported by immunofluorescent data [32]. Using immunofluorescence, *Brennan et al.* demonstrated that H_2O_2 treated cultured adult rat ventricular cardiomyocytes exhibited greater nuclear and myofibrillar localisation [32]. In an attempt to identify potential interaction partners of disulfide bound PKARIα after H_2O_2 treatment a number of immunofluorescent co-stains were made in freshly isolated mouse ventricular cardiomyocytes with PKARIα and other major structural and Ca^{2+} handling proteins. Immunofluorescent imaging of these cells however revealed a highly variable staining signal for the PKARIα antibody. For example in Figure 2.12A the PKARIα stain exhibits a more striated patterns while in Figure 2.2B the PKARIα is diffuse throughout the cell. Immunofluorescent PKARIα were repeated a number of times and failed

to show a consistent signal. Therefore, immunofluorescent co-localisation experiments in cardiomyocytes could not be made with confidence. In retrospect, culturing of mouse cardiomyocytes overnight prior to H_2O_2 treatments should have been employed as this would have allowed the redox-state of the cells to stabilize and likely would have produced a more consistent fluorescent signal.

1.21 Molecular biology

1.21.1 Tissue homogenisation

Tissues were homogenized on ice with a Polytron grinder to 10% (w/v) samples in homogenisation buffer. An aliquot was re-suspended in an equal volume of non-reducing SDS sample buffer (SB) containing maleimide. Samples were then boiled (95 °C, 5 min), centrifuged (25,000 rcf, 5 min) and labelled "non-reduced". Aliquots were then removed and 5% (v/v) β-mercaptoethanol added to yield a reduced sample.

1.21.2 Cardiomyocyte homogenisation

All homogenisation was undertaken at 4 °C. Cells were centrifuged (1,000 g, 1 min), re-suspended in cell-homogenisation buffer and vortexed. Cells were then centrifuged (2,000 g, 10 minutes) the supernatant removed and snap-frozen in liquid nitrogen. Protein concentrations were assessed using Pierce BCA Protein Assay Kit according to the manufacturer's instructions.

1.21.3 Fractionation

Cardiac homogenate (200 µl) was centrifuged at 4 °C (5 min, 25,000 rcf) and the resultant supernatant added to 200 µl of SB (soluble fraction). The pellet was re-suspended in 200 µl homogenisation buffer containing 1% Triton X-100 and centrifuged (5 min, 25,000 rcf). The resultant supernatant was added to 200 µl of SB (insoluble fraction) and the pellet re-suspended in 200 µl of sample buffer (pellet). Therefore, yielding 3 separate fractions. Markers of the

cytosol (GAPDH), membrane (α1NaKATPase) and myofilaments (cTnI) revealed these proteins to be abundant in the soluble, insoluble and pellet fractions respectively (Figure 2.13).

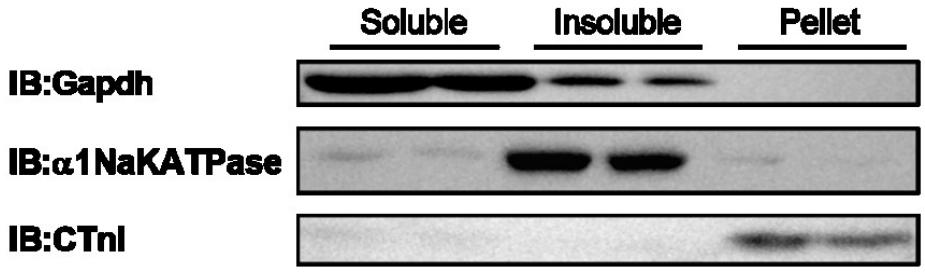

Figure 2.13. Immunoblot of subcellular markers following fractionation of cardiac homogenates. Cardiac homogenates were centrifuged in the absence and presence of 1 % Triton X-100 yielding a soluble, insoluble and pellet fraction. Immunoblots of GAPDH, α1NaKATPase and cTnI identified these fractions as primarily cytosolic, membrane and myofilament rich fractions respectively (n = 2).

1.21.4 Western blotting

10 µl of tissue homogenates as prepared in 2.6.1 or 40 ug of cardiomyocyte protein as determined in 2.6.2 in SB were loaded per well. SDS-PAGE and semi dry transfer protocols were run with BioRad Protean and Trans-Blot Turbo systems using the manufacturer's pre-cast gels, PVDF membranes, running and transfer buffers according to the manufacturer's instruction. Membranes were blocked, and antibodies incubated in, PBS-Tween-20 containing 5 % (wt/vol) fat free milk (Premier International Foods, UK). Membranes were incubated in primary antibodies for 2 hours at room temperature or overnight at 4 °C and HRP-conjugated secondary antibodies for 1 hour at room temperature. Incubations were separated by 3 15 minute PBS-Tween-20 washes. Blots were developed on autoradiographic film (GE Healthcare, UK) using chemiluminescence (ECL, Thermo Scientific, Illinois, US) in a film developer (Fuji, JPN). Densitometry was conducted with Image Studio Lite. All immunoblots showing dimeric and monomeric PKARIα were run from non-reduced samples. A table of all antibodies used in this thesis can be found in Appendix 2. SuperSignal West Femto Maximum Sensitivity Substrate (Thermo Scientific, Illinois, US) was used as chemiluminescence for immunoblots of DRP1 and S637 as normal ECL failed to produce signal on immunoblots.

1.21.5 Coomassie Brilliant Blue staining

Following exposure of membranes on autoradiographic film, membranes were rinsed in de-ionised water and protein loading stained using Coomassie Brilliant Blue. Membranes were gently shaken in the stain for 10 minutes and de-stained for approximately 1 hour until a clear separation of background and stain was visible. Staining was used to confirm that both protein transfer from gel to blot and protein loading were uniform.

1.21.6 DRP1 and pDRP1-S637 antibody selection

Prior to assessing changes in DRP1 localisation or phosphorylation is was necessary to find antibodies that produced a clear reliable signal. The chosen antibodies had been used in published work and were therefore tested (Table2).

Table 2. Antibodies tested for DRP1 and pDRP1-S637. Table displays the antibodies that were tested, their product numbers, company from which they were ordered, species in which they were raised, dilutions used and incubation times. All antibodies were incubated in 5 % milk in PBS-T.

Name	Code	Company	Species	Concentration	Incubation
DRP1 [154]	8570	Cell Signalling	Rabbit	1:1000	Overnight, 4 °C
DRP1 [155]	32898	Santa Cruz	Rabbit	1:1000	Overnight, 4 °C
pS637 [55]	6319	Cell Signalling	Rabbit	1:1000	Overnight, 4 °C
pS637 [55]	4867	Cell Signalling	Rabbit	1:1000	Overnight, 4 °C

Antibodies were tested on immunoblots of cardiac homogenates from mice IP injected with isoprenaline as a positive control for pDRP1-S637. Homogenates were centrifuged to yield soluble and insoluble fractions. Phosphorylation of DRP1-S637 was detected at its appropriate molecular weight (82kDa) using Cell Signalling DRP1-S637 antibody #4867 and total DRP1 was clearest with Cell signalling antibody #8570 (Figure 2.14). These antibodies were therefore used in all further experiments.

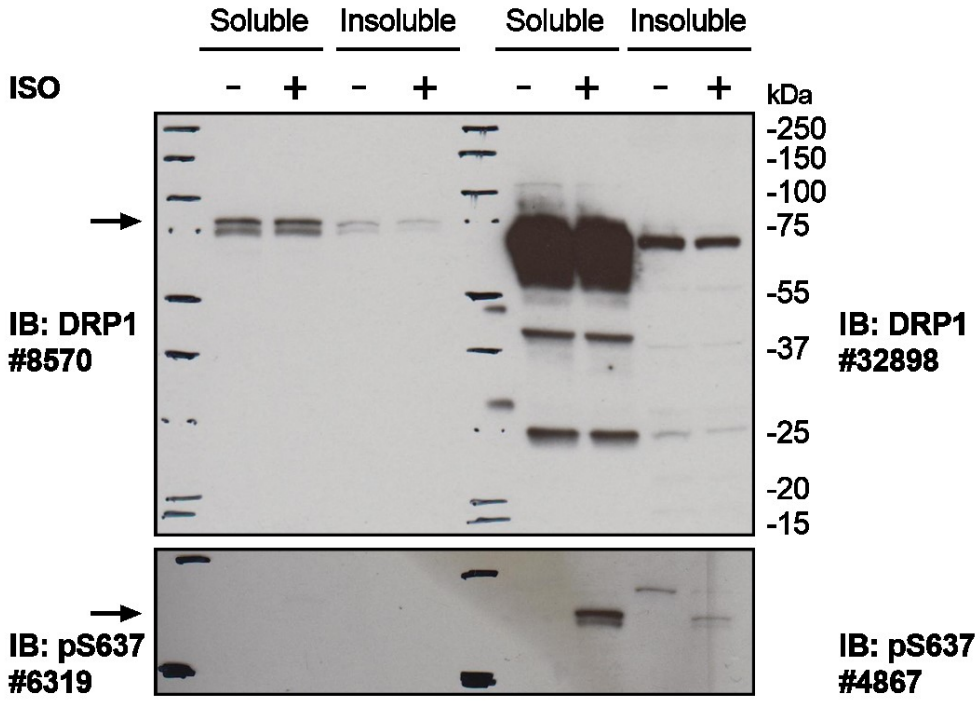

Figure 2.14. Selection of appropriate antibodies for DRP1 and pS637. Immunoblot of DRP1 and S637 in soluble and insoluble heart fractions using commercially available antibodies following intraperitoneal injection of isoprenaline (1mg/kg). **(Top)** Left, Cell Signalling antibody number 8570, right Santa Cruz antibody number 32898. **(Bottom)** Left, Cell Signalling antibody number 6319, right Cell Signalling antibody number 4867 (n = 1).

1.21.7 Polymerase chain reaction

DNA was isolated from mice ear clippings using the Qiagen DNAeasy tissue kit according to the manufacturer's instructions. The PCR reaction for genotyping of PKARIα C17S KI was developed by Tactonic Artemis. A DNA-free master mix was made and 36 µl per DNA sample aliquoted into PCR tube racks on ice. DNA (4 µl) was then added to each aliquot of master mix and the samples placed in a thermal cycler (Eppendorf) upon cessation of the cycle samples were held at 4 °C. DNA electrophoresis was conducted on a 2 % agarose gel in tris-acetate ethylenediaminetetraacetic (TAE) buffer containing 0.01 % gelRed Nucleic Acid Gel Stain (Biotium) for DNA visualisation. The first lane was loaded with 5 µl of the 100 bp DNA step ladder (Promega), and 15 µl of PCR product were loaded in adjacent lanes. Samples run to the end of the gel and gentoypes assessed by visualising DNA fragments under UV light.

1.22 Protein crosslinking

Protein-protein interactions can be investigated using crosslinking compounds. These agents stabilise interactions that may be otherwise weak or transient making their identification more readily detectable. If H_2O_2 brought PKARIα, DRP-1 or D-AKAP into proximity with other proteins this would be evident by an increase in labelling in crosslinked samples immunoblotted for these proteins.

First a screen of the amine-amine crosslinking compounds bis-sulfosuccinimidyl-suberate (BS3), disuccinimidyl glutarate (DSG) and ethylene glycol bis-succinimidyl succinate (EGS) containing spacer arms lengths of 11.4 Å, 7.7 Å and 16.1 Å respectively were used to identify an effective agent. Hearts were homogenized in liquid nitrogen using a mortar and pestle and made to 10 % (w/v) homogenates in PBS lysis buffer containing 100 mM maleimide. Homogenates were then centrifuged at 4 °C (25,000 rcf, 5 min), the supernatant removed and rotated at room temperature (30 min) in 2 mM BS3, EGS or DSG. The reaction was terminated by incubation with 100 mM Tris-HCL pH 7.4 (15 min) and samples re-suspended in an equal volume of SB containing 5 % (v/v) β-mercaptoethanol (Figure 2.15).

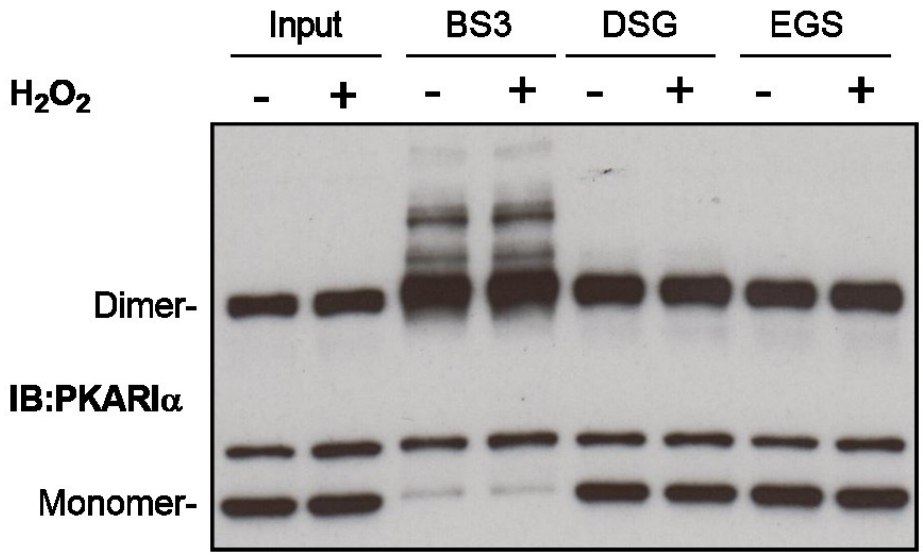

Figure 2.15. BS3 and not DSG or EGS effectively crosslinks PKARIα. Immunoblot of PKARIα from mouse hearts perfused with H_2O_2 (100 μM) for 5 minutes and the resultant homogenates crosslinked with bis-sulfosuccinimidyl-suberate (BS3), disuccinimidyl glutarate (DSG) or ethylene glycol bis-succinimidyl succinate (EGS) for 30 minutes. K-HB with Na-pyruvate.

Incubation of cardiac homogenates with 3 different crosslinking compounds showed that BS3 and not DSG or EGS successfully bound PKARIα to other proteins as evidenced by labelling above the dimeric weight of the protein (Figure 2.15). BS3 was therefore used in all succeeding crosslinking experiments. Hearts treated with H_2O_2 and subsequently crosslinked with BS3 were then probed for DRP1 and D-AKAP1. If H_2O_2 increased the association of either protein with PKARIα an increase in labelling of immunoblots for DRP1 or D-AKAP1 above their molecular weight would be anticipated in treated hearts and absent in controls.

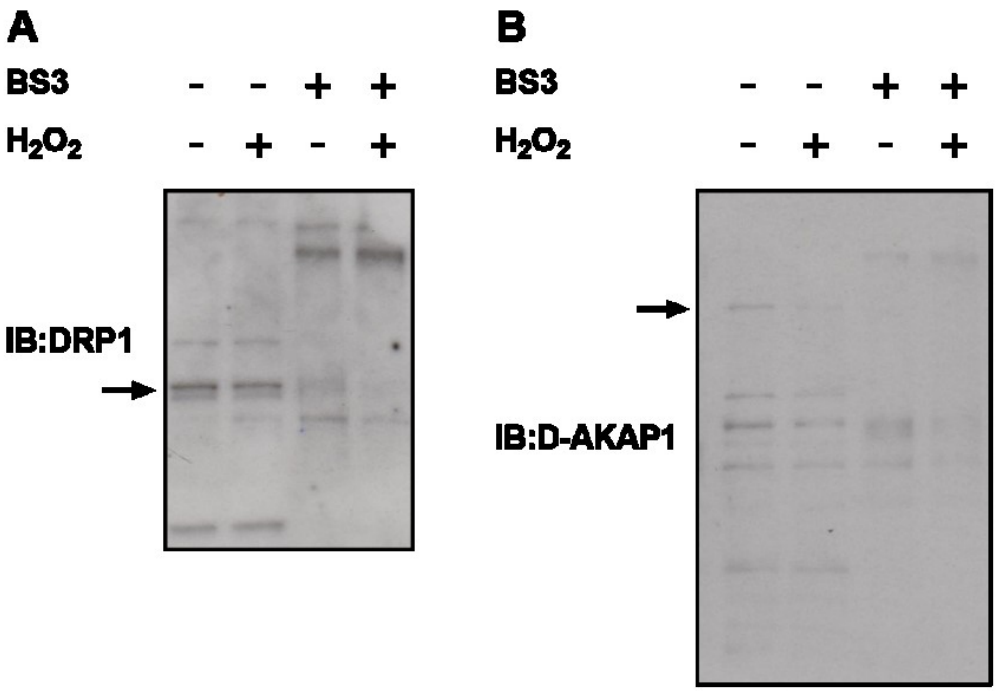

Figure 2.16. No difference in DRP1 or D-AKAP1 labelling in cross-linked homogenates from hearts perfused with H_2O_2. Mouse hearts were perfused with H_2O_2 (100 μM) for 5 minutes and the resultant homogenates cross-linked with BS3 in the presence of maleimide for 30 minutes. Left, immunoblot of DRP1. Right, immunoblot of D-AKAP1. K-HB with Na-pyruvate.

No difference in labelling of crosslinked samples from H_2O_2 perfused hearts were seen in immunoblots of DRP1 or D-AKAP1 (Figure 2.16), indicating that the treatment did not increase their association with other proteins. H_2O_2 may result in subtle changes in protein association not readily detectable by crosslinking alone. Therefore, to enrich the concentration of bound PKARIα after crosslinking we used cAMP affinity chromatography.

1.23 Affinity pull down using cAMP agarose

Purification of PKA using cAMP gels has previously been employed to co-capture the holoenzyme with both its AKAPs and associated substrates [156-159]. 2-(6-aminohexylamino)-adenosine- 3', 5'- cyclic monophosphate (2-AHA-cAMP), a commercially available conjugate of cAMP immobilised on agarose beads by a flexible aminohexylamino spacer arm at position 2' of the adenine ring (Biolog, A 054-06), was used to purify PKARIα. Hearts were homogenized in liquid nitrogen using a mortar and pestle and made to 10 % (w/v) homogenates in PBS lysis buffer. Homogenates were vortexed, an aliquot added to sample buffer and designated "Input". To reduce non-specific 2-AHA-cAMP beads were washed in PBS lysis buffer containing 0.5 % bovine serum albumin (BSA). Homogenates were then incubated with 10 % (v/v) 2-AHA-cAMP slurry and rotated at 4 °C for 2 hours. Homogenates were then centrifuged (1,500 g, 2 min), the flow-through added to an equal volume of SB and designated "unbound". Beads were washed 4 times with PBS lysis buffer and once prior to elution with triton-free PBS lysis buffer. Beads were eluted with SB and designated "capture". Equal protein concentrations were added to all lanes.

Several steps were first taken to optimize the capture of PKARIα. Firstly, 10mM cAMP or SDS-sample buffer was used to assess which solution more effectively eluted PKARIα from 2-AHA-cAMP (Figure 2.17A). Secondly, 500 µg or 1000 µg of homogenate was used to assess which concentration was necessary to effectively capture PKARIα (Figure 2.7B). Finally, homogenates were also incubated with varying concentrations of 2-AHA-cAMP to assess which concentration optimally captured PKARIα (Figure 2.7C).

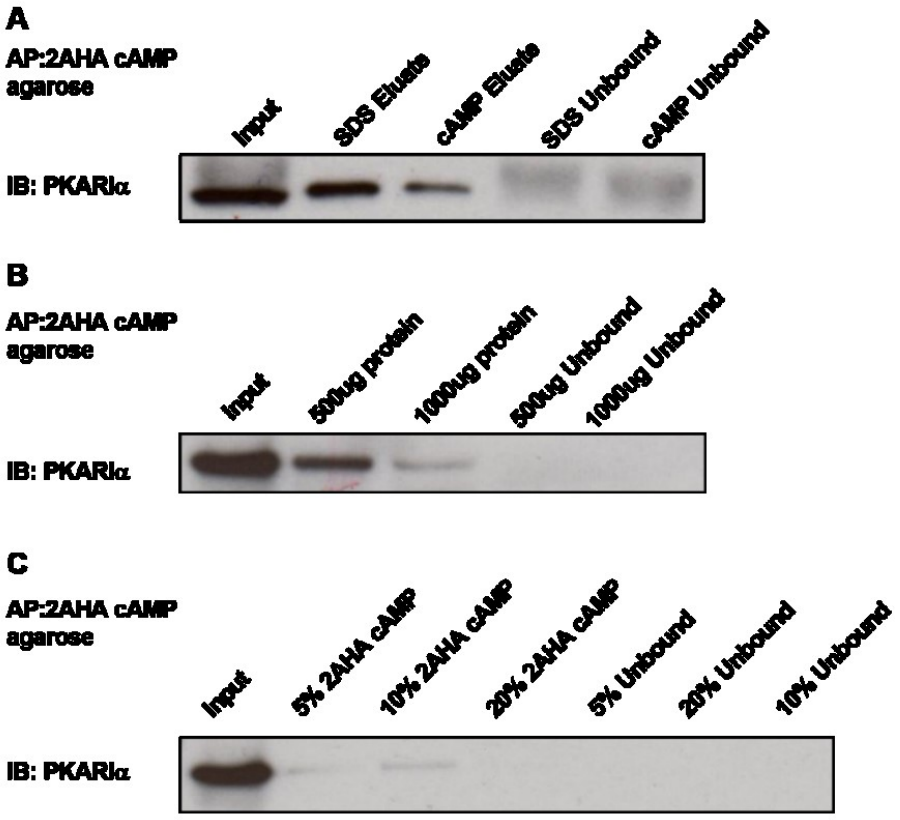

Figure 2.17. Development of 2-AHA-cAMP affinity purification of PKA in cardiac homogenates. Immunoblots of affinity purified PKARIα **(A)** Cardiac homogenates were incubated with 2-AHA-cAMP agarose and eluted with SDS sample buffer or cAMP (10 mM) **(B)** 0.5 and 1mg of cardiac homogenate was incubated with 2-AHA-cAMP **(C)** Cardiac homogenates were incubated in 5, 10 and 20% 2-AHA-cAMP. Protein concentration between Input, Capture and Unbound equal in all above experiments.

These experiments showed that SB was more effective at eluting PKARIα than a molar excess of cAMP (Figure 2.7A). Additionally, 500 μg of homogenate appeared sufficient to capture PKARIα (Figure 2.7B). Finally, incubation of samples with 10 % (v/v) 2-AHA-cAMP appeared to be the optimal concentration of ligand to bind the kinase (Figure 2.7C). These parameters were therefore used in subsequent experiments involving hearts perfused with H_2O_2.

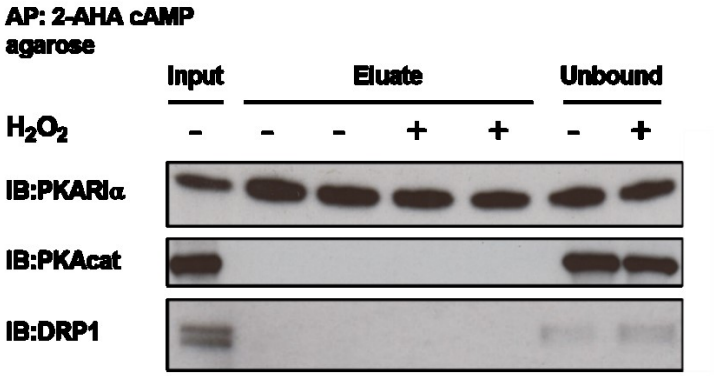

Figure 2.18. 2-AHA-cAMP effectively captures PKARIα but not PKA-cat or DRP1. Immunoblots of PKARIα, PKA-cat and DRP1 from PKA purified from hearts treated for 5 minutes with H_2O_2 using 2-AHA-cAMP agarose. Protein concentration equal between all lanes. K-HB with Na-pyruvate.

PKARIα was effectively captured using 2-AHA-cAMP but neither PKA-cat nor DRP1 were co-captured (Figure 2.18). This is expected as cAMP, although necessarily conjugated to agarose to purify the protein, also catalyses the release of the holoenyme's catalytic subunits. Though this reduces the probability of co-capturing PKA substrates, this potential pitfall was anticipated to be mitigated in succeeding experiments as the samples were first crosslinked stabilizing associations.

1.23.1 Affinity purification of crosslinked proteins

Finally, cardiac homogenates from hearts perfused with H_2O_2 were first crosslinked and then captured with 2-AHA-cAMP in order to first stabilize interactions and then enrich the capture. This showed that H_2O_2 reduced the amount of PKA captured (Figure 2.19). For experiments involving affinity pull down an aliquot of cross-linked homogenate prior to re-suspension in SB was used. Silver staining was completed using the PlusOne Silver Staining Kit (GE Healthcare Life Sciences) as per the manufacturer's guidelines.

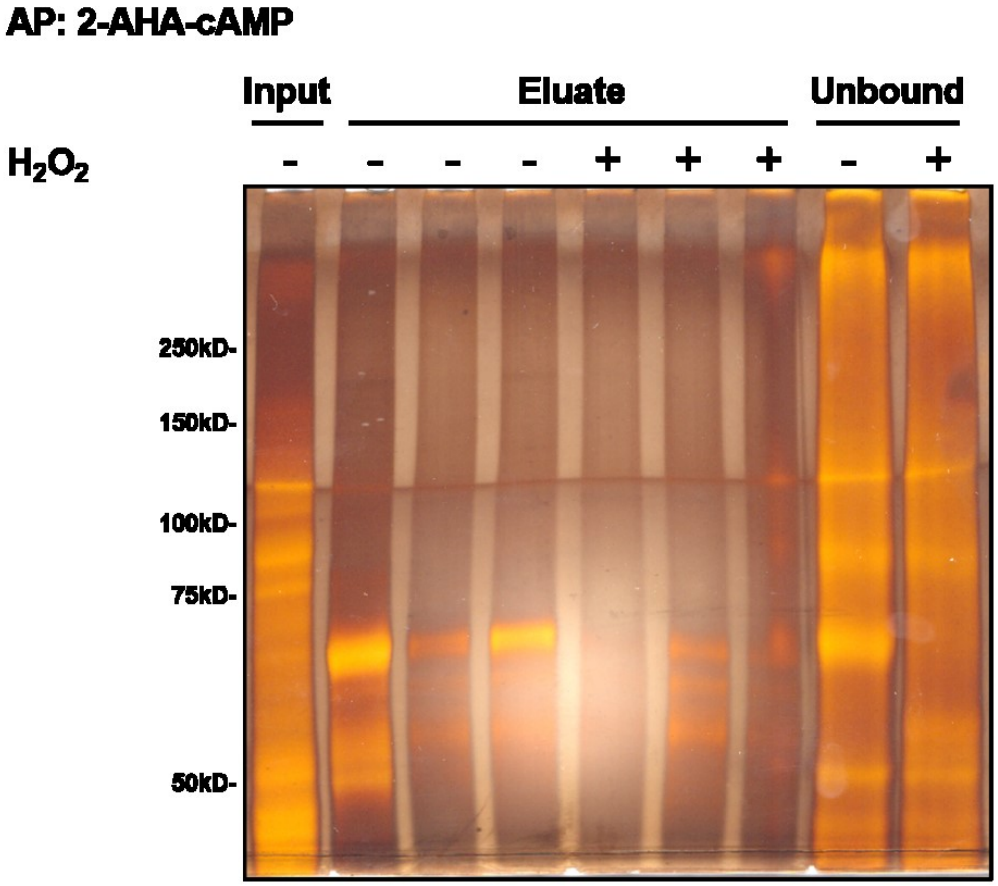

Figure 2.19. Cross-linking and subsequent affinity purification of PKA using 2-AHA-cAMP captures PKA in control but not H_2O_2 perfused hearts. Silver stain of tris-glycine gel loaded with H_2O_2 perfused heart homogenate cross-linked prior to 2-AHA-cAMP purification. All lanes loaded with equal concentrations of protein. K-HB with Na-pyruvate.

To assess if PKARIα interacted with DRP1 or D-AKAP1 and whether this was influenced by the presence of disulfide bonds between PKARIα subunits mouse hearts were perfused with H_2O_2 and subject to several methods routinely used to capture protein interactions. Despite the use of crosslinking compounds, cAMP-agarose and both in tandem no co-purification of PKARIα and DRP1 or D-AKAP1 was observed.

PKARIα was successfully crosslinked as evidenced by the formation of higher molecular weight complexes in the presence of BSE (Figure 2.15). If H_2O_2 influenced the interaction between PKARIα, DRP1 and D-AKAP1 greater labelling of these proteins should be observed in immunoblots. Although numerous attempts were made, no clear difference in labelling of these proteins were seen (Figure 2.16). As an alternative approach, immobilisation of PKARIα using cAMP-agarose was used. This approach has been employed numerous times in the

literature to successfully co-capture PKA with both its AKAPs and associated substrates [156-159]. Several attempts were first utilised to optimize PKARIα capture which included using different elutants and varying the concentration of homogenate and 2-AHA cAMP agarose (Figure 2.17). In each case PKARIα was successfully captured, however neither the catalytic subunit of PKA nor DRP1 were co-purified and no apparent impact of H_2O_2 on these potential interactions was seen (Figure 2.18). Nucleotide binding to PKA initiates the release of its catalytic subunits, therefore it is perhaps not surprising that PKA-cat and DRP1 were not co-purified. Probing of captured samples for D-AKAP1 were unfortunately unsuccessful. In a final attempt to identify a DRP1-PKARIα interaction homogenates from Langendorff H_2O_2 perfused hearts were first covalently cross linked and PKA then captured with cAMP agarose (Figure 2.19). This was anticipated to first stabilize PKARIα interactions and then enrich them, permitting their visual identification as bands on a silver stained Tris-glycine gel that could be subsequently cut out, digested and identified with mass spectrometry. Unfortunately, this protocol failed to capture any clear difference in banding pattern between H_2O_2 treated and untreated hearts and was therefore not further pursued (Figure 2.19). Finally, in later experiments the addition of Na-pyruvate was identified as potently attenuating H_2O_2 induced protein oxidation (detailed in section 4.6). As Na-pyruvate was included in the K-HB of all the above cross-linking experiments this factor likely contributed to the failure to identify changes in PKARIα association with DRP1 and D-AKAP1 in response to H_2O_2.

1.24 Reagents

Unless otherwise stated all reagents used in the following experiments were purchased from Sigma-Aldrich (St. Louis, MO). Buffer compositions are found in Appendix 2.

1.25 Statistics

Data are presented as mean ± standard error of the mean (SEM). Sample numbers are denoted by "n". Unpaired Student's *t*-test, one-way Analysis of Variance (one-way ANOVA) with Tukey *post hoc* test and repeated measures two-way ANOVA with multiple comparisons between groups were used where appropriate and are indicated in figure legends. Data were analysed using GraphPad Prism 6 (GraphPad Software, Inc). *P*-values <0.05 were considered significant.

Results

1.26 Fraction of cardiac homogenates

To assess compartment specific changes in the localisation of DRP1 to mitochondria it was necessary to separate soluble from insoluble proteins. This was achieved through centrifugation in the absence of detergent. Antibodies to the mitochondrial markers D-AKAP1 and the mitochondrial pyruvate carrier 2 (BRP44) were then used to determine if this provided efficient separation of mitochondria from soluble proteins.

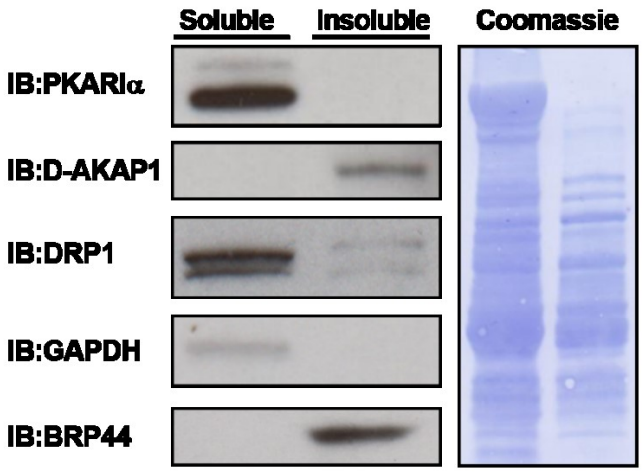

Figure 3.1. Centrifugation in the absence of detergent efficiently separates mitochondrial from soluble proteins. (Left) Immunoblot of PKARIα, DAKAP1, DRP1, GAPDH and BRP44 in samples centrifuged in the absence of detergent. D-AKAP1 and BRP44 show exclusive localisation to the insoluble fraction. GAPDH and PKARIα are entirely soluble while the majority of DRP1 is also soluble **(Right)** Coomassie stain of PVDF membrane showing distinct protein separation between soluble and insoluble fractions (n = 2). K-HB without Na-pyruvate.

Both D-AKAP1 and BRP44 show exclusive localisation to the insoluble pellet while DRP1, PKARIα and GAPDH are restricted to the soluble fraction of cardiac homogenates. This suggests fractionation in the absence of detergent is an efficient means of separating mitochondrial from soluble proteins. Therefore providing a rapid assay for the assessment of whether proteins of interest, namely PKARIα and DRP1, alter their localisation with mitochondria following interventions modulating cAMP and oxidant concentrations.

1.27 Langendorff perfusion of hearts with H_2O_2

Mouse hearts were Langendorff perfused with 100 µM H_2O_2 for 5 minutes. Centrifugation of heart homogenate in the absence of detergent yielded soluble and insoluble fractions. Immunobloting in the absence of reducing agent was used to assses alteration in disulfide PKARIα in response to H_2O_2

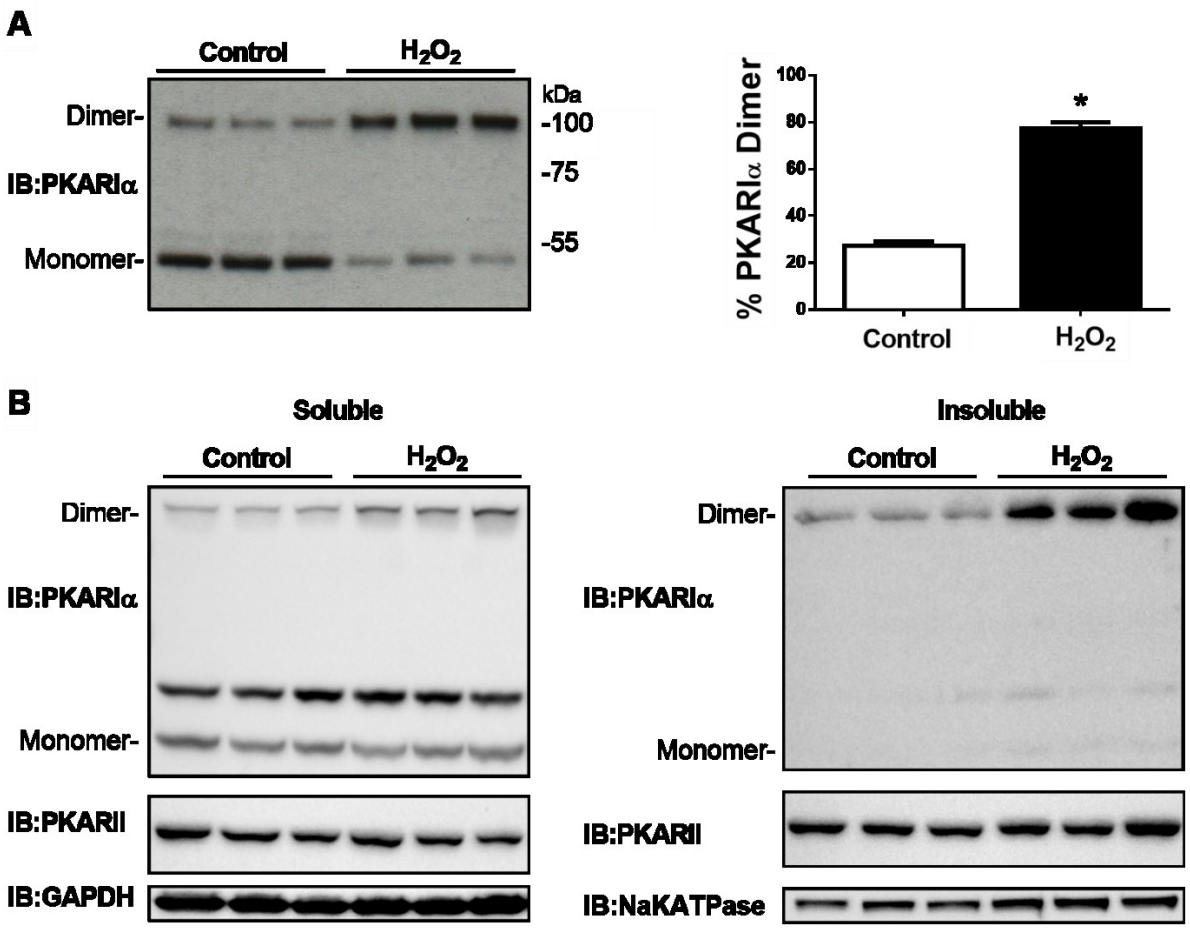

Figure 3.2. H_2O_2 induces a disulfide dimer of PKARIα which translocates to the insoluble fraction of cardiac homogenates while PKARII is unchanged. Mouse hearts were perfused for 5 minutes with 100 µM H_2O_2 and immediately snap frozen in liquid nitrogen. Cardiac homogenates were centrifuged (25,000 rcf, 5 min) in the absence of detergent generating soluble and insoluble fractions. **(A)** Immunoblot of PKARIα in non-reducing sample buffer from uncentrifuged homogenate **(B)** Immunoblot of soluble (left) and insoluble (right) PKARIα and PKARII, GAPDH and NaKATPase were used as loading controls for soluble and insoluble immunoblots respectively. Data analysed using students t-test (n=3±SEM, *$p<0.05$). K-HB without Na-pyruvate.

Perfusion with H_2O_2 increased the amount of disulfide PKARIα from 27 % to 77% ($p<0.05$) (Figure 3.2A). Disulfide, but not monomeric PKARIα, was significantly ($p<0.05$) increased in the insoluble fraction of hearts in response to H_2O_2 (Figure 3.2B). No change in localisation of PKARII was observed in response to H_2O_2 (Figure 3.2B).

1.28 24 hours starvation induced changes in cardiac PKARIα and DRP1

Starvation was used to trigger an increase in cAMP and ROS as well as induce mitochondrial recruitment of DRP1. Animal chow was removed from starved animals for 24 hours after which blood glucose was measured and the animals sacrificed.

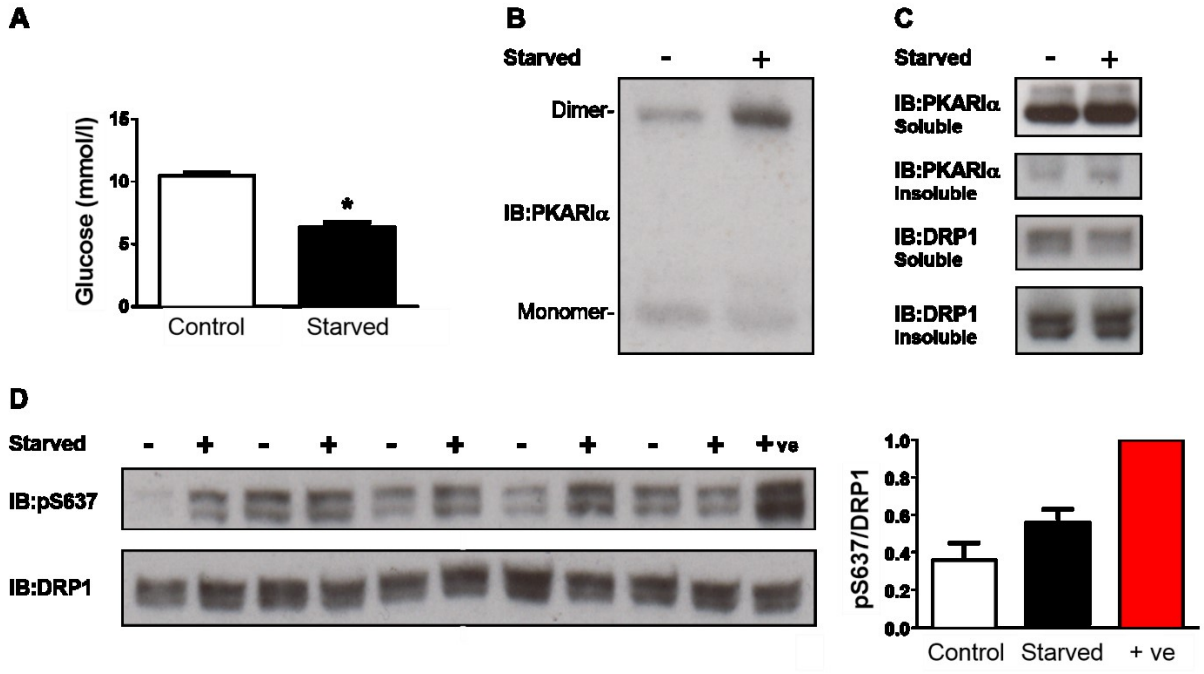

Figure 3.3. Starvation of mice for 24 hours results in PKARIα dimer formation but does not change kinase localisation or phosphorylation of DRP1 S637. Food was removed from cages at 9 am, 24 hours later blood glucose levels were measured and animals sacrificed. **(A)** Blood glucose levels following 24 hours starvation. **(B)** Immunoblot of PKARIα **(C)** Immunoblot of PKARIα and DRP in soluble and insoluble fractions of cardiac homogenates. **(D)** Left, immunoblot of DRP1 and S637 with an isoprenaline injected mouse used as positive control (+ve) for S637 phosphorylation. Right, densitometry quantification of S637/DRP1 (n=5, ±SEM,*$p<0.05$).

24 hour starvation reduced blood glucose levels by 42 % from 10.4 to 6.3 mmol/L ($p<0.05$) and led to a 12.7 % increase in percent disulfide PKARIα ($p<0.05$), (Figure 3.3A and 3.3B). No difference in pDRP1-S637 or PKARIα and DRP1 localisation was observed in response to

24 hours starvation (Figure 3.3C and 3.3D). Fat, muscle and liver samples were also excised from starved mice and immunoblotted. This revealed that fat and muscle samples showed highly variable disulfide PKRIα levels while those observed in liver were relatively stable (data not shown). For this reason liver tissue, as opposed to fat and muscle were also further examined.

1.28.1 24 hours starvation induced changes in liver PKARIα and DRP1

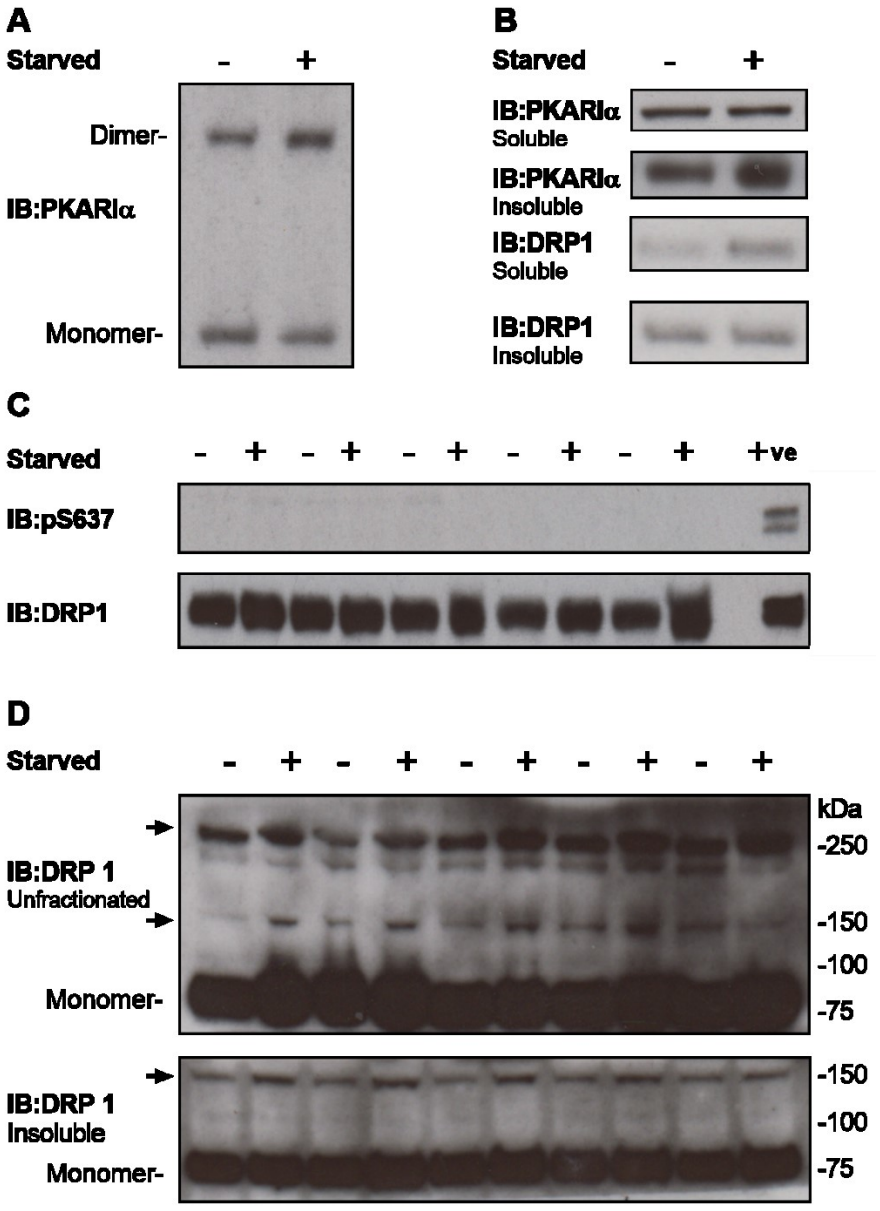

Figure 3.4. Starvation induced liver PKARIα dimerization and translocation, DRP1 forms higher molecular weight complexes and its soluble abundance is increased. (A) Immunoblot of PKARIα. **(B)** Immunoblot of PKARIα and DRP in soluble and insoluble fractions of liver homogenates. **(C)** Immunoblot of DRP1 and S637 with an isoprenaline injected mouse used as positive control (+ve) for S637 phosphorylation. **(D)** Immunoblot of DRP1 in unfractionated and soluble fractions at high exposure (n=5, ±SEM).

Starvation increased the percent disulfide PKARIα in the liver by 16 % ($p<0.05$) (Figure 3.4A). A significant ($p<0.05$) increase in insoluble PKARIα and soluble DRP1 was also observed following starvation (Figure 3.4B). No signal for pDRP1-S637 was seen in liver homogenates (Figure 3.4C) and there can be confidence in these results as the positive control sample also generated a robust pDRP1 signal at the anticipated weight of this protein. The samples were re-run several times and additional positive controls analysed, however no discernible signal at the correct weight could be observed and, therefore, assessment of pDRP1-S637 in liver samples was not pursued further. Long exposures of DRP1 immunoblots revealed higher molecular weight complexes in unfractionated and insoluble fractions after starvation (Figure 3.4D). As it is unclear at which time point changes in DRP1 modulation and ROS production in response to starvation are initiated a shorter duration of 12 hours starvation was also investigated.

1.28.2 12 hours starvation induced changes in PKARIα and DRP1

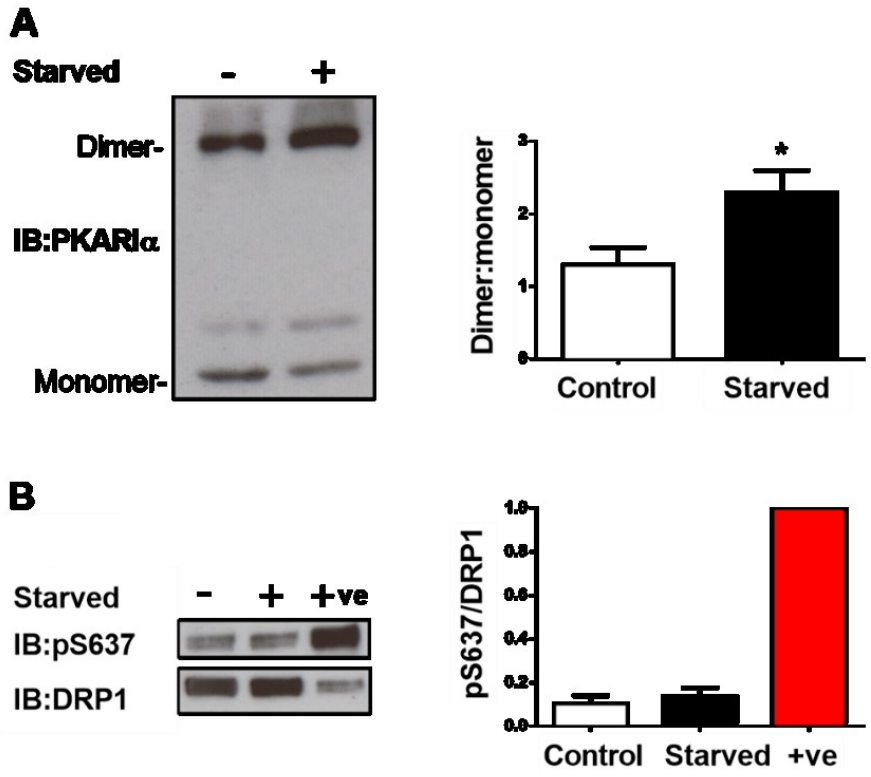

Figure 3.5. Starvation of mice for 12 hours results in PKARIα dimer formation but not change in DRP1-S637 phosphorylation in cardiac tissue. (A) Left, immunoblot of PKARIα. Right, densitometry quantification of disulfide to monomeric PKARIα ratio **(B)** Immunoblot of DRP and S637 with an isoprenaline injected mouse used as positive control (+ve) for S637 phosphorylation. Right, densitometry quantification of S637/DRP1. (n=5, ±SEM, *$p<0.05$).

12 hours starvation increased percent disulfide PKARIα in the heart by 19 % ($p<0.05$) (Figure 3.5A), but did not alter the levels of pDRP1-S637 (Figure 3.5B). Liver samples were not assessed due to failure in previous experiments to observe any pDRP1-S637 signal (Figure 3.4C).

1.29 24 hours starvation of PKARIα C17S KI mice

Starvation of mice for 24 hours increased disulfide PKARIα formation and its presence in the insoluble fraction of liver homogenates. Although the pDRP-S637 signal was not detected in liver samples, soluble DRP1 was seen to increase and higher molecular weight complexes form in response to starvation. Both of these traits are consistent with DRP1 phosphorylation by PKA. To assess whether these factors were modulated by disulfide PKARIα, 24 hour starvation experiments were repeated using the "redox dead" PKARIα C17S KI mouse.

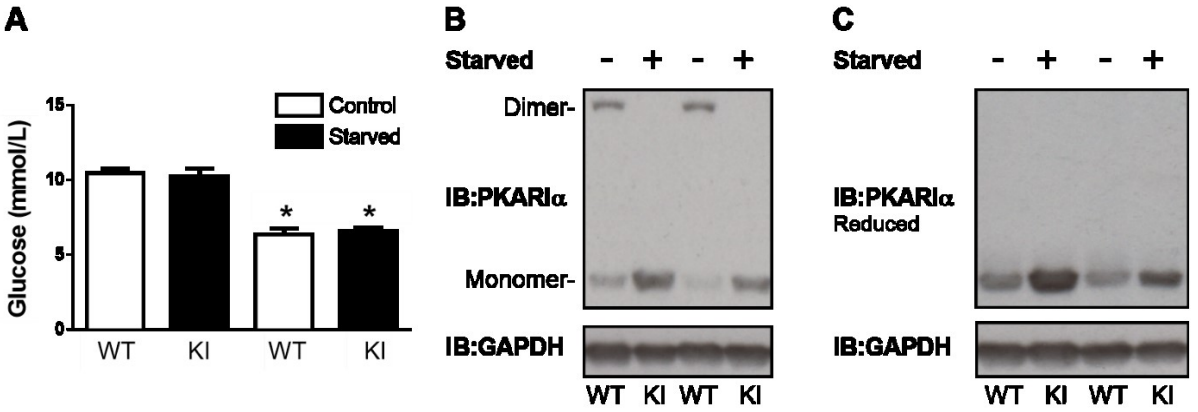

Figure 3.6. PKARIα C17S KI mice show no difference in blood glucose response to 24 hour starvation compared to WT littermates but show basally elevated PKARIα expression in hearts. Food was removed from cages at 9am, 24 hours later blood glucose levels were measured and animals sacrificed **(A)** Blood glucose measurements following starvation. **(B)** Immunoblot of PKARIα and GAPDH. **(C)** Immunoblot of reduced PKARIα and GAPDH. KI: PKARIα C17S, WT: wildtype (n=3, ±SEM, *$p<0.05$).

24 hours starvation reduced blood glucose levels by 39 % ($p<0.05$), with no difference in this glycaemic response between WT or KI mice (Figure 3.6A). The proportion of disulfide PKARIα increased from 43 % to 72 % ($p<0.05$) in WT animals in response to starvation, which was not observed in KIs (Figure 3.6B). Basal PKARIα expression was elevated 1.2 fold ($p<0.05$) in KIs compared to WTs (Figure 3.6C).

1.29.1 Starvation induced changes in DRP1 in PKARIα C17S KI mice

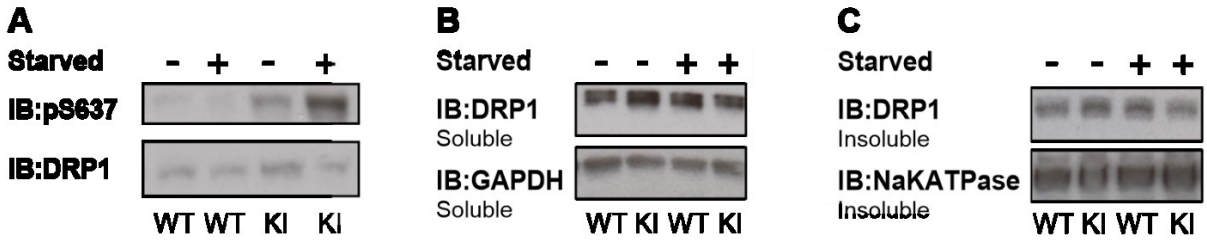

Figure 3.7. PKARIα C17S KI mice show higher levels of S637 phosphorylation after 24 hours starvation which does not change DRP1 localisation in hearts. Food was removed from mice for 24 hours after which they were sacrificed. **(A)** Immunoblot of DRP1 and S637. **(B)** Immunoblot of soluble DRP1 and GAPDH. **(C)** Immunoblot of insoluble DRP1 and NaKaATPase. KI: PKARIα C17S, WT: wildtype (n=3).

DRP1-S637 showed a trend toward increased basal phosphorylation in hearts from KI animals (Figure 3.7A). Following starvation DRP1-S637 phosphorylation was significantly increased in KIs but unchanged in WT animals ($p<0.05$) (Figure 3.7A). A trend toward elevated soluble DRP1 was seen basally in KIs and after starvation in both WT and KI animals (Figure 3.7B). No significant change in insoluble DRP1 was observed between either genotype in response to starvation (Figure 3.7C). To assess if changes in phosphorylation after starvation in KIs was DRP1 specific, total PKA substrate phosphorylation was also assessed.

1.29.2 "Total" PKA-substrate phosphorylation in PKARIα C17S KI mice

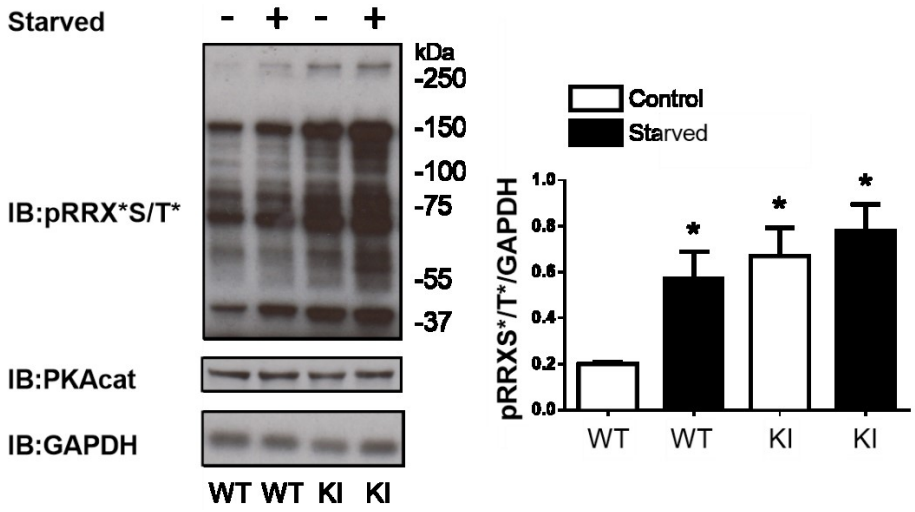

Figure 3.8. PKARIα C17S KI mice show higher levels of basal PKA substrate phosphorylation and no change in PKA catalytic subunit expression in heart. Food was removed from mice for 24 hours after which they were sacrificed. Left, immunoblot of PKA substrate phosphorylation (pRRXS*/T*), PKAcat and GAPDH in WT and KI animals before and after starvation. Right, densitometry quantification of PKA substrate phosphorylation. KI: PKARIα C17S, WT: wildtype (n=3, ±SEM, *p<0.05).

24 hours starvation induced a significant ($p<0.05$) increase in PKA substrate phosphorylation in WT but not KI mice, although the latter displayed significantly ($p<0.05$) elevated basal PKA-substrate phosphorylation (Figure 3.8). No change in PKA-cat expression was observed between genotypes (Figure 3.8).

1.29.3 Starvation induced changes in mitochondrial and autophagy associated proteins

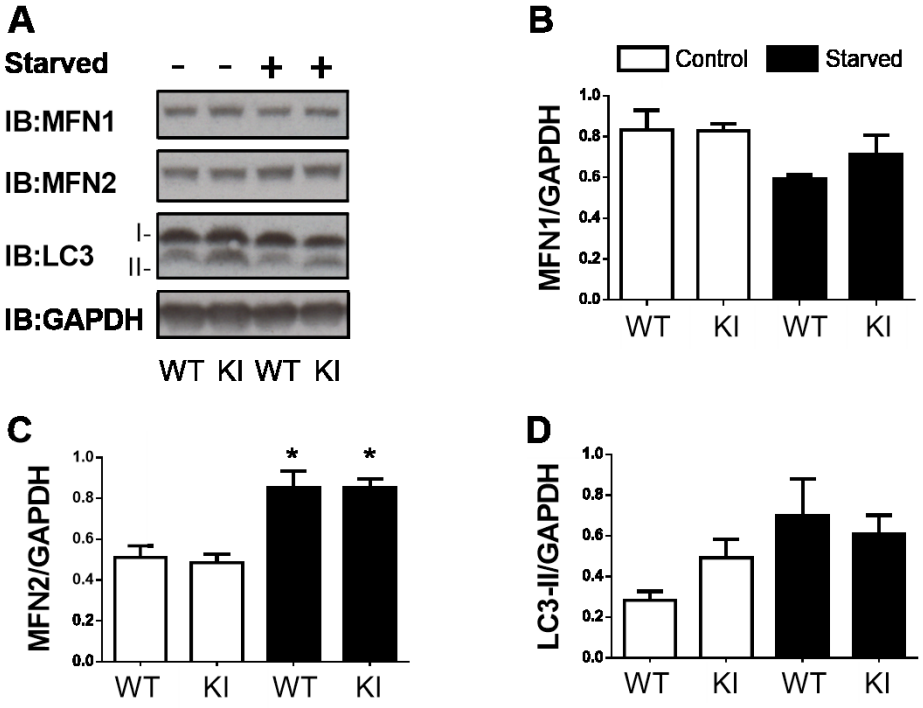

Figure 3.9. 24 hours starvation results in elevated levels of MFN 2 but not MFN1 and PKARIα C17S KI show high basal levels of LC3-II in hearts. Food was removed from mice for 24 hours after which they were sacrificed. **(A)** Immunoblots of MFN1, MFN2, LC3 showing LC3-I and LC3-II, and GAPDH. **(B)** Densitometry quantification of MFN1/GAPDH. **(C)** Densitometry quantification of MFN2/GAPDH. **(C)** Densitometry quantification of LC3-II/GAPDH. KI: PKARIα C17S, WT: wildtype (n=3, ±SEM, *p<0.05).

MFN2 but not MFN1 expression was significantly ($p<0.05$) increased in both genotypes in response to 24 hours starvation (Figure 3.9B and 3.9C). KI mice showed a trend toward basally increased LC3-II levels and no significant changes were observed following starvation (Figure 3.9D).

1.30 Initial concomitant perfusion with H_2O_2 and isoprenaline

The purpose of these experiments was to answer the following questions. 1) Is increased disulfide PKARIα associated with a concomitant increase in pPKA-substrate? 2) Do elevated levels of cAMP affect PKARIα disulfide formation? 3) What is the impact on pPKA-substrate phosphorylation when both disulfide PKARIα and cAMP are elevated in parallel?

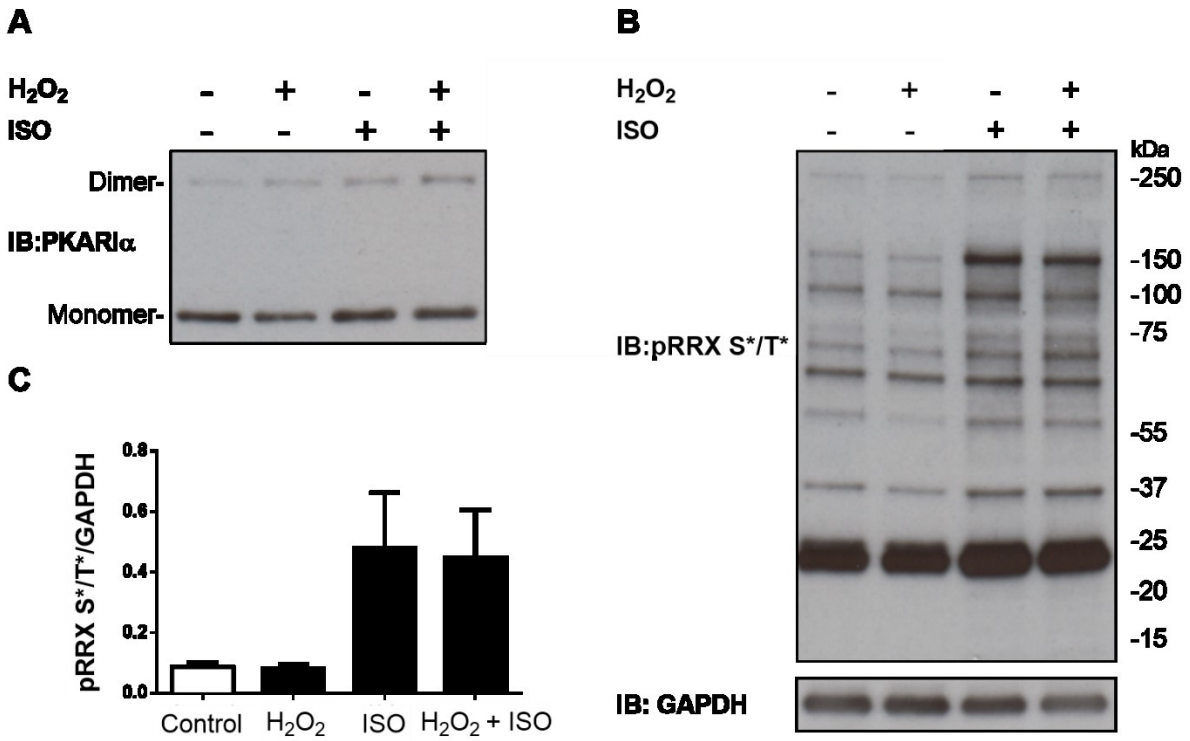

Figure 3.10. Perfusion of hearts with 100 µM H_2O_2 failed to induce disulfide PKARIα. Hearts were stabilized for 20 minutes prior to perfusion with 100 µM H_2O_2, 10 nM isoprenaline, or both agonists simultaneously for 5 minutes, control hearts were time matched and perfused exclusively with K-HB. **(A)** Immunoblot of PKARIα **(B)** Immunoblot of PKA substrate phosphorylation and GAPDH. **(C)** Densitometry of PKA substrate phosphorylation/GAPDH. Analysis, one-way ANOVA with Tukey post hoc test (n=5, ±SEM). K-HB with Na-pyruvate.

H_2O_2, isoprenaline or both these agents administered concomitantly had no impact on PKARIα disulfide formation (3.10A). Isoprenaline increased pPKA-substrate which was not affected by H_2O_2 (Figure 3.10C). Perfusion with H_2O_2 is routinely used to increase disulfide PKARIα therefore this result was unexpected and additional experiments were carried out to try and understand why oxidation of the kinase was not observed. To exclude contaminated H_2O_2 as the problem further experiments were independently undertaken using newly ordered, previously unopened H_2O_2, additionally studies with higher oxidant concentrations were performed. PKGIα was immunoblotted as it readily forms a disulfide dimer in the presence of H_2O_2 and could therefore serve as a positive control for protein oxidation [50].

1.30.1 Pefusion with unopened and increasing doses of H_2O_2

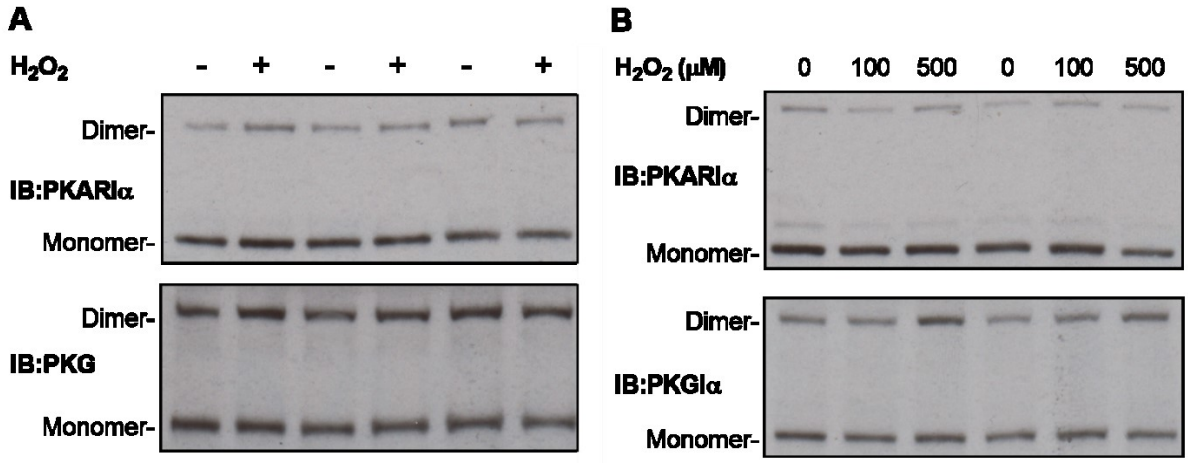

Figure 3.11. Perfusion of hearts with unopened or higher doses of H_2O_2 fail to induce PKARIα and PKGα disulfide dimerization. Hearts were stabilized for 20 minutes prior to perfusion with H_2O_2, control hearts were time matched and perfused exclusively with K-HB. **(A)** Immunoblot of PKARIα (top) and PKGIα (bottom) in hearts perfused with 100 μM H_2O_2 for 10 minutes, n=5 **(B)** Immunoblot of PKARIα (top) and PKGIα (bottom) in hearts perfused (10 min) with 100 μM and 500 μM H_2O_2 (n=2). K-HB with Na-pyruvate.

Perfusion of hearts with newly ordered, previously unused H_2O_2 failed to induce any change in PKARIα or PKGIα disulfide formation (Figure 3.11A) indicating that the results in Figure 3.10A were not a result of a technical issue with the PKARIα antibody or because of degraded H_2O_2. Perfusion of hearts with 500 μM H_2O_2 did not affect PKARIα but induced a significant increase in PKGIα disulfide formation (Figure 3.11B). However, typically 50 μM H_2O_2 is sufficient to induce disulfides in PKARIα or PKGIα indicating that other factors were mitigating the peroxide's effectiveness. Following discussions with laboratory members conducting related experiments, it was determined that Na-pyruvate was a constituent of the K-HB I was using, but was often not included. Although Na-pyruvate stabilizes contractile function (Figure 2.3), it may have been responsible for the attenuated oxidation PKARIα in these experiments. Therefore, the perfusion experiments were repeated, exposing the hearts to H_2O_2 in the absence or presence of Na-pyruvate to control for this variable.

1.30.2 Perfusion with H_2O_2 in the absence of Na-pyruvate

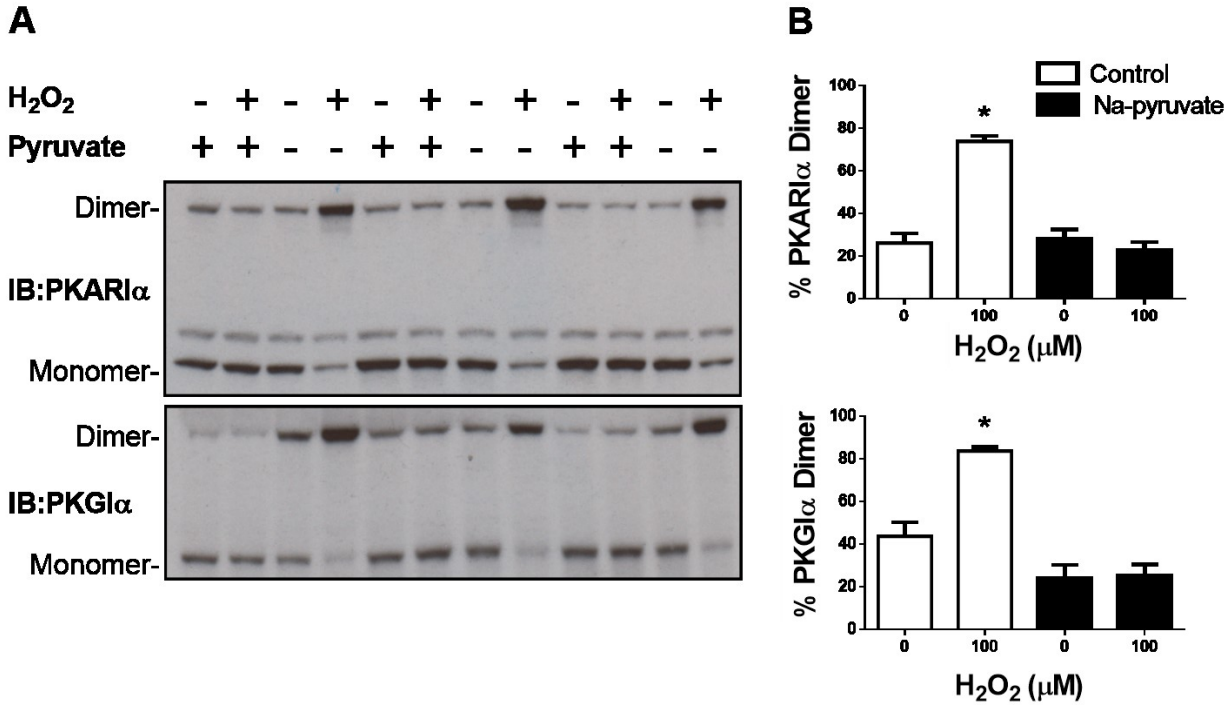

Figure 3.12. Na-pyruvate attenuates the oxidation of PKARIα and PKGIα by H_2O_2. Hearts were perfused using K-HB with or without 2 mM Na-pyruvate. Following a 20 minutes stabilisation period H_2O_2 (100 μM) was added to the buffer and hearts perfused for a further 5 minutes. Control hearts were time matched hearts perfused using K-HB with or without 2 mM Na-pyruvate. **(A)** Top, immunoblot of PKARIα. Bottom, immunoblot of PKGIα. **(B)** Top, densitometry quantification of PKARIα dimer expressed as a percent of total PKARIα. Bottom, densitometry quantification of PKGIα dimer expressed as a percent of total PKGIα. Analysis, one-way ANOVA with Tukey post hoc test (n=3, ±SEM, *$p<0.05$).

Removal of Na-pyruvate from the K-HB led to 1.8 fold and 0.9 fold increase ($p<0.05$) in percent disulfide PKARIα and PKGIα respectively in response to H_2O_2 (Figure 3.12). No change in either kinase was observed when hearts were perfused with H_2O_2 in the presence of Na-pyruvate.

1.30.3 Cardiac function in response to H_2O_2 in the presence and absence of Na-pyruvate

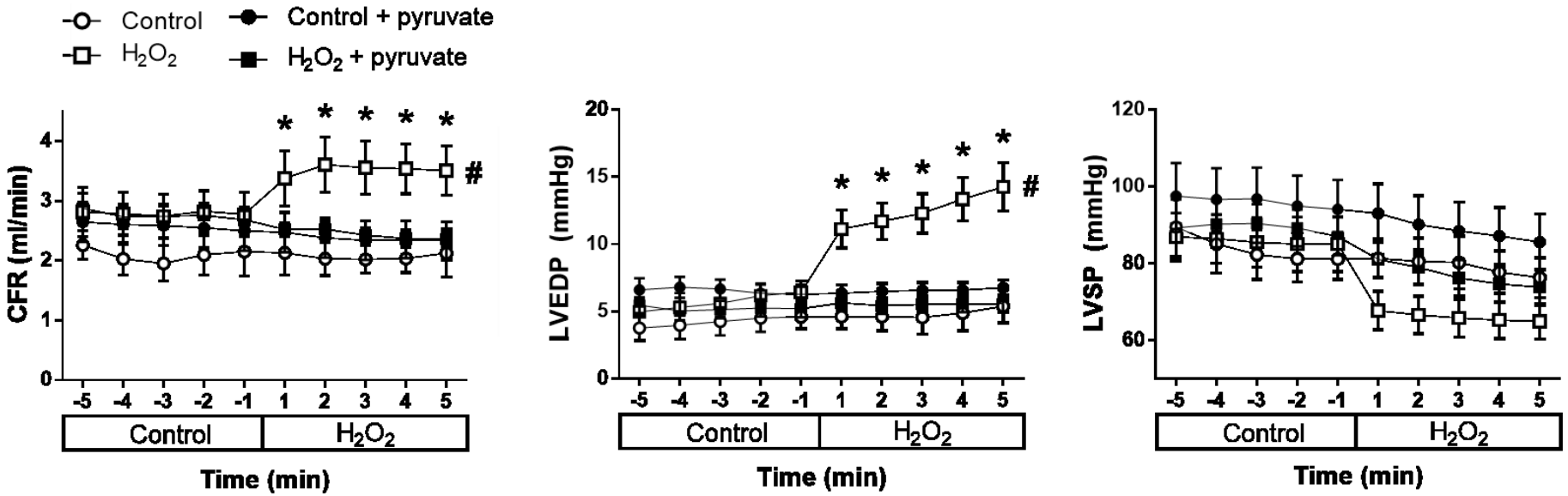

Figure 3.13. Na-pyruvate abolishes H_2O_2 induced changes in CFR and LVEDP. Hearts were perfused using K-HB with or without 2 mM Na-pyruvate. Following a 20 minutes stabilisation period H_2O_2 (100 µM) was added to the buffer and hearts perfused for a further 5 minutes. Control hearts were time matched hearts perfused using K-HB with or without 2 mM Na-pyruvate. **(Left)** Average coronary flow rate (CFR) values 5 minutes pre and post treatment. **(Middle)** Average left ventricular end diastolic pressure (LVEDP) values 5 minutes pre and post treatment. **(Right)** Average left ventricular systolic pressure values 5 minutes pre and post treatment. * $p<0.05$ difference from Control group (Repeated measures Two way ANOVA, multiple comparison between groups). # $p<0.05$ area under the curve (AUC) difference from Control group during 5 minutes post treatment (One way ANOVA, Tukey post hoc test). Control n=8, H_2O_2 n=12, Control + Na-pyruvate n=8, H_2O_2 + Na-pyruvate n=9, ±SEM.

As well as attenuating disulfide PKARIα formation, Na-pyruvate also attenuated H_2O_2 induced changes in cardiac performance (Figure 3.13). Perfusion of hearts with H_2O_2 increased CFR by 49% and LVEDP by 106 % at all time points post treatment ($p<0.05$) and showed a trend toward reducing LVSP by 29 %. These physiological alteration in response to H_2O_2 were entirely attenuated by the presence of Na-pyruvate in the K-HB.

1.31 Concomitant perfusion with H_2O_2 and isoprenaline in the absence of Na-pyruvate

Having found that Na-pyruvate efficiently blocks H_2O_2-induced PKARIα disulfide formation, it was not used in all subsequent experiments. Perfusion of mouse hearts with H_2O_2 alone or in combination with isoprenaline were then repeated in the absence of Na-pyruvate.

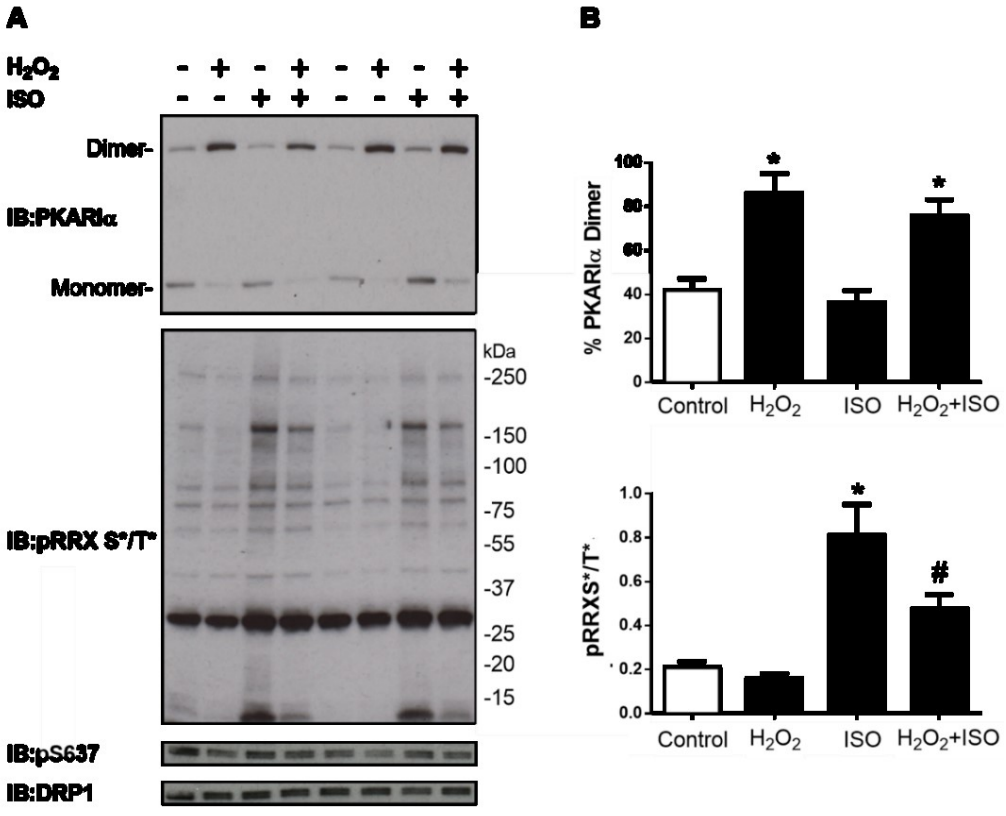

Figure 3.14. Concurrent perfusion with H_2O_2 and isoprenaline does not affect PKARIα dimerization or pDRP1-S637 but reduces PKA substrate phosphorylation. Following a 20 minute stabilisation period hearts were perfused with 100 µM H_2O_2, 10 nM isoprenaline, or both substances in tandem for 5 minutes. Control hearts were time-matched and perfused with K-HB throughout. **(A)** Immunoblot of PKARIα, PKA substrate phosphorylation (pRRXS*/T*), pS637 and DRP1. **(B)** Top, densitometry quantification of disulfide PKARIα expressed as a percent of total PKARIα. Bottom, densitometry quantification of PKA substrate phosphorylation. Analysis, one-way ANOVA with Tukey post hoc test, *$p<0.05$ difference from control, #$p<0.05$ difference from ISO (n=5, ±SEM). K-HB without Na-pyruvate.

Concurrent perfusion with isoprenaline and H_2O_2 or H_2O_2 alone produced a similar increase of approximately 90 % ($p<0.05$) in percent disulfide PKARIα compared to controls (Figure 3.14). Phosphorylation of PKA-substrate was unaltered by H_2O_2 and increased 2.9 fold ($p<0.05$) by isoprenaline (Figure 3.14). H_2O_2 abrogated isoprenaline induced PKA-substrate phosphorylation by 41 % ($p<0.05$). No changes in pDRP1-S637 were observed under any conditions.

1.31.1 Cardiac function in response to concomitant perfusion with H_2O_2 and isoprenaline

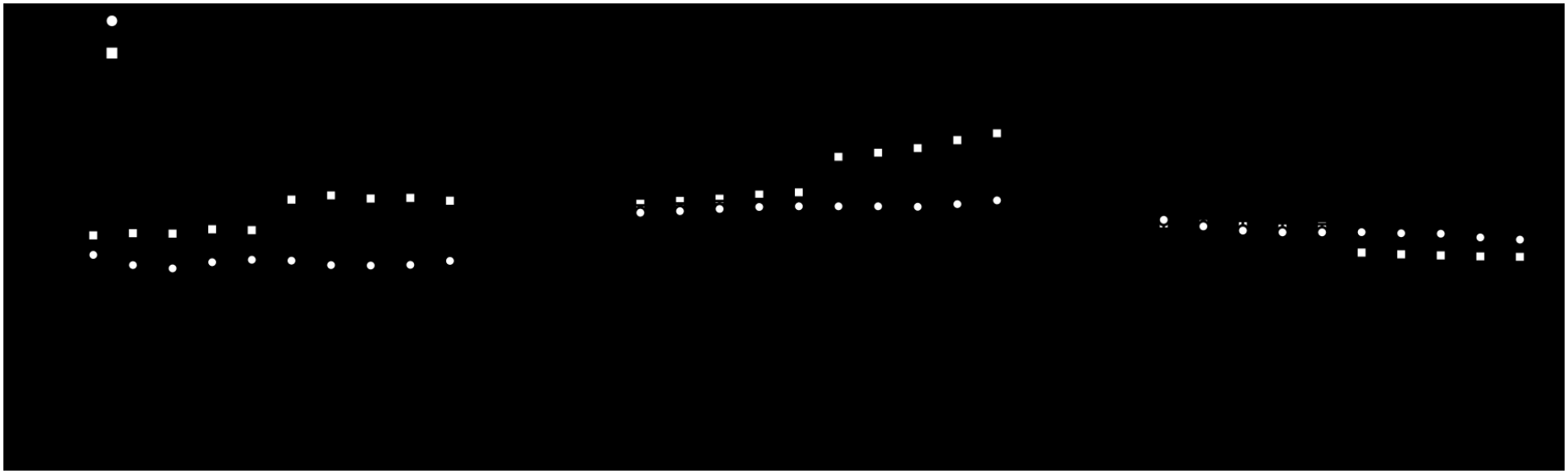

Figure 3.15. H_2O_2 attenuates isoprenaline induced changes in CFR, LVEDP and LVSP. Following a 20 minute stabilisation period hearts were perfused with 100 μM H_2O_2, 10 nM isoprenaline, or both substances in tandem for 5 minutes. Control hearts were time-matched and perfused with K-HB throughout. **(Left)** Average coronary flow rate (CFR) values 5 minutes pre and post treatment. **(Middle)** Average left ventricular end diastolic pressure (LVEDP) values 5 minutes pre and post treatment. **(Right)** Average left ventricular systolic pressure values 5 minutes pre and post treatment. * $p<0.05$ difference from Control group (Repeated measures Two way ANOVA, multiple comparison between groups). # $p<0.05$ area under the curve (AUC) difference from Control group during five minutes post treatment (One way ANOVA, Tukey post hoc test). Control n=8, H_2O_2 n=12, ISO=7, H_2O_2 + ISO n=6, ±SEM) K-HB without Na-pyruvate.

Administering isoprenaline for 5 minutes increased CFR by 144 % and LVSP by 74 % ($p<0.05$), both of which were attenuated by concurrent perfusion with H_2O_2 (Figure 3.15). LVEDP was significantly decreased by isoprenaline ($p<0.05$) and this was also attenuated by concurrent perfusion with H_2O_2. To assess whether disulfide PKARIα was responsible for the reduction in pPKA-substrate seen in response to concurrent perfusion with H_2O_2 and isoprenaline the above experiments were repeated with PKARIα C17S KI and WT littermate mice.

1.32 Perfusion of PKARIα C17S KI mice with H_2O_2 and isoprenaline

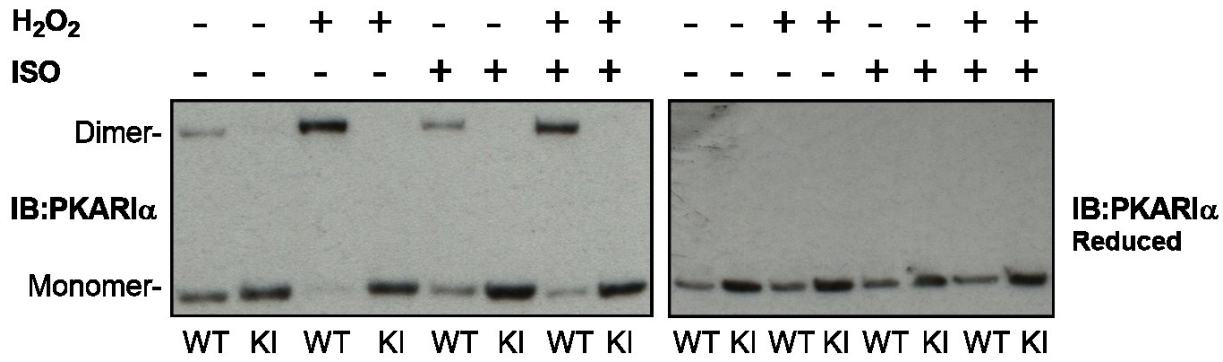

Figure 3.16. Perfusion of KI or WT mice with H_2O_2 and isoprenaline. Following a 20 minute stabilisation period hearts were perfused with 100 μM H_2O_2, 10 nM isoprenaline, or both substances in tandem for 5 minutes. Control hearts were time-matched and perfused with K-HB throughout. **(Left)** Immunoblot of PKARI α. **(Right)** Immunoblot of PKARIα run under reducing conditions. KI: PKARIα C17S, WT: wildtype (n=3). K-HB without Na-pyruvate.

H_2O_2 increased the percent disulfide PKARIα in WT hearts, and the concomitant presence of isoprenaline did not modulate this ($p<0.05$). Isoprenaline alone had no impact on disulfide formation in WTs. Hearts from KI mice showed no disulfide form of PKARIα, but did show an 88 % ($p<0.05$) increase in PKAIα expression.

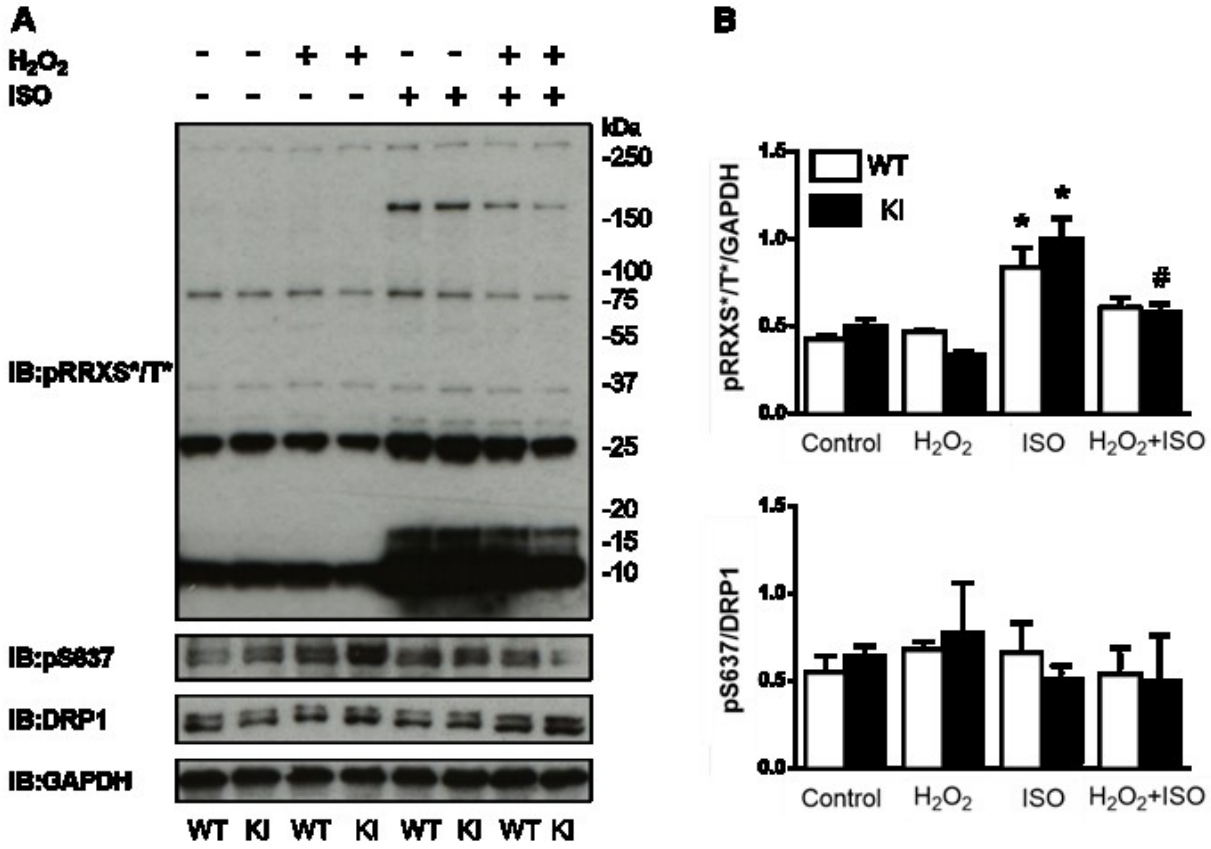

Figure 3.17. Disulfide PKARIα is not responsible for H_2O_2 induced reductions in isoprenaline sensitivity. Following a 20 minute stabilisation period hearts were perfused with 100 µM H_2O_2, 10 nM isoprenaline, or both substances in tandem for 5 minutes. Control hearts were time-matched and perfused with K-HB throughout. **(Left)** Immunoblot of PKA substrate phosphorylation, pS637, DRP1 and GAPDH. **(Right)** Top, densitometry quantification of PKA substrate phosphorylation normalised to GAPDH. Bottom, densitometry quantification of pS637 normalised to total DRP1. KI: PKARIα C17S, WT: wildtype. * $p<0.05$ difference from control. # $p<0.05$ difference from ISO. (n=3, ±SEM). K-HB without Na-pyruvate.

Neither WT nor KI animals showed significant alterations in pPKA-substrate in response to H_2O_2. In contrast, isoprenaline increased pPKA-substrate by 98 % and 101 % in hearts from WT and KI animals respectively ($p<0.05$). The presence of H_2O_2 attenuated isoprenaline-induced changes in pPKA-substrate to a similar extent in both WT and KI mice. No difference in pDRP1-S637 was observed between WT and KI animals or between condition.

Discussion

1.33 Brief summary of results

The aim of this thesis was to investigate factors influencing disulfide PKARIα formation and the impact of this oxidation event on the phosphorylation of substrates of this kinase. PKARIα formed a disulfide-dimer during perfusions with H_2O_2, which was associated with its translocation to the insoluble fraction of cardiac homogenates. 12 or 24 hours starvation of mice increased disulfide PKARIα formation, translocation and PKA-substrate phosphorylation, as detected by a pan-specific 'total' PKA substrate antibody, but not specific phosphorylation of DRP1-S637. To assess the potential role of disulfide PKARIα in mediating these changes PKARIα-C17S KI and WT mice were also starved for 24 hours. Unexpectedly, in heart and liver tissue PKARIα-C17S KI mice showed a basal elevation in PKA-substrate phosphorylation and increased PKARIα expression, as well as an increase in DRP1-S637 phosphorylation following starvation. Langendorff perfusion experiments showed that Na-pyruvate blocked oxidation events associated with H_2O_2. Biochemically, this was evidenced by Na-pyruvates attenuation of H_2O_2 induced cysteine oxidation and physiologically as an attenuation of H_2O_2 mediated changes in LVEDP and CFR. Disulfide PKARIα formation in response to H_2O_2 was not impacted by elevating cardiac cAMP with the β-adrenergic agonist isoprenaline. However, H_2O_2 did attenuate isoprenaline-induced elevations in PKA-substrate phosphorylation, which physiologically was reflected by a blunted CFR, LVEDP and LVSP responsiveness to isoprenaline. To assess whether these changes were dependent on disulfide PKARIα the above experiments were repeated using PKARIα-C17S KI and WT mice. Both PKARIα-C17S KI and WT mice displayed a similar reduction in PKA-substrate phosphorylation during concomitant perfusions with H_2O_2 and isoprenaline. This indicates that reduced isoprenaline sensitivity in the presence of H_2O_2 is not dependent on disulfide PKARIα. Taken together, the above findings indicate that PKARIα activity is modulated by both its oxidation to a disulfide dimer or through cAMP binding. However, the interplay between these two factors may be more complex than anticipated as evidenced by a failure of cellular models to translate to ex vivo and in vivo scenarios.

1.34 Subcellular localization of DRP1, PKARIα and D-AKAP1

Fractionation by centrifugation in the absence of detergent showed PKARIα and GAPDH to be exclusively soluble, DRP1 to be almost entirely soluble, and as expected while D-AKAP1 and BRP44 (both mitochondrial markers) were insoluble (Figure 3.1). The presence of D-AKAP1 and BRP44 in the insoluble but not soluble fraction suggests centrifugation successfully separated mitochondrial from soluble proteins and thus could be used as a rapid assay to study changes in the protein mitochondrial localisation. Basally a high level of interaction between PKARIα and DRP1 via D-AKAP1 appears unlikely as neither the kinase nor GTPase strongly co-fractionate with the scaffold protein. However, as shown in Figure 3.2B in the presence of H_2O_2 PKARIα forms a disulfide dimer which is recruited to the same fraction as D-AKAP1. Interestingly, DRP1 is recruited to mitochondrial fractions under various conditions including: hypoxia; ischaemic injury; Ca^{2+} overload; hyperglycemia and starvation [65, 67, 68, 93]. Although the recruitment of DRP1 to the mitochondria has repeatedly been shown using fluorescently labelled proteins [56, 65, 67, 68, 93], the exact mechanisms mediating this remain unclear. A number of DRP1 post-translational modifications have been identified, as summarised in Figure 1.7. For example, phosphorylation of DRP1-S616 by CDK1 positively regulates DRP1 association with mitochondria and is important during mitotic cell division [63]. Calcineurin-mediated dephosphorylation of DRP1-S637 induced by elevated cytosolic Ca^{2+}, following mitochondrial depolarization using the mitochondrial uncouplers FCCP and arachidonic acid, is similarly seen to drive DRP1 translocation to mitochondria [65]. In line with this, *Slupe et al.* identified a DRP1 calcineurin docking motif which promotes mitochondrial remodelling and ischaemic neuronal injury [66]. DRP1-S637 phosphorylation by PKA is seen to inhibit DRP1 fission activity by decreasing the interaction of its GED domain with its GTP-binding and middle domains this slowing GTP hydrolysis [55]. While sumolyation, and ubiquitination promote its fission of mitochondria [53, 60]. It is due to this wide array of conditions that modulate DRP1 that a number of experimental approaches were initially studied, as detailed in the Materials and Methods section of Chapter 2.

1.35 H_2O_2 induces disulfide dimer formation and translocation of PKARIα

Perfusion of Langendorff perfused hearts with H_2O_2 increased the percentage disulfide PKARIα from 27% to 77 % (Figure 3.2A). These findings are in line with previous experiments showing that PKARIα forms a disulfide dimer in response to oxidants such as H_2O_2 or the nitric oxide donor nitrocysteine [32, 137]. It was previously established that Cys17 and Cys38 are responsible for the pair of interprotein disulfides that can form between the PKARIα regulatory subunits. Conformationally, the two RIα subunits lie antiparallel to one another on the D/D interface of the holoenzyme directly flanking its interaction with the a-helix of AKAPs (Figure 1.4). As previously explained in section 1,7 systematic mutation of these residues to alanine reduce the kinase's affinity for D-AKAP2 [38]. This suggests that oxidation of Cys17 and 38 is a critical mechanism for targeting PKARIα to its scaffold proteins. Adding further credence to this model are structural comparisons of membrane and cytosolic PKARIα. Using electrospray ionization mass spectrometry, *Boeshans et al.* reported a higher extent of disulfide formation in membrane versus cytosolic localised PKARIα [160]. As PKARIα is primarily soluble (Figure 3.1) alteration in its affinity for scaffold AKAP proteins is likely an important modification to target its activity. Oxidation of PKARIα to a disulfide dimer led to aggregation of the disulfide bound form of the kinase in the insoluble fraction of mouse hearts (Figure 3.2B). Based on the aforementioned studies, it is probable that this re-localisation is mediated through a disulfide-induced increase in the affinity of PKARIα for its membrane bound scaffold AKAPs [32]. It was hypothesized that increased association between PKARIα and D-AKAPs should facilitate substrate-induced dissociation of the tetramer to enhance phosphorylation. Indeed, *Brennan et al.* reported that H_2O_2 induced-disulfide PKARIα was also increased in membrane fractions and associated with PKA substrate phosphorylation [32]. Alterations in substrate phosphorylation following disulfide PKARIα formation are explored in further detail below in section 4.4. PKARII localisation was unchanged during H_2O_2 perfusions further clarifying that oxidation induced re-localisation is a specific trait of PKARIα (Figure 3.2B). This observation is also consistent with the view that the PKARII is primarily membrane bound under basal conditions through its association with AKAPs [161].

1.36 In vivo regulation of disulfide PKARIα

In vivo starvation of mice was chosen to instigate a possible PKARIα-DRP1 interaction via D-AKAP1 as these conditions have previously been shown to result in increased PKA-dependent DRP1-S637 phosphorylation [57]. As described in section 1.13, starvation has also been shown to result in the production of both oxidants and cAMP, factors which based on our hypothesised model of PKARIα activation are expected to result in maximal phosphorylation of DRP1-S637 [57, 108, 162-164]. It was hypothesized that nutrient deprivation for 12 or 24 hours would instigate mitochondrial electron transport chain leak as a result of increased ATP demand therefore causing ROS levels to rise. The redox sensitive regulatory subunits of PKARIα would then perhaps become oxidised to form a disulfide dimer, increasing its affinity for D-AKAP1. On binding to D-AKAP1, PKARIα would then be sensitized to cAMP which as a result of GPCR agonism induced by starvation would also be elevated. Both elevated ROS and cAMP levels would therefore together induce the full dissociation of PKARIα leading to the prevention of mitochondrial fission through DRP1-S637 phosphorylation. The specific role of disulfide dimerized PKARIα in mediating these changes would then potentially be confirmed using PKARIα C17S KI mice. The principal approach taken was to withhold food from mice for 12 or 24 hour periods. A starved metabolic state was confirmed by blood glucose measurements immediately after the duration of starvation and changes in the oxidative, phosphorylation and subcellular localisation of PKARIα and DRP1 were assessed by immunoblotting.

1.36.1 Starvation induces PKARIα disulfide formation

These experiments confirmed that removal of food for 24 hours induced a starved state as evidenced by a significant reduction in blood glucose levels (Figure 3.3A). As described above, a central tenet to the hypothesis was that starvation would elevate both intracellular ROS and cAMP levels. Here it is shown that starvation precipitates a robust increase in the production of oxidants as evidenced by the oxidation of PKARIα to a disulfide dimer in heart (Figure 3.3B and 3.4A) and liver (Figure 3.5A) following 12 and 24 hour periods of starvation. Similarly, the observed elevation of "total" PKA-substrate phosphorylation during starvation is strongly indicative of increased cAMP production (Figure 3.8). Though ROS are generated by NOX,

xanthine oxidase and NOS, during starvation their source has been principally attributed to mitochondrial electron chain leakage [105]. As such DCF-DA staining, a purported H_2O_2 sensitive fluorescent probe, exhibits co-localisation with mitochondria during nutrient deprivation. Similarly, mitochondrial targeted SOD2 over expression is also seen to reduce total O_2^- levels during starvation [111]. Hence, two hypotheses are proposed for mitochondrial, as opposed to NOX production of ROS during starvation. The first posits that during starvation the energetic demand of the cell increases against a deficit in available substrate which mitochondria attempt to compensate for by increasing ATP production leading to electron leak [105]. The second proposes that a currently unknown factor may transduce upstream nutrient deprivation signals to mitochondria [105]. These results provided justification for the selection of starvation as a scenario in which ROS production were elevated and show for the first time that during this physiologically-relevant intervention PKARIα becomes oxidised.

1.36.2 Starvation induced PKARIα translocation

Following from this it was anticipated that starvation induced-disulfide PKARIα would exhibit increased affinity for its scaffold AKAPs, in particular D-AKAP1. Indeed, 24 hours starvation elevated the percent of liver disulfide PKARIα which was associated with its increased co-fractionation with D-AKAP1 (Figure 3.4). This is in line with previous results showing that perfusion of hearts with H_2O_2 led to translocation of disulfide PKARIα and shows translation of our model from an *ex vivo* to *in vivo* physiological context (Figure 3.2B). Though, PKARIα translocation was observed in liver homogenates, no change in the localisation of the kinase was observed in heart tissue following 24 hours starvation (Figure 3.3C). Two reasons may account for this. Firstly, although PKARIα was significantly oxidised in heart and liver the latter exhibited a larger total percent of disulfide PKARIα after starvation, therefore increasing the probability of observing its translocation relative to the former. Secondly, failure to observe PKARIα translocation in cardiac tissue may be a reflection of starvation inducing a more subtle increase in ROS than H_2O_2 perfusions. During Langendorff experiments PKARIα disulfide formation approaches maximal levels as replenished H_2O_2 is continuously circulated through the myocardium. Under physiological conditions, such as in starvation, it is likely that enzymatic (SOD, catalase and gluthathione peroxidase) and non-enzymatic (ascorbic acid, thioredoxin and flavonoids) scavenging systems are more capable of buffering endogenous

intracellular oxidant production. These scavenging systems may therefore be recycling disulfide PKARIα back to its reduced state, decreasing its location in the insoluble fraction and so limiting the likelihood of observing its translocation.

1.36.3 Starvation induced changes in the phosphorylation of PKA substrates

Based on my hypothesised model of activation, the factors considered above should result in the dissociation of PKARIα inducing phosphorylation of its substrates, in particular DRP1-S637. Indeed, "total" PKA-substrate phosphorylation was elevated following 24 hour starvation (Figure 3.8). In addition a trend toward elevated DRP1-S637 phosphorylation in cardiac tissue was observed after 24 hours starvation (Figure 3.3D) but unchanged after 12 hours (Figure 3.5B). On immunoblots from liver samples no DRP1-S637 phosphorylation signal was observed despite a positive control (cardiac homogenate from a mouse intraperitoneally injected with isoprenaline), indicating that the antibody worked appropriately (Figure 3.4C). A number of additional studies analysing liver samples from isoprenaline-injected mice as positive controls showed no phosphorylation signal for DRP1-S637 at its correct molecular weight therefore a valid assessment of the phospho-status of DRP1 in liver could not be made. S637 phosphorylation inhibits GTP hydrolysis, trapping DRP1 at the OMM which consequently self assembles into large oligomeric complexes incompatible with mitochondrial fission [64, 67]. In other words DRP1-S637 phosphorylation increases the localisation of DRP1 at the mitochondria in the form of oligomeric complexes. Therefore, the anticipated result of DRP-S637 phosphorylation was the increased presence of DRP1 oligomeric complexes in insoluble fractions after starvation. In line with this, high molecular weight complexes were observed on immunoblots of liver DRP1 after starvation which were also confirmed to be present in insoluble fractions (Figure 3.4D). DRP1 oligomerization is an essential precursor to fission and well described in the literature [165, 166]. OMM DRP1 self-assembles into oligomers by forming cross bridges between adjacent middle and GED domains [165]. Upon encirclement of the mitochondria DRP1 oligomers then constricts in a GTPase-dependent manner severing the organelle [166, 167]. Although this observation fits well with the described effects of PKA mediated DRP1-S637 phosphorylation, namely the accumulation of OMM DRP1, failure to identify a specific phosphor-DRP1 signal precluded a possible causative association [64]. A schematic of these findings is presented below.

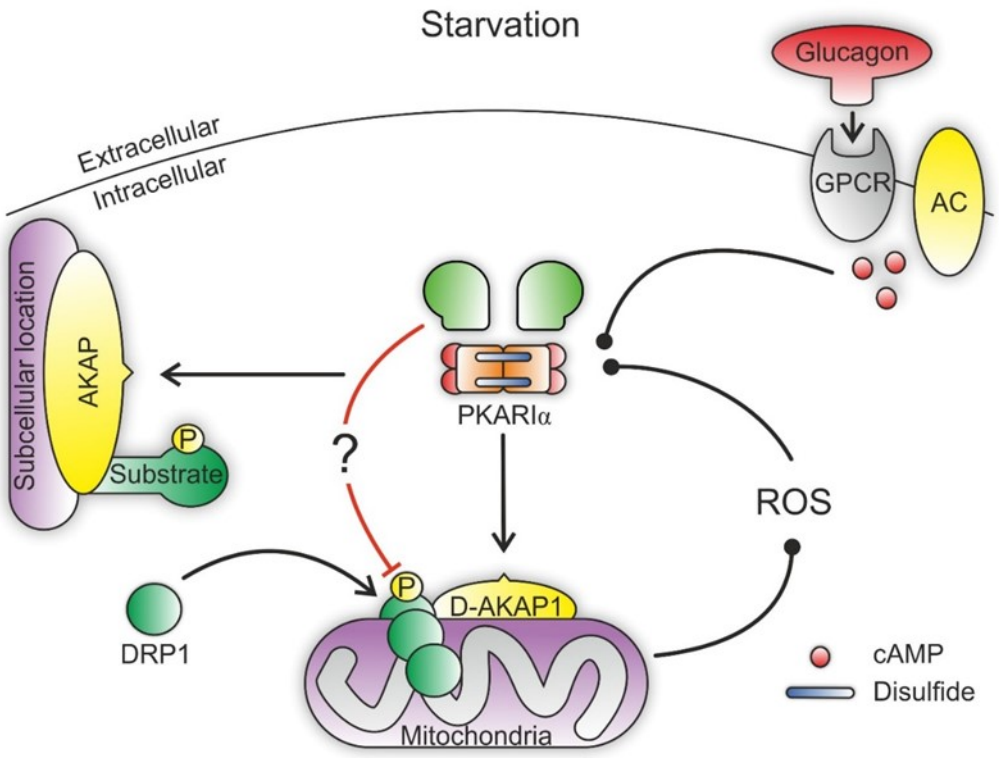

Figure 4.1. PKARIα modulation during starvation. During starvation glucagon is released to maintain blood glucose levels. Binding of glucagon to g-protein coupled receptors (GPCR) triggers an increase in intracellular cAMP via adenylate cyclase (AC). Mitochondrial metabolism is increased to compensate for the energetic deficit induced by starvation leading to electron transport chain leak and ROS production. PKARIα becomes oxidized to its disulfide form increasing its affinity for D-AKAP1 at the mitochondria and other AKAPs which sensitize the kinase to cAMP. PKARIα then fully dissociates to phosphorylate its substrates however, whether disulfide PKARIα is involved in the phosphorylation of DRP1 remains unclear.

Additionally, in liver starvation also increased soluble DRP1 levels. This observation, though in contrast to the previous point, is also consistent with some reports of DRP1-S637 phosphorylation. *Cereghetti et al.* showed that the uncoupling agents FCCP and arachidonic acid dephosphorylated DRP1-S637 leading to its mitochondrial accumulation which was attenuated by a phosphomimetic DRP1-S637D mutation [65]. Phosphomimetic mutations in the assessment of DRP1 function are however problematic as they operate under the presumption that phospho-regulation of DRP1 is a single step process. This therefore neglects the possibility that it may arrest DRP1 function at a premature stage of its recruitment potentially confounding experimental interpretations. However, *ex vivo* and *in vivo* models of cardiac dysfunction (I/R and KCL-induced cardiac arrest, respectively) have shown that DRP1-S637 dephosphorylation is associated with increased mitochondrial DRP1 [68, 69]. To

summarize, in liver 24 hours starvation increased disulfide and insoluble PKARIα. Concurrently, DRP1 was increased in soluble fractions and higher molecular weight complexes were observed on DRP1 immunoblots. Taken together, the above factors are compelling evidence for a role of disulfide-PKARIα in mediating these events.

1.36.4 Starvation induced changes in liver DRP1-S637

Unfortunately, failure to observe a DRP1-S637 phosphorylation signal on immunoblots from liver samples precluded drawing any causative associations. If PKARIα was phosphorylating liver DRP1-S637 the anticipated effect of this would be inhibition of DRP1 fission activity resulting in elongated mitochondria. Indeed, liver electron micrographs from mice starved for 12 hours do exhibit elongated mitochondria [57]. Although the authors provide extensive evidence to suggest this is mediated by PKA-dependent inhibitory phosphorylation of DRP1-S637 this was not directly shown in liver tissue [57]. In contrast to liver, no change in DRP1 localisation was observed in heart samples after 12 or 24 hours starvation. This discrepancy between tissues may be explained by distinct differences between cardiac and hepatic mitochondria. For example, mitochondria in liver have an approximate 8 fold higher rate of proteolytic activity than those from cardiomyocytes [168]. In other words mitochondrial networks, which critically depend on DRP1 for their modulation, are more dynamic in liver than in heart. This difference in activity may account for the current discrepancies observed between liver and heart samples.

Though a number of promising results in liver were obtained, the failure to observe a DRP1-S637 phosphorylation signal presented a major hurdle. It prevented conclusions being drawn about potential case-and effect, and so also limited the enthusiasm for further related experiments. The inability to observe changes in the phospho-status of DRP1 in interventions of specific interest was a major issue which I encountered. To potentially overcome this problem 2 additional approaches could be employed. As has previously been performed, DRP1 might be immunoprecipitated to enrich the protein prior to immunoblotting with a phospho-specific S637 antibody or indirectly with the pan PKA-substrate antibody, as used in this thesis [56, 57]. Alternatively, the Phos-tag method could potentially be used to monitor changes in the phospho-status of DRP1 [169].

1.37 PKARIα C17S KI show basal elevation in "total" PKA-substrate phosphorylation

PKARIα C17S KI and WT animals exhibited similar reductions in blood glucose levels after starvation and as anticipated disulfide PKARIα was elevated in WT but not KI mice (Figure 3.6B). Unexpectedly, and previously unobserved in this colony, KI mice displayed a greater than 1-fold increase in expression of PKARIα, compared to WT in heart (Figure 3.6C) and liver samples. It was hypothesised that KI animals harbouring a mutation precluding disulfide formation, would have decreased AKAP affinity, thereby reducing DRP1-S637 and "total" PKA-substrate phosphorylation during starvation. This was not observed, in fact contrary to our expectations PKARIα C17S KI mice showed a trend toward elevated basal DRP-S637 phosphorylation which was significantly increased by starvation (Figure 3.7A). Furthermore, analysis of "total" PKA-substrate phosphorylation revealed that this was not specific to DRP1 but reflected a broad basal elevation in substrate phosphorylation (Figure 3.8).

This result is diametrically opposite our hypothesized model in which disulfide PKARIα would have enhanced affinity for its scaffold proteins, thus elevated substrate phosphorylation (Figure 1.7**)**. To prevent disulfide formation between opposing RIα subunits it was necessary to mutate one of two cysteines. Although the PKARIα C17S KI mutation prevents disulfide formation between subunits it potentially leaves the remaining cysteine 38 available for oxidative modification. Both cysteines are located in the D/D domain of PKARIα which directly interacts with the amphipathic helix of AKAPs (Figure 1.4B). Instead of forming an inter-RIα disulfide bond, upon KI mutation of C17S the remaining cysteine thiol may now form an inter-protein disulfide with its associated AKAPs. PKARIα anchored in this way to AKAPs, in the presence of elevated cAMP as in starvation, could then exacerbate PKARIα substrate phosphorylation as observed. Sequence analysis of both D-AKAP1 and D-AKAP2 show no cysteine residues within their respective amphipathic helices, though this does not exclude disulfide exchange occurring with currently unidentified D-AKAPs. Though D-AKAP1 may not interact via a thiol with PKARIα, it is notable that in a recent proteome wide screen using cysteine-reactive small-molecule fragments both PKARIα and D-AKAP1 were identified as redox active [170]. Alternatively, the current model presumes that Cys17 is the sensing thiol, i.e. the first to become oxidised to sulfenic acid before being resolved to a disulfide by its opposing Cys38

residue. Its mutation to a serine thereby precludes disulfide formation. However if Cys38 is the sensing thiol, upon oxidation to sulfenic acid and unable to resolve to a disulfide due to the C17S mutation it could be further stepwise oxidised to a sulfinic and then sulfonic acid that may have functional impact (Figure 1.1). Oxidative modification to sulfonic acid is irreversible and may therefore also mediate PKARIα activity. Identifying whether Cys38 forms a sulfenic acid in the KI mouse could be assessed using dimedone-based reagents which specifically alkylate and trap cysteine sulfenic acids [171]. If Cys38 were the sensing thiol, labelling would be minimal in WTs as the sulfenic acid would be quickly resolved to a disulfide by Cys17. However, in the KI, Cys38 could not form a disulfide with Cys17 and would therefore be trapped in its sulfenic state evidenced by an increase in dimedone labelling.

In KI mice DRP1-S637 phosphorylation was significantly increased by starvation (Figure 3.7). As previously discussed this was contrary to expectations and may be accounted for by the aforementioned reasons however, it also raises an important question. Namely, if S637 phosphorylation was anticipated to modulate DRP1 localisation why then in KI animals displaying significantly elevated S637 phosphorylation was DRP1 localisation unchanged? This may suggest the fractionation did not adequately separate both fractions to detect changes in protein localisation. However this is perhaps unlikely as alterations in PKARIα and DRP1 localisation were previously demonstrated using the same method (Figure 3.2B). An alternative approach may have been to use a commercially available mitochondria isolation kit such as the Mitochondria Isolation Kit for Tissue by ThermoFisher which has previously been used to show changes in DRP1 localisation [68]. Commercially available kits however are not without their caveats, especially as their constituents are unlisted because they are proprietary, and so it can be unclear how such methods actually work.

1.37.1 Increased RIα expression in PKARIα C17S KI mice

KI mice displayed a significant increase in RIα subunit expression in both heart and liver but no change in PKA-cat expression (Figure 3.6C). The expected impact of this can be interpreted in two ways. Firstly, as the regulatory subunits localise PKARIα to a specific set of AKAPs and therefore also its substrate, an increase in RIα expression may be expected to enhance "total" PKA-substrate phosphorylation through increased targeting of the kinase to AKAPs. In

accordance with this, PKA-substrate phosphorylation is decreased in human dilated cardiomyopathy, which is associated with a concurrent reduction in both PKARI and PKARII subunit expression [172]. An alternative interpretation focuses on regulatory subunit sequestration of catalytic subunit activity. As PKA-cat levels remained unchanged while PKARIα expression was elevated, an increase in the ratio of PKARIα:PKA-cat may be anticipated to reduce "total" PKA-substrate phosphorylation through catalytic subunit inactivation. Importantly this reasoning would only be true in circumstances of unaltered cAMP levels, which were not measured in this study. *Han et al.* measured the phosphorylation state and expression of PKA regulatory and catalytic subunits in failing human myocardium [173]. PKA substrate phosphorylation was decreased despite post-translational modification of PKARII and PKA-cat that favoured catalytic subunits release and affinity for its substrate [173]. The authors found that a concurrent increase in PKARIα expression may be compensating for this by sequestering PKA-cat activity [173].

Previous research conducted in 2012 on the colony used in this work reported a basal increase in kidney and liver PKARIα expression but no change was observed in cardiac tissue [174]. It is possible that this upregulation is a compensatory mechanism against deficient PKARIα activity incurred as a consequence of the cysteine mutation. For example, disulfide PKARIα-mediated ERK phosphorylation was recently seen to be critical for angiogenic signalling [37]. Using Doppler imaging and immunostained tumour sections *Burgoyne et al.* showed that PKARIα C17S KI mice were deficient in angiogenesis after hind limb ischaemia and tumour implant [37]. In line with this, elevated PKARIα expression is associated with numerous cancers including cholangiocarcinoma [175], melanoma [176], ovarian cancer [177] and colorectal cancer [178]. No tumours, however, have been identified during studies involving dissection of PKARIα C17S KI mice. Conversely, mutations in the *PRKAR1A* gene are associated with approximately 75 % of patients with Carney Complex, a multiple endocrine neoplasia in which patients develop skin pigmentation and Schwannomas [179].

1.37.2 Starvation increases MFN2 expression

Starvation increased cardiac MFN2 levels in both PKARIα C17S KI and WT animals (Figure 3.9C). Mitochondrial fusion begins with the tethering of two separate mitochondria and this is critically dependent on the presence of MFN1 and MFN2 [167]. MFN1 and MFN2 are localised to the OMM and extend their carboxyl terminals into the cytosol, forming homo or hetero interactions with MFN1 and MFN2 of adjacent mitochondria [52]. Increased MFN2 expression therefore suggests that mitochondria are in pro-fusion state during starvation. Mitochondria elongation in response to starvation has previously been reported [180]. *Gomes et al.* showed that in response to nutrient deprivation mitochondria enlarge, possess higher cristae levels, are protected from autophagic degradation and increase ATP synthesis [57]. Interestingly, mitochondria also donate membranes for autophagosome formation during starvation and this process is attenuated by MFN2 depletion [181]. Therefore, it is likely MFN2 upregulation is an adaptive response to nutrient scarcity.

The ubiquitously expressed cytosolic microtubule-associated protein 1A/1B-light chain 3 (LC3-I) is an essential component of autophagosome formation [182]. During autophagy LC3-I is conjugated to LC3-phosphatidylethanolamine conjugate (LC3-II), which associates with autophagosomal membranes and degraded upon fusion with lysosomes [182, 183]. As such LC3-II is a routine marker of starvation-induced autophagy [182]. A trend toward increased LC3-II in response to starvation was observed in WT animals but was not significant (Figure 3.9D). Though a broadly used indicator of autophagosome formation, LC3-II measurement with immunoblotting is not without its caveats. Principally, LC3-II itself is degraded during autophagy [182]. It is therefore recommended that LC3-II be assessed with or without lysosomal protease inhibitors which were not used in the present study and may account for our failure to observe an increased LC3-II in response to starvation [183]. LC3-II formation appeared, though not significantly, basally elevated in PKARIα C17S KI mice (Figure 3.9D). P62 is commonly examined in tandem with LC3 as it binds both LC3 and ubiquitin and its accumulation is an indicator of dysfunctional autophagy [182]. To assess whether elevated LC3-II observed in PKARIα C17S KI mice impacted on autophagy, P62 levels were also examined but found unchanged (Figure S7). Despite this, elevated LC3-II in PKARIα C17S KI mice presents an interesting avenue for further study as LC3-II is negatively regulated by

PKA [184]. Therefore, in KI mice this negative regulation may be compromised resulting in elevated LC3-II.

1.38 Na-pyruvate attenuates H_2O_2 induced oxidation of PKARIα and PKGIα

Initial experiments with isoprenaline and H_2O_2 failed to increase the percentage of PKARIα disulfide dimer (Figure 3.10A). As this method was previously effective at inducing disulfides (Figure 3.2A), additional experiments were undertaken to establish why in this instance it was not. H_2O_2 is a highly reactive substance and decomposed by most transition metals as well as catalase [185]. Despite cautions taken in the laboratory to limit degradation, it is possible that H_2O_2 can become contaminated and so decompose, therefore new H_2O_2 was ordered and perfusions performed again. Additionally, as batch to batch variation in antibody specificity is possible PKGIα disulfide dimer formation was used as a control for H_2O_2 induced protein oxidation. However, experiments using newly ordered (Figure 3.11A) and increasing doses of H_2O_2 (Figure 3.11B) again failed to increase disulfide PKARIα or PKGIα dimer levels and so the factors considered above were ruled out as responsible. Following discussions with other laboratory members using similar protocols it was identified that Na-pyruvate was not included in their perfusion buffer. Removal of Na-pyruvate from my perfusion buffer dramatically altered the effectiveness of H_2O_2 to induce disulfide PKARIα and PKGIα dimers (Figure 3.12) and also enhanced both CFR and LVEDP (Figure 3.13).

Pyruvate is a critical intermediate in the citric acid cycle and is produced by the breakdown of glucose during glycolysis [186]. Pyruvate is used to produce energy by the following mechanisms: Decarboxylation of pyruvate by the pyruvate dehydrogenase complex produces acetyl-CoA an essential input to the citric acid cycle. Carboxylation of pyruvate by pyruvate carboxylase produces oxaloacetate which replenishes key citric acid cycle intermediates and is also used during gluconeogenesis [186]. Pyruvate can also be transaminated to alanine or in the absence of oxygen reduced to lactate [187]. During Langendorff perfusion cardiac function can undergo regular cyclic fluctuations in contractility and coronary flow (Figure 2.3) rendering valid comparisons between experiments problematic. The addition of Na-pyruvate has previously been shown to mitigate this [113]. As alterations in contractile function were an important index in these experiments Na-pyruvate had been added to obviate problems caused by variability due to fluctuation in contractility.

Pyruvate undergoes rapid decarboxylation in the presence of H_2O_2 yielding acetate, H_2O and CO_2 [185, 186, 188]. Attention was first brought to its used in oxidants treated cell culture experiments by *Giandomenico et al.* who reported differences in H_2O_2 stability across various culture mediums [189]. By systematically measuring H_2O_2 degradation in response to cell culture components the authors found Na-pyruvate to be a highly efficient scavenger of the oxidant [189]. Cognisance of pyruvate content in experiments using exogenous application of oxidants has since been confirmed and cautioned by several other groups [190-193]. Na-pyruvate caused a striking reduction in both the ability of H_2O_2 to induce disulfide PKARIα (Figure 3.12) and its physiological impacts on CFR and LVEDP (Figure 3.13). Rather than infer that it is in this case cardio-protective, for the aforementioned reasons, it is most likely Na-pyruvate's presence in the buffer greatly reduced the effective lifetime of H_2O_2 prior to reaching the myocardium. Investigating whether pre-perfusion with Na-pyruvate can attenuate cardiac dysfunction and disulfide PKARIα formation in response to H_2O_2 treatment or oxidant generating interventions such as I/R therefore present an interesting avenue of further investigation. It is worth mentioning that Na-pyruvate showed a tendency to increase CFR and LVSP under control conditions relative to hearts perfused in its absence (Figure 3.13) as well as reduce basal levels of disulfide PKGIα (Figure 3.12). Similar inotropic results as well as protective effects have been reported during I/R injury, myocardial infarction and cardioplegia, and are thought to be mediated by pyruvate-dependent increased energy production or free radical scavenging [113, 194-199]. These results verify that these cardio-protective effects may also be mediated through pyruvates scavenging of H_2O_2.

1.39 PKARIα disulfide formation is unaffected by β-adrenergic stimulation

Binding of cAMP to PKA induces a conformational change in the kinase resulting in the release of its catalytic subunits [21]. PKGIα is similarly altered by interaction with its nucleotide cGMP, which prevents its formation of disulfide dimers [5]. Whether cAMP mediates PKARIα disulfide formation between its regulatory subunits was assessed by elevating cardiac cAMP levels with the non-selective β-adrenoreceptor agonist isoprenaline in the presence and absence of H_2O_2. Isoprenaline alone or in combination with H_2O_2 did not affect disulfide formation (Figure 3.14). Unlike PKGIα, whose nucleotides bind close to its disulfide forming cysteines, the cAMP binding domains and disulfide cysteines formed by PKARIα are not in close

proximity [5]. This may therefore preclude an impact of cAMP on PKARIα disulfide formation. Compartmentalisation of cAMP signalling is well described and regulated by numerous factors such as PDEs and the particular GPCR or adenylate cyclase activated [200, 201]. Isoprenaline-induced elevations in cAMP are reportedly constrained to the particulate fraction, while PGE1 increases soluble cAMP [202]. Using cAMP sensors specifically targeted to RI and RII domains *Benedetto et al.* showed that isoprenaline induced elevations in cAMP were only detected by the RII sensor, while the RI sensor exclusively responded to PGE1 [203]. Therefore, PGE1 may have been a more effective agonist to discriminately target cAMP to PKARIα.

1.39.1 H_2O_2 attenuates myocardial isoprenaline sensitivity

As described in section 1.8, PKARIα, but not PKARII shows increased responsiveness to cAMP in the presence of substrate [48]. This substrate-induced sensitivity to cAMP results in potentiated PKA activity for a given cAMP concentration and reduces the rate of PKARIα-PKA-cat re-association [48, 49, 204]. This led to the proposal that both substrate and cAMP are necessary for full dissociation of PKA-cat subunits and therefore full activation of PKARIα. Furthermore, mutation of the cysteines necessary for PKARIα disulfide formation reduce the kinase's affinity for D-AKAP2 [33]. It was hypothesised that disulfide formation between the RIα subunits would enhance the association of the kinase with its AKAPs, which when in proximity with its substrate would be sensitised to cAMP leading to complete disassociation and activation of PKARIα (Figure 1.6). "Total" PKA-substrate phosphorylation was unchanged in the presence of H_2O_2 but was elevated, as anticipated, by isoprenaline. However, this elevation was unexpectedly attenuated by H_2O_2 (Figure 3.14) and mirrored by a simultaneous attenuation of CFR, LVEDP and LVSP responsiveness to isoprenaline in the presence of H_2O_2 (Figure 3.15). These findings are summarised in the figure below. Unexpectedly, DRP1-S637 phosphorylation was unchanged during all interventions studied.

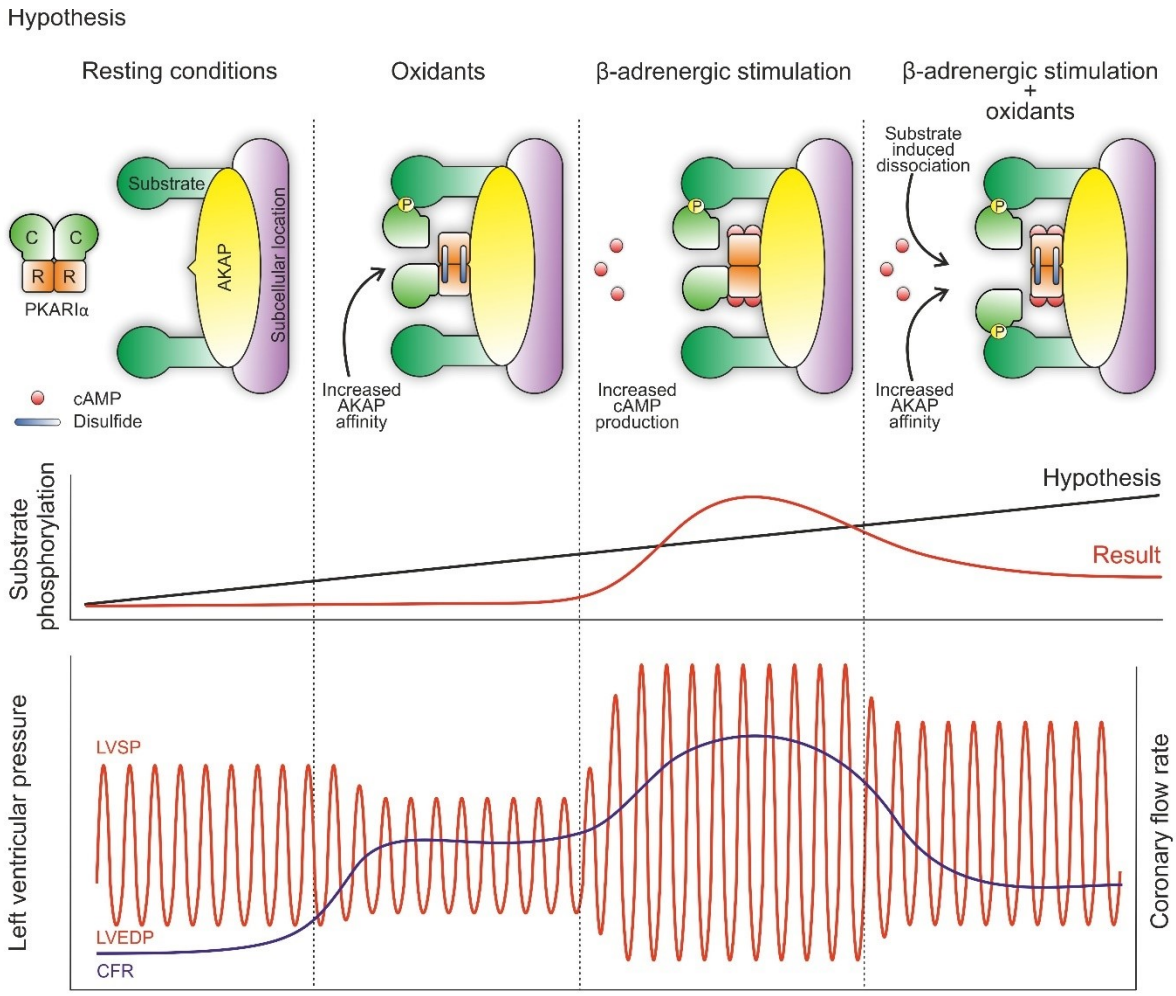

Figure 4.2. Summary of hypothesized and achieved results in Langendorff perfusion experiments. Top, hypothesized model of substrate phosphorylation in the presence of oxidants and β-adrenergic stimulation. Middle, schematic representation of hypothesized and achieved substrate phosphorylation results. Bottom, schematic representation of physiological changes in cardiac function during H_2O_2 and isoprenaline perfusions. Left ventricular systolic pressure (LVSP), left ventricular end diastolic pressure (LVEDP) and coronary flow rate (CFR).

In contrast to the current study, previous work has shown an impact of H_2O_2 on substrate phosphorylation. Treatment of freshly isolated or overnight cultured rat ventricular myocytes with H_2O_2 has previously been shown to induce the phosphorylation of PLB and cTnI which was largely, but not entirely, attenuated by the presence of the PKA inhibitor H98 [35]. Similarly, treatment of bovine aortic endothelial cells with H_2O_2 or vascular endothelial growth factor induces PKARIα disulfide formation and PKA site specific phosphorylation of ERK which is absent in aorta from PKARIα C17S KI mice [37]. In addition, it has also been shown that treatment of cells with isoprenaline, PGE1 or directly with cAMP in the presence of H_2O_2 shows a trend toward potentiated "total" PKA-substrate phosphorylation beyond exposure to

either chemical alone [205]. Although this was not observed in cardiomyocytes it was reliably detected in HEK293 or vascular smooth muscle cells, as well as aortic rings under cell culture conditions [205]. This is in contrast to the current results showing that rather than potentiating "total" PKA-substrate phosphorylation, in hearts the presence of oxidants and cAMP reduces phosphorylation levels below the levels achieved by β-adrenoreceptor agonism alone (Figure 3.14). Interestingly this phenomenon was not observed in initial perfusion experiments (Figure 3.10B), further supporting the hypothesis that pyruvate contributes to the decomposition, and thus effectiveness, of H_2O_2. The subsequent loss of phosphorylation due to H_2O_2 was accompanied by a concurrent reduction in all indices of cardiac function in response to isoprenaline (Figure 3.15). Both the LVSP and CFR response to isoprenaline was significantly attenuated, while LVEDP changes were entirely abolished by H_2O_2 (Figure 3.15). The disparity between these findings may stem from several methodological limitations.

Though examined under culture conditions, all of the results in cells considered above had yet to be replicated at organ level. Furthermore, although PKA substrates were observed to be phosphorylated in response to H_2O_2 in adult rat ventricular myocytes, this was not observed in vascular smooth muscle cells, HEK cells or aortic rings [205]. In line with this, previous experiments involving H_2O_2 perfused mouse hearts failed to identify any change in a number of PKA substrates using site-specific phospho antibodies [174]. In cellular experiments showing perpetuated "total" PKA-substrate phosphorylation after exposure to cAMP agonists and H_2O_2 the concentrations of H_2O_2 used were at least 2-fold and often 5-fold higher than those utilised in the current study. Additionally, the incubation periods used were twice as long as those in the current study [205]. Both factors are important as PKA substrate phosphorylation has also been shown to exhibit a bell-shaped curve in response to increasing concentrations of H_2O_2 [35]. Therefore, shorter incubation periods with lower concentrations of H_2O_2 may account for the disparity in the current results. Moreover, culture experiments all involved pre-treatment of cells prior to concomitant treatments, which is in contrast to the current study which involved only concomitant exposure [205]. Furthermore, cardiomyocyte monoculture experiments may not be translatable to whole heart scenarios as the myocardium is composed of several distinct cell types. Indeed, using a combination of genetic tools and cellular markers *Pinto et al.* recently revised estimates of cardiac tissue composition to be primarily endothelial cells (55%) followed by cardiomyocytes (32%) and then fibroblasts (13%) [206]. Therefore, although specific changes may be reliably induced in cell culture

preparations these pathways may not be translatable as they do not reflect *in vivo* changes in the intracellular environment of heterocellular organs.

H_2O_2 when exogenously applied is also an indiscriminate, non-specific cell-wide oxidant that targets PKARIα, but is also fully capable of modifying other proteins - including those involved in PKA substrate phosphorylation. For example, PKA-cat contains a cysteine near its active site that when S-gluthathionylated, inhibits the activity of the kinase [207]. Similarly, when oxidised at its metal centre, the serine-threonine protein phosphatase-1 (PP1) is also inactivated [208]. Assessing H_2O_2 induced alterations in PKA substrate phosphorylation is further complicated by the oxidants concurrent activation of redox sensitive PKG. This is particularly confounding as PKG phosphorylates a number of residues that are also regulated by PKA. For example, the cardiac myosin binding protein c (cMyBP-C) serine residues 273, 282 and 302 are all phosphorylated by both PKA and PKG [209, 210]. Similarly, cTnI Ser23/24 are regulated by both PKA and PKG [26]. In line with this, oxidant-dependent PKA substrate phosphorylation in cardiomyocytes was only partially attenuated by H89 suggesting alternative pathways, such as those mentioned above, may also contribute to H_2O_2-induced changes in phosphorylation [35]. Therefore, it is possible that any PKARIα disulfide-dependent changes in phosphorylation are masked by concurrent oxidation of other mediators of PKA substrate phosphorylation. In summary, significant differences in the concentrations of H_2O_2 used, duration of exposure, method of application and the non-specific nature of H_2O_2 may account for the discrepancy between the current results and those observed in cell culture preparations.

1.39.2 DRP1-S637 phosphorylation is unchanged by H_2O_2 or isoprenaline

Unexpectedly DRP1-S637 phosphorylation was unchanged during all eight Langendorff conditions under which it was examined. This is particularly perplexing for two reasons. Firstly, half of the conditions contained isoprenaline at concentrations sufficient to induce significant elevations in "total" PKA-substrate phosphorylation. Secondly, isoprenaline and other cAMP elevating agents such as forskolin are routinely used as a positive control for DRP1-S637 phosphorylation [56, 57, 64]. In addition calcineurin, which dephosphorylates DRP1-S637, is itself subject to inactivation by H_2O_2. Using purified calcineurin and mutants harbouring a Met 406 to Leu exchange, *Carruthers & Stemmer* showed that methionine

oxidation by H_2O_2 reduced the affinity of calmodulin for calcineurin more than 3-fold, disrupting the enzymes activation [211]. This adds a further credence to the expectation of altered DRP1-S637 phosphorylation during perfusion experiments. These results therefore raise the question of whether the means by which S637 phosphorylation was assessed was sufficiently sensitive to detect changes in the proteins phospho-status. Evidence refuting this is presented in Figure 2.4, as DRP1-S637 phosphorylation shows a clear dose-response to increasing concentration of isoprenaline. On the other hand the observation that direct perfusion of isoprenaline to the myocardium, at concentrations adequate to induce ample increases in "total" PKA-substrate phosphorylation, did not affect S637 phosphorylation. This indicates that alternative methods of assessment are warranted. Examples of these methods are described in section 4.3.1.

1.39.3 H_2O_2 attenuates isoprenaline induced alterations in contractile function

The impact of β-adrenergic receptor agonists on cardiac performance are well characterized, resulting in increased inotropy, chronotropy and lusitropyas via mechanisms described in Figure 1.3 [21, 23]. Enhanced contractility, myocardial relaxation and coronary vasodilation were readily seen in response to isoprenaline (Figure 3.15). Pacing of hearts precluded the observation of chronotropic variability. If H_2O_2 induced similar the phosphorylation of PKA-substrates typically attributed to PKARII in response to β-adrenoreceptor activation, the expected profiles of their contractile indices should be comparable. Though this is true for CFR, both LVSP and LVEDP show divergent responses to isoprenaline and H_2O_2 (Figure 3.15). It could therefore be suggested that disulfide PKARIα and cAMP-activated PKARII induce divergent responses in contractile function. However, as H_2O_2 failed to induce any change in "total" PKA-substrate phosphorylation this argument cannot be made (Figure 3.14). As previously mentioned H_2O_2 likely oxidises many different free protein thiols, a clear ramification of which is activation of other redox sensitive proteins that modulate cardiac function such as PKGIα. Disulfide PKGIα has previously been shown to mitigate LVSP responsiveness to isoprenaline. Indeed, when PKGIα is inhibited, an inotropic response to H_2O_2 is seen in rat hearts [137]. Therefore, it is possible that activation of alternative signalling pathways by H_2O_2 is masking contractile changes induced by disulfide PKARIα.

1.39.4 Disulfide PKARIα does not mediate H_2O_2 induced changes in isoprenaline sensitivity

H_2O_2 increased PKARIα disulfide formation, which in the presence of elevated cAMP, was associated with a decrease in "total" PKA substrate phosphorylation (Figure 3.14). By contrast, PKARIα C17S KI mice which cannot form disulfides showed elevated "total" PKA-substrate phosphorylation (Figure 3.8). In other words, in both cases the presence or absence of disulfide PKARIα appeared to be associated with a concurrent change in "total" PKA-substrate phosphorylation. Taken together this data suggested that disulfide bound PKARIα, instead of facilitating substrate phosphorylation, may in fact be preventing it. To test this hypothesis, additional perfusion experiments were performed with PKARIα C17S KI and WT mice. If disulfide bound PKARIα was responsible for decreasing isoprenaline-induced "total" PKA-substrate phosphorylation in the presence of H_2O_2, it was anticipated that this effect would be absent in KI but not WT mice. KI mice showed no disulfide form of the kinase under any conditions, but did show increased PKARIα expression (Figure 3.16). WT mice displayed similar increases in disulfide PKARIα in response to H_2O_2 in the presence or absence of isoprenaline. "Total" PKA-substrate phosphorylation was similar between genotypes under all conditions suggesting that H_2O_2 induced disulfide bound PKARIα is not responsible for the decreases in phosphorylation observed during concurrent perfusions (Figure 3.17). In contrast to previous experiments (Figure 3.8) KI preparations did not display basal elevations in "total" PKA-substrate phosphorylation, which would be a plausible, anticipated consequence. Langendorff experiments were conducted *ex vivo* and involved the excision, cannulation and perfusion of hearts under artificial conditions for a 35 minute period. In contrast, the previous experiments involved excision and immediate snap-freezing of hearts in liquid nitrogen. Due to the speed at which tissues were isolated and frozen the latter experiments are therefore likely a better reflection of the in situ phospho-status of PKA substrate in KI mice. Differences in physiological indices of cardiac function between KI and WT mice could not be viably assessed due to small sample sizes.

Though the above reduction in isoprenaline sensitivity in the presence of oxidants appears independent of disulfide PKARIα formation it is nonetheless a striking observation. These results therefore highlight the strong potential interplay between oxidant and β-adrenergic-induced PKA signalling. Attenuation of cardiac β-adrenoceptor signal transduction has been

reported in the presence of H_2O_2. In rat heart membranes treated with H_2O_2, a decrease in β1 and β2-adrenoceptor density was observed as well as reduced adenylate cyclase activity responsiveness to isoprenaline, effects which were abrogated by the H_2O_2 decomposing enzyme catalase [212]. Similarly, perfusion of rat hearts with H_2O_2 has been reported to reduce β-adrenoceptor density and depress both adenylate cyclase activity and the positive-inotropic response to isoprenaline [213]. Perturbations of β-adrenoceptors sensitivity and density following H_2O_2 treatment have also been reported in intestinal, tracheal, and lung parenchymal tissue [214, 215]. Therefore, the reduced responsiveness to isoprenaline in the presence of H_2O_2 may be explained by the oxidant concurrently reducing β-adrenergic responsiveness.

Finally, catecholamines are readily degraded by oxidative reactions catalysed by oxygen, light, acidic conditions and heavy metal [216]. Though isoprenaline and H_2O_2 were added separately to the perfusion buffer minutes prior to its use, it is possible that oxidative degradation of isoprenaline catalysed by H_2O_2 occurred within the same time window. Degradation of isoprenaline produces aminochromes which are further oxidised to various reactive intermediates and free radicals [217]. Accordingly, in cardiomyocytes and H9C2 cells this degradation is accompanied by a concomitant increase in ROS production [218, 219]. However, no additional increase in disulfide PKARIα was observed during combined perfusions with H_2O_2 and isoprenaline compared to H_2O_2 alone, suggesting the agent may not have been degraded.

1.40 Summary and future work

Previous cellular and *in vitro* studies have shown that in response to oxidants PKARIα forms disulfide bonds between its regulatory subunits which are associated with both enhanced affinity for its scaffold AKAPs and phosphorylation of its substrates [32, 33]. In addition, PKARIα substrate also sensitises the kinase to its nucleotide cAMP to induce its activation [49]. The purpose of this thesis was to examine the interplay of these factors on PKARIα substrate phosphorylation and disulfide dimer formation *in vivo*. To this end, a number of in vivo and ex vivo approaches were undertaken that involved the application of exogenous oxidants and the cAMP agonist isoprenaline or scenarios in which elevations in both factors were thought to occur.

These experiments revealed that perfusion of hearts with the oxidant H_2O_2 led to the formation of disulfide bonds between the regulatory subunits of PKARIα. Disulfide bound PKARIα then exhibited enhanced affinity for its AKAPs, as evidenced by co-fractionation of the kinase with D-AKAP1 after perfusions. However, these changes were not associated with any change in substrate phosphorylation. PKARIα disulfide formation was unaffected by the presence of cAMP, however during concomitant perfusions with H_2O_2 and isoprenaline cardiac sensitivity to the cAMP agonist was reduced. This was evidenced at the protein level by reduced "total" PKA-substrate phosphorylation and physiologically as a blunted response in CFR, LVEDP and LVSP responsiveness to isoprenaline. Using the "redox dead" PKARIα C17S KI mouse these changes were seen, however they occur independently of disulfide formation. These changes may instead stem from H_2O_2 concomitantly inducing additional signalling events. Oxidant induced PKARIα disulfide formation was also verified *in vivo* in the context of starvation. Oxidation of PKARIα to a disulfide dimer was robustly seen in response to various periods of starvation and associated with both co-fractionation of the kinase with its scaffold protein D-AKAP1 and increased "total" PKA-substrate phosphorylation. Clarifying the contribution of disulfide PKARIα to this increase was difficult as basally PKARIα C17S KI mice displayed both increased RIα expression and "total" PKA-substrate phosphorylation. Although no change in phosphorylation of the mitochondrial D-AKAP1 associated protein DRP1 was observed during starvation, several promising results in livers were obtained. These included; increased PKARIα disulfide formation and translocation, the formation of DRP1 higher molecular weight complexes and increased soluble DRP1. These findings are indicative of DRP1-S637 phosphorylation. However as no increase in DRP1-S637 was detected using commercially available antibodies further experiments utilizing phospho-capture resins or immune-precipitated DRP1 may allow this to be confirmed.

The failure to replicate cell culture experiments may be a consequence of several factors. Unlike cell monocultures, the current experiments were undertaken in heterocellular organs exposed to lower concentration of H_2O_2 for shorter time periods. Furthermore, H_2O_2 is a highly reactive oxidant and it would seem prudent to assume its exogenous application has many off target effects, its use to oxidise PKARIα is therefore not without its own limitations. Due to these factors experiments using cardiomyocytes isolated from PKARIα C17S KI and WT mice would be a valid complimentary approach. Of particular concern is the observation that KI mice unable to form disulfides in fact display a basal elevation in substrate phosphorylation.

This may be accounted for by the concurrent increase in RIα expression observed in these mice which may unspecifically saturate AKAPs in an effort to compensate for decreased targeting due to the Cys17 to Ser KI mutation. Taken together these findings suggest a more intricate model of PKARIα activation than is seen in other redox-sensitive kinases. For example, PKGIα is activated independently by cGMP or oxidants and binding of its nucleotide precludes its formation of a disulfide dimer [5]. However unlike PKARIα, the regulatory and catalytic units of PKGIα are fused into a single subunit [220]. This conformational difference may therefore account for a more complex method of PKARIα regulation by cAMP and disulfide bond formation.

Critical to this and previous work is the hypothesis that disulfide-mediated increases in PKARIα-AKAP affinity, which have been clearly demonstrated, facilitate an increase in PKA-substrate phosphorylation [33]. Although this would seem logical this facet of PKARIα activation has yet to be fully substantiated *in vitro*. Therefore future work involving *in vitro* kinase activity assays using recombinant PKARIα in its disulfide and reduced state may be undertaken to clarify this point. Mitochondrial networks are generally reported in terms of aspect ratio (i.e. length/width) which in cardiomyocytes and liver is typically around 1.5. However, in other cells types, such as mouse embryonic fibroblasts a mitochondrial aspect ratio of approximately 6 is typical [52]. In addition, these networks display rapid rates of mitochondrial fusion and fission compared to the relatively slow turnover seen in cardiomyocytes [52]. Therefore, examination of PKARIα mediated DRP1-S637 phosphorylation in cell types typically exhibiting more dynamic changes in mitochondrial fusion and fission events may be a more promising avenue of investigation than in cardiac tissue. In addition, encouraging results indicative of a PKARIα mediated change in liver DRP1 during starvation were identified. Further investigation of the phospho-status of DRP1-S637 using alternative methods may be informative. As the implication of DRP1-S637 phosphorylation is inhibition of its mitochondrial fission activity a method of assessing changes in mitochondrial morphology would also be necessary. This could perhaps be accomplished by using electron microscopy or immunohistochemistry of liver tissue sections. For example, if PKARIα phosphorylates DRP1-S637 during starvation, mitochondria from these interventions should be larger and this difference should be absent in PKARIα C17S KI mice.

In conclusion, PKARIα is a ubiquitous kinase replete within the cardiovascular system and subject to post-translational modification by both cAMP and oxidants. *Ex vivo* Langendorff perfusion experiments demonstrated that in response to H_2O_2 PKARIα forms a disulfide dimer which translocates to membrane fractions. This model of PKARIα oxidation was then replicated *in vivo* in the context of starvation. The targets of starvation induced disulfide bound PKARIα remain to be fully elucidated, although promising results suggest that in liver starvation induced disulfide PKARIα may target the mitochondrial fission protein DRP1.

PKARIα can be activated by β-adrenergic stimulation or through its oxidation to a disulfide dimer. How these two events are integrated by PKARIα to impact the phosphorylation of its substrates remains unclear as evidenced by a failure of translation between cellular and organ models. In addition, Na-pyruvate was identified as potently attenuating H_2O_2 induced cysteine oxidation. This is of particular methodological importance to experiments involving the exogenous application of oxidants, as numerous culture mediums and perfusion solutions include Na-pyruvate. Finally, a complete understanding of the factors regulating PKARIα is important as PKA is a critical regulator of inotropy, lusitropy and chronotropy in the heart and numerous cardiac pathologies such as ischaemic injury, heart disease and myocardial infarction are associated with excessive β-adrenergic stimulation and ROS production.

Bibliography

1. Wu RF, M.Z., Liu Z, Terada LS. , *Nox4-derived H2O2 mediates endoplasmic reticulum signaling through local Ras activation.* Mol Cell Biol, 2010. **30**: p. 3553–3568.
2. Datla, S.R., et al., *Poldip2 controls vascular smooth muscle cell migration by regulating focal adhesion turnover and force polarization.* Am J Physiol Heart Circ Physiol, 2014. **307**(7): p. H945-57.
3. Clempus RE, S.D., Dikalova AE, Pounkova L, Jo P, Sorescu GP, Schmidt HH, Lassègue B, Griendling KK. , *Nox4 is required for maintenance of the differentiated vascular smooth muscle cell phenotype.* Arterioscler Thromb Vasc Biol, 2007. **27**: p. 42–48.
4. Aslan, M. and T. Ozben, *Oxidants in receptor tyrosine kinase signal transduction pathways.* Antioxid Redox Signal, 2003. **5**(6): p. 781-8.
5. Burgoyne, J.R., et al., *cGMP-dependent activation of protein kinase G precludes disulfide activation: implications for blood pressure control.* Hypertension, 2012. **60**(5): p. 1301-8.
6. Frantz, S., J. Bauersachs, and G. Ertl, *Post-infarct remodelling: contribution of wound healing and inflammation.* Cardiovasc Res, 2009. **81**(3): p. 474-81.
7. Giacco, F. and M. Brownlee, *Oxidative stress and diabetic complications.* Circ Res, 2010. **107**(9): p. 1058-70.
8. Wagner, S., et al., *Redox regulation of sodium and calcium handling.* Antioxid Redox Signal, 2013. **18**(9): p. 1063-77.
9. Prysyazhna, O., O. Rudyk, and P. Eaton, *Single atom substitution in mouse protein kinase G eliminates oxidant sensing to cause hypertension.* Nat Med, 2012. **18**(2): p. 286-90.
10. Birukov, K.G., *Cyclic stretch, reactive oxygen species, and vascular remodeling.* Antioxid Redox Signal, 2009. **11**(7): p. 1651-67.
11. Zweier, J.L. and M.A. Talukder, *The role of oxidants and free radicals in reperfusion injury.* Cardiovasc Res, 2006. **70**(2): p. 181-90.
12. Fortuno, A., et al., *Association of increased phagocytic NADPH oxidase-dependent superoxide production with diminished nitric oxide generation in essential hypertension.* J Hypertens, 2004. **22**(11): p. 2169-75.
13. Higashi, Y., et al., *Endothelial function and oxidative stress in renovascular hypertension.* N Engl J Med, 2002. **346**(25): p. 1954-62.
14. Murdoch, C.E., et al., *Endothelial NADPH oxidase-2 promotes interstitial cardiac fibrosis and diastolic dysfunction through proinflammatory effects and endothelial-mesenchymal transition.* J Am Coll Cardiol, 2014. **63**(24): p. 2734-41.
15. Carroll, J., et al., *Bovine complex I is a complex of 45 different subunits.* Journal of Biological Chemistry, 2006. **281**(43): p. 32724-32727.
16. Chen, Y.R. and J.L. Zweier, *Cardiac mitochondria and reactive oxygen species generation.* Circ Res, 2014. **114**(3): p. 524-37.
17. Brown, D.I. and K.K. Griendling, *Regulation of signal transduction by reactive oxygen species in the cardiovascular system.* Circ Res, 2015. **116**(3): p. 531-49.
18. Hanschmann, E.M., et al., *Thioredoxins, glutaredoxins, and peroxiredoxins--molecular mechanisms and health significance: from cofactors to antioxidants to redox signaling.* Antioxid Redox Signal, 2013. **19**(13): p. 1539-605.
19. Biteau, B., J. Labarre, and M.B. Toledano, *ATP-dependent reduction of cysteine-sulphinic acid by S. cerevisiae sulphiredoxin.* Nature, 2003. **425**(6961): p. 980-4.
20. Broniowska, K.A. and N. Hogg, *The chemical biology of S-nitrosothiols.* Antioxid Redox Signal, 2012. **17**(7): p. 969-80.

21. Johnston, A.S., S.E. Lehnart, and J.R. Burgoyne, *Ca(2+) signaling in the myocardium by (redox) regulation of PKA/CaMKII.* Front Pharmacol, 2015. **6**: p. 166.
22. Benovic, J.L., et al., *Regulation of adenylyl cyclase-coupled beta-adrenergic receptors.* Annu Rev Cell Biol, 1988. **4**: p. 405-28.
23. Bers, D.M., *Cardiac excitation-contraction coupling.* Nature, 2002. **415**(6868): p. 198-205.
24. Hulme, J.T., et al., *Beta-adrenergic regulation requires direct anchoring of PKA to cardiac CaV1.2 channels via a leucine zipper interaction with A kinase-anchoring protein 15.* Proc Natl Acad Sci U S A, 2003. **100**(22): p. 13093-8.
25. Hofmann, F., et al., *L-type CaV1.2 calcium channels: from in vitro findings to in vivo function.* Physiol Rev, 2014. **94**(1): p. 303-26.
26. Layland, J., R.J. Solaro, and A.M. Shah, *Regulation of cardiac contractile function by troponin I phosphorylation.* Cardiovasc Res, 2005. **66**(1): p. 12-21.
27. Li, L., et al., *Phosphorylation of phospholamban and troponin I in beta-adrenergic-induced acceleration of cardiac relaxation.* Am J Physiol Heart Circ Physiol, 2000. **278**(3): p. H769-79.
28. Wehrens, X.H., et al., *Ryanodine receptor/calcium release channel PKA phosphorylation: a critical mediator of heart failure progression.* Proc Natl Acad Sci U S A, 2006. **103**(3): p. 511-8.
29. Lehnart, S.E., et al., *Stabilization of cardiac ryanodine receptor prevents intracellular calcium leak and arrhythmias.* Proc Natl Acad Sci U S A, 2006. **103**(20): p. 7906-10.
30. Shan, J., et al., *Phosphorylation of the ryanodine receptor mediates the cardiac fight or flight response in mice.* J Clin Invest, 2010. **120**(12): p. 4388-98.
31. Shan, J., et al., *Role of chronic ryanodine receptor phosphorylation in heart failure and beta-adrenergic receptor blockade in mice.* J Clin Invest, 2010. **120**(12): p. 4375-87.
32. Brennan JP, B.S., Burgoyne JR, Fuller W, Schroder E, Wait R, Begum S, Kentish JC, and Eaton P. , *Oxidantinduced activation of type I protein kinase A is mediated by RI subunit interprotein disulfide bond formation.* J Biol Chem, 2006. **281**: p. 21827-21836.
33. Sarma, G.N., et al., *Structure of D-AKAP2:PKA RI complex: insights into AKAP specificity and selectivity.* Structure, 2010. **18**(2): p. 155-66.
34. Zick, S.K. and S.S. Taylor, *Interchain disulfide bonding in the regulatory subunit of cAMP-dependent protein kinase I.* J Biol Chem, 1982. **257**(5): p. 2287-93.
35. Brennan, J.P., et al., *Oxidant-induced activation of type I protein kinase A is mediated by RI subunit interprotein disulfide bond formation.* J Biol Chem, 2006. **281**(31): p. 21827-36.
36. Leon DA, H.F., Banky P, Taylor SS., *A stable alpha-helical domain at the N terminus of the RIalpha subunits of cAMP-dependent protein kinase is a novel dimerization/docking motif.* J Biol Chem, 1997. **. 272**: p. 28431–28437.
37. Burgoyne, J.R., et al., *Deficient angiogenesis in redox-dead Cys17Ser PKARIalpha knock-in mice.* Nat Commun, 2015. **6**: p. 7920.
38. Sarma GN, K.F., Kim C, von Daake S, Chen L, Wang BC, & Taylor SS. , *Structure of D-AKAP2:PKA RI complex: Insights into AKAP specificity and selectivity.* Structure, 2010. **18** p. 155–166.
39. Esseltine, J.L. and J.D. Scott, *AKAP signaling complexes: pointing towards the next generation of therapeutic targets?* Trends Pharmacol Sci, 2013. **34**(12): p. 648-55.
40. Rogne, M., et al., *Mutually exclusive binding of PP1 and RNA to AKAP149 affects the mitochondrial network.* Hum Mol Genet, 2009. **18**(5): p. 978-87.
41. Banky, P., et al., *Isoform-specific differences between the type Ialpha and IIalpha cyclic AMP-dependent protein kinase anchoring domains revealed by solution NMR.* J Biol Chem, 2000. **275**(45): p. 35146-52.
42. Gold, M.G., et al., *Molecular basis of AKAP specificity for PKA regulatory subunits.* Mol Cell, 2006. **24**(3): p. 383-95.
43. Affaitati, A., et al., *Essential role of A-kinase anchor protein 121 for cAMP signaling to mitochondria.* J Biol Chem, 2003. **278**(6): p. 4286-94.

44. Banky, P., L.J. Huang, and S.S. Taylor, *Dimerization/docking domain of the type Ialpha regulatory subunit of cAMP-dependent protein kinase. Requirements for dimerization and docking are distinct but overlapping.* J Biol Chem, 1998. **273**(52): p. 35048-55.
45. Huang, L.J., et al., *NH2-Terminal targeting motifs direct dual specificity A-kinase-anchoring protein 1 (D-AKAP1) to either mitochondria or endoplasmic reticulum.* J Cell Biol, 1999. **145**(5): p. 951-9.
46. Yang, S., W.H. Fletcher, and D.A. Johnson, *Regulation of cAMP-dependent protein kinase: enzyme activation without dissociation.* Biochemistry, 1995. **34**(19): p. 6267-71.
47. Kopperud, R., et al., *Formation of inactive cAMP-saturated holoenzyme of cAMP-dependent protein kinase under physiological conditions.* J Biol Chem, 2002. **277**(16): p. 13443-8.
48. Vigil, D., et al., *Differential effects of substrate on type I and type II PKA holoenzyme dissociation.* Biochemistry, 2004. **43**(19): p. 5629-36.
49. Viste, K., et al., *Substrate enhances the sensitivity of type I protein kinase a to cAMP.* J Biol Chem, 2005. **280**(14): p. 13279-84.
50. Burgoyne, J.R., et al., *Cysteine redox sensor in PKGIa enables oxidant-induced activation.* Science, 2007. **317**(5843): p. 1393-7.
51. Lin, R.Y., S.B. Moss, and C.S. Rubin, *Characterization of S-AKAP84, a novel developmentally regulated A kinase anchor protein of male germ cells.* J Biol Chem, 1995. **270**(46): p. 27804-11.
52. Song, M. and G.W. Dorn, 2nd, *Mitoconfusion: noncanonical functioning of dynamism factors in static mitochondria of the heart.* Cell Metab, 2015. **21**(2): p. 195-205.
53. Figueroa-Romero, C., et al., *SUMOylation of the mitochondrial fission protein Drp1 occurs at multiple nonconsensus sites within the B domain and is linked to its activity cycle.* Faseb j, 2009. **23**(11): p. 3917-27.
54. Cho, D.H., et al., *S-nitrosylation of Drp1 mediates beta-amyloid-related mitochondrial fission and neuronal injury.* Science, 2009. **324**(5923): p. 102-5.
55. Chang, C.R. and C. Blackstone, *Cyclic AMP-dependent protein kinase phosphorylation of Drp1 regulates its GTPase activity and mitochondrial morphology.* J Biol Chem, 2007. **282**(30): p. 21583-7.
56. Cribbs, J.T. and S. Strack, *Reversible phosphorylation of Drp1 by cyclic AMP-dependent protein kinase and calcineurin regulates mitochondrial fission and cell death.* EMBO Rep, 2007. **8**(10): p. 939-44.
57. Gomes, L.C., G. Di Benedetto, and L. Scorrano, *During autophagy mitochondria elongate, are spared from degradation and sustain cell viability.* Nat Cell Biol, 2011. **13**(5): p. 589-98.
58. Han, X.J., et al., *CaM kinase I alpha-induced phosphorylation of Drp1 regulates mitochondrial morphology.* J Cell Biol, 2008. **182**(3): p. 573-85.
59. Gawlowski, T., et al., *Modulation of dynamin-related protein 1 (DRP1) function by increased O-linked-beta-N-acetylglucosamine modification (O-GlcNAc) in cardiac myocytes.* J Biol Chem, 2012. **287**(35): p. 30024-34.
60. Nakamura, N., et al., *MARCH-V is a novel mitofusin 2- and Drp1-binding protein able to change mitochondrial morphology.* EMBO Rep, 2006. **7**(10): p. 1019-22.
61. Wang, H., et al., *Parkin ubiquitinates Drp1 for proteasome-dependent degradation: implication of dysregulated mitochondrial dynamics in Parkinson disease.* J Biol Chem, 2011. **286**(13): p. 11649-58.
62. Kashatus, J.A., et al., *Erk2 phosphorylation of Drp1 promotes mitochondrial fission and MAPK-driven tumor growth.* Mol Cell, 2015. **57**(3): p. 537-51.
63. Taguchi, N., et al., *Mitotic phosphorylation of dynamin-related GTPase Drp1 participates in mitochondrial fission.* J Biol Chem, 2007. **282**(15): p. 11521-9.
64. Merrill, R.A., et al., *Mechanism of neuroprotective mitochondrial remodeling by PKA/AKAP1.* PLoS Biol, 2011. **9**(4): p. e1000612.

65. Cereghetti, G.M., et al., *Dephosphorylation by calcineurin regulates translocation of Drp1 to mitochondria.* Proc Natl Acad Sci U S A, 2008. **105**(41): p. 15803-8.
66. Slupe, A.M., et al., *A calcineurin docking motif (LXVP) in dynamin-related protein 1 contributes to mitochondrial fragmentation and ischemic neuronal injury.* J Biol Chem, 2013. **288**(17): p. 12353-65.
67. Kim, H., et al., *Fine-tuning of Drp1/Fis1 availability by AKAP121/Siah2 regulates mitochondrial adaptation to hypoxia.* Mol Cell, 2011. **44**(4): p. 532-44.
68. Sharp, W.W., et al., *Dynamin-related protein 1 (Drp1)-mediated diastolic dysfunction in myocardial ischemia-reperfusion injury: therapeutic benefits of Drp1 inhibition to reduce mitochondrial fission.* Faseb j, 2014. **28**(1): p. 316-26.
69. Sharp, W.W., et al., *Inhibition of the mitochondrial fission protein dynamin-related protein 1 improves survival in a murine cardiac arrest model.* Crit Care Med, 2015. **43**(2): p. e38-47.
70. Otera, H., et al., *Mff is an essential factor for mitochondrial recruitment of Drp1 during mitochondrial fission in mammalian cells*. J Cell Biol, 2010. **191**(6): p. 1141-58.
71. Palmer, C.S., et al., *MiD49 and MiD51, new components of the mitochondrial fission machinery.* EMBO Rep, 2011. **12**(6): p. 565-73.
72. Palmer, C.S., et al., *Adaptor proteins MiD49 and MiD51 can act independently of Mff and Fis1 in Drp1 recruitment and are specific for mitochondrial fission.* J Biol Chem, 2013. **288**(38): p. 27584-93.
73. Huang, P., C.A. Galloway, and Y. Yoon, *Control of mitochondrial morphology through differential interactions of mitochondrial fusion and fission proteins.* PLoS One, 2011. **6**(5): p. e20655.
74. Frank, S., et al., *The role of dynamin-related protein 1, a mediator of mitochondrial fission, in apoptosis.* Dev Cell, 2001. **1**(4): p. 515-25.
75. Cassidy-Stone, A., et al., *Chemical inhibition of the mitochondrial division dynamin reveals its role in Bax/Bak-dependent mitochondrial outer membrane permeabilization.* Dev Cell, 2008. **14**(2): p. 193-204.
76. Parone, P.A., et al., *Inhibiting the mitochondrial fission machinery does not prevent Bax/Bak-dependent apoptosis.* Mol Cell Biol, 2006. **26**(20): p. 7397-408.
77. Szabadkai, G., et al., *Drp-1-dependent division of the mitochondrial network blocks intraorganellar Ca2+ waves and protects against Ca2+-mediated apoptosis.* Mol Cell, 2004. **16**(1): p. 59-68.
78. Ashrafian, H., et al., *A mutation in the mitochondrial fission gene Dnm1l leads to cardiomyopathy.* PLoS Genet, 2010. **6**(6): p. e1001000.
79. Ikeda, Y., et al., *Endogenous Drp1 mediates mitochondrial autophagy and protects the heart against energy stress.* Circ Res, 2015. **116**(2): p. 264-78.
80. Song, M., et al., *Mitochondrial fission and fusion factors reciprocally orchestrate mitophagic culling in mouse hearts and cultured fibroblasts.* Cell Metab, 2015. **21**(2): p. 273-85.
81. Kageyama, Y., et al., *Parkin-independent mitophagy requires Drp1 and maintains the integrity of mammalian heart and brain.* EMBO J, 2014. **33**(23): p. 2798-813.
82. Pennanen, C., et al., *Mitochondrial fission is required for cardiomyocyte hypertrophy mediated by a Ca2+-calcineurin signaling pathway.* J Cell Sci, 2014. **127**(Pt 12): p. 2659-71.
83. Zepeda, R., et al., *Drp1 loss-of-function reduces cardiomyocyte oxygen dependence protecting the heart from ischemia-reperfusion injury.* J Cardiovasc Pharmacol, 2014. **63**(6): p. 477-87.
84. Ong, S.B., et al., *Inhibiting mitochondrial fission protects the heart against ischemia/reperfusion injury.* Circulation, 2010. **121**(18): p. 2012-22.
85. Givvimani, S., et al., *Mitochondrial division/mitophagy inhibitor (Mdivi) ameliorates pressure overload induced heart failure.* PLoS One, 2012. **7**(3): p. e32388.
86. Qi, X., et al., *A novel Drp1 inhibitor diminishes aberrant mitochondrial fission and neurotoxicity.* J Cell Sci, 2013. **126**(Pt 3): p. 789-802.

87. Disatnik, M.H., et al., *Acute inhibition of excessive mitochondrial fission after myocardial infarction prevents long-term cardiac dysfunction.* J Am Heart Assoc, 2013. **2**(5): p. e000461.
88. Sharp, W.W., *Dynamin-related protein 1 as a therapeutic target in cardiac arrest.* J Mol Med (Berl), 2015. **93**(3): p. 243-52.
89. Merrill, R.A. and S. Strack, *Mitochondria: a kinase anchoring protein 1, a signaling platform for mitochondrial form and function.* Int J Biochem Cell Biol, 2014. **48**: p. 92-6.
90. Song, M., et al., *Super-suppression of mitochondrial reactive oxygen species signaling impairs compensatory autophagy in primary mitophagic cardiomyopathy.* Circ Res, 2014. **115**(3): p. 348-53.
91. Granger, D.N. and P.R. Kvietys, *Reperfusion injury and reactive oxygen species: The evolution of a concept.* Redox Biol, 2015. **6**: p. 524-51.
92. Giordano, F.J., *Oxygen, oxidative stress, hypoxia, and heart failure.* J Clin Invest, 2005. **115**(3): p. 500-8.
93. Ong, S.B. and D.J. Hausenloy, *Mitochondrial morphology and cardiovascular disease.* Cardiovasc Res, 2010. **88**(1): p. 16-29.
94. Ratcliffe, N.A. and P.E. King, *Ultrastructural changes in the mitochondria of the acid gland of Nasonia vitripennis (Walker) (Pteromalidae: Hymenoptera) induced by starvation.* Z Zellforsch Mikrosk Anat, 1969. **99**(3): p. 459-68.
95. Wilson, J.W. and E.H. Leduc, *Mitochondrial changes in the liver of essential fatty acid-deficient mice.* J Cell Biol, 1963. **16**: p. 281-96.
96. Zauner, C., et al., *Resting energy expenditure in short-term starvation is increased as a result of an increase in serum norepinephrine.* Am J Clin Nutr, 2000. **71**(6): p. 1511-5.
97. Leiter, L.A., et al., *Catecholamine responses to hypocaloric diets and fasting in obese human subjects.* Am J Physiol, 1984. **247**(2 Pt 1): p. E190-7.
98. Walter, R.M., et al., *The effect of adrenergic blockade on the glucagon responses to starvation and hypoglycemia in man.* J Clin Invest, 1974. **54**(5): p. 1214-20.
99. Zhang, J., et al., *Insulin disrupts beta-adrenergic signalling to protein kinase A in adipocytes.* Nature, 2005. **437**(7058): p. 569-73.
100. Mayo, K.E., et al., *International Union of Pharmacology. XXXV. The glucagon receptor family.* Pharmacol Rev, 2003. **55**(1): p. 167-94.
101. Unger, R.H., *Glucagon physiology and pathophysiology in the light of new advances.* Diabetologia, 1985. **28**(8): p. 574-8.
102. McKnight, G.S., *Cyclic AMP second messenger systems.* Curr Opin Cell Biol, 1991. **3**(2): p. 213-7.
103. Bradshaw, R.A., Stahl, P.D. , *Encylopedia of Cell Biology* 2015, Cambridge MA: Academic Press
104. Filomeni, G., et al., *Under the ROS...thiol network is the principal suspect for autophagy commitment.* Autophagy, 2010. **6**(7): p. 999-1005.
105. Filomeni, G., D. De Zio, and F. Cecconi, *Oxidative stress and autophagy: the clash between damage and metabolic needs.* Cell Death Differ, 2015. **22**(3): p. 377-88.
106. Murphy, M.P., *How mitochondria produce reactive oxygen species.* Biochem J, 2009. **417**(1): p. 1-13.
107. Scherz-Shouval, R. and Z. Elazar, *ROS, mitochondria and the regulation of autophagy.* Trends Cell Biol, 2007. **17**(9): p. 422-7.
108. Scherz-Shouval, R., et al., *Reactive oxygen species are essential for autophagy and specifically regulate the activity of Atg4.* Embo j, 2007. **26**(7): p. 1749-60.
109. Chen, Y. and S.B. Gibson, *Is mitochondrial generation of reactive oxygen species a trigger for autophagy?* Autophagy, 2008. **4**(2): p. 246-8.
110. Yu, L., et al., *Autophagic programmed cell death by selective catalase degradation.* Proc Natl Acad Sci U S A, 2006. **103**(13): p. 4952-7.
111. Chen, Y., M.B. Azad, and S.B. Gibson, *Superoxide is the major reactive oxygen species regulating autophagy.* Cell Death Differ, 2009. **16**(7): p. 1040-52.

112. Ferretti, A.C., et al., *Protein kinase A signals apoptotic activation in glucose-deprived hepatocytes: participation of reactive oxygen species.* Apoptosis, 2012. **17**(5): p. 475-91.
113. Wang, Q.D., et al., *Cyclic fluctuations in the cardiac performance of the isolated Langendorff-perfused mouse heart: pyruvate abolishes the fluctuations and has an anti-ischaemic effect.* Acta Physiol Scand, 2002. **175**(4): p. 279-87.
114. Sutherland, F.J., et al., *Mouse isolated perfused heart: characteristics and cautions.* Clin Exp Pharmacol Physiol, 2003. **30**(11): p. 867-78.
115. Johanns, M., et al., *AMPK antagonizes hepatic glucagon-stimulated cyclic AMP signalling via phosphorylation-induced activation of cyclic nucleotide phosphodiesterase 4B.* Nat Commun, 2016. **7**: p. 10856.
116. Hearse, D.J., et al., *Xanthine oxidase: a critical mediator of myocardial injury during ischemia and reperfusion?* Acta Physiol Scand Suppl, 1986. **548**: p. 65-78.
117. Chambers, D.E., et al., *Xanthine oxidase as a source of free radical damage in myocardial ischemia.* J Mol Cell Cardiol, 1985. **17**(2): p. 145-52.
118. Ikeda, Y., et al., *PR-39, a proline/arginine-rich antimicrobial peptide, exerts cardioprotective effects in myocardial ischemia-reperfusion.* Cardiovasc Res, 2001. **49**(1): p. 69-77.
119. Paradies, G., et al., *Decrease in mitochondrial complex I activity in ischemic/reperfused rat heart: involvement of reactive oxygen species and cardiolipin.* Circ Res, 2004. **94**(1): p. 53-9.
120. Chouchani, E.T., et al., *Ischaemic accumulation of succinate controls reperfusion injury through mitochondrial ROS.* Nature, 2014. **515**(7527): p. 431-5.
121. Chouchani, E.T., et al., *A Unifying Mechanism for Mitochondrial Superoxide Production during Ischemia-Reperfusion Injury.* Cell Metab, 2016. **23**(2): p. 254-63.
122. Perkins, K.A., et al., *The effects of modulating eNOS activity and coupling in ischemia/reperfusion (I/R).* Naunyn Schmiedebergs Arch Pharmacol, 2012. **385**(1): p. 27-38.
123. Granville, D.J., et al., *Reduction of ischemia and reperfusion-induced myocardial damage by cytochrome P450 inhibitors.* Proc Natl Acad Sci U S A, 2004. **101**(5): p. 1321-6.
124. Bianchi, P., et al., *Oxidative stress by monoamine oxidase mediates receptor-independent cardiomyocyte apoptosis by serotonin and postischemic myocardial injury.* Circulation, 2005. **112**(21): p. 3297-305.
125. Yang, C., et al., *Early ischaemic preconditioning requires Akt- and PKA-mediated activation of eNOS via serine1176 phosphorylation.* Cardiovasc Res, 2013. **97**(1): p. 33-43.
126. Asai, M., et al., *PKA rapidly enhances proteasome assembly and activity in in vivo canine hearts.* J Mol Cell Cardiol, 2009. **46**(4): p. 452-62.
127. Khaliulin, I., J.E. Parker, and A.P. Halestrap, *Consecutive pharmacological activation of PKA and PKC mimics the potent cardioprotection of temperature preconditioning.* Cardiovasc Res, 2010. **88**(2): p. 324-33.
128. Dorsch, M., et al., *Morphine-Induced Preconditioning: Involvement of Protein Kinase A and Mitochondrial Permeability Transition Pore.* PLoS One, 2016. **11**(3): p. e0151025.
129. Huang, M.H., et al., *Therapeutic synergy and complementarity for ischemia/reperfusion injury: beta1-adrenergic blockade and phosphodiesterase-3 inhibition.* Int J Cardiol, 2016. **214**: p. 374-80.
130. Chung, Y.W., et al., *Targeted disruption of PDE3B, but not PDE3A, protects murine heart from ischemia/reperfusion injury.* Proc Natl Acad Sci U S A, 2015. **112**(17): p. E2253-62.
131. Huang, M.H., et al., *Heart protection by combination therapy with esmolol and milrinone at late-ischemia and early reperfusion.* Cardiovasc Drugs Ther, 2011. **25**(3): p. 223-32.
132. Edwards, H.V., J.D. Scott, and G.S. Baillie, *PKA phosphorylation of the small heat-shock protein Hsp20 enhances its cardioprotective effects.* Biochem Soc Trans, 2012. **40**(1): p. 210-4.
133. Nishida, H., et al., *Infarct size limitation by adrenomedullin: protein kinase A but not PI3-kinase is linked to mitochondrial KCa channels.* Cardiovasc Res, 2008. **77**(2): p. 398-405.
134. Song, M., et al., *Interdependence of Parkin-Mediated Mitophagy and Mitochondrial Fission in Adult Mouse Hearts.* Circ Res, 2015. **117**(4): p. 346-51.

135. Kamga Pride, C., et al., *Nitrite activates protein kinase A in normoxia to mediate mitochondrial fusion and tolerance to ischaemia/reperfusion.* Cardiovasc Res, 2014. **101**(1): p. 57-68.
136. Gao, D., et al., *Dynasore protects mitochondria and improves cardiac lusitropy in Langendorff perfused mouse heart.* PLoS One, 2013. **8**(4): p. e60967.
137. Burgoyne, J.R. and P. Eaton, *Transnitrosylating nitric oxide species directly activate type I protein kinase A, providing a novel adenylate cyclase-independent cross-talk to beta-adrenergic-like signaling.* J Biol Chem, 2009. **284**(43): p. 29260-8.
138. Franco, S.J., et al., *Calpain-mediated proteolysis of talin regulates adhesion dynamics.* Nat Cell Biol, 2004. **6**(10): p. 977-83.
139. Zhang, Z., et al., *Multiple alphaII-spectrin breakdown products distinguish calpain and caspase dominated necrotic and apoptotic cell death pathways.* Apoptosis, 2009. **14**(11): p. 1289-98.
140. Guo, A., et al., *Molecular Determinants of Calpain-dependent Cleavage of Junctophilin-2 Protein in Cardiomyocytes.* J Biol Chem, 2015. **290**(29): p. 17946-55.
141. Parascandola, J., *Dinitrophenol and bioenergetics: an historical perspective.* Mol Cell Biochem, 1974. **5**(1-2): p. 69-77.
142. Harper, J.A., K. Dickinson, and M.D. Brand, *Mitochondrial uncoupling as a target for drug development for the treatment of obesity.* Obes Rev, 2001. **2**(4): p. 255-65.
143. Luz, A.L., et al., *Mitochondrial Morphology and Fundamental Parameters of the Mitochondrial Respiratory Chain Are Altered in Caenorhabditis elegans Strains Deficient in Mitochondrial Dynamics and Homeostasis Processes.* PLoS One, 2015. **10**(6): p. e0130940.
144. Schlagowski, A.I., et al., *Mitochondrial uncoupling reduces exercise capacity despite several skeletal muscle metabolic adaptations.* J Appl Physiol (1985), 2014. **116**(4): p. 364-75.
145. Egan, D.F., et al., *Phosphorylation of ULK1 (hATG1) by AMP-activated protein kinase connects energy sensing to mitophagy.* Science, 2011. **331**(6016): p. 456-61.
146. Kim, J., et al., *AMPK and mTOR regulate autophagy through direct phosphorylation of Ulk1.* Nat Cell Biol, 2011. **13**(2): p. 132-41.
147. Qi, Z., et al., *Antioxidant supplement inhibits skeletal muscle constitutive autophagy rather than fasting-induced autophagy in mice.* Oxid Med Cell Longev, 2014. **2014**: p. 315896.
148. Jung, E.H., et al., *AMPK activation by liquiritigenin inhibited oxidative hepatic injury and mitochondrial dysfunction induced by nutrition deprivation as mediated with induction of farnesoid X receptor.* Eur J Nutr, 2015.
149. Saito, S., et al., *Glucose Fluctuations Aggravate Cardiac Susceptibility to Ischemia/Reperfusion Injury by Modulating MicroRNAs Expression.* Circ J, 2016. **80**(1): p. 186-95.
150. Wu, W., et al., *FUNDC1 regulates mitochondrial dynamics at the ER-mitochondrial contact site under hypoxic conditions.* Embo j, 2016. **35**(13): p. 1368-84.
151. Zhang, L., et al., *Reactive oxygen species effect PASMCs apoptosis via regulation of dynamin-related protein 1 in hypoxic pulmonary hypertension.* Histochem Cell Biol, 2016. **146**(1): p. 71-84.
152. Shen, T., et al., *The Critical Role of Dynamin-Related Protein 1 in Hypoxia-Induced Pulmonary Vascular Angiogenesis.* J Cell Biochem, 2015. **116**(9): p. 1993-2007.
153. Tekin, D., A.D. Dursun, and L. Xi, *Hypoxia inducible factor 1 (HIF-1) and cardioprotection.* Acta Pharmacol Sin, 2010. **31**(9): p. 1085-94.
154. Hoshino, A., et al., *Cytosolic p53 inhibits Parkin-mediated mitophagy and promotes mitochondrial dysfunction in the mouse heart.* Nat Commun, 2013. **4**: p. 2308.
155. Khraiwesh, H., et al., *Mitochondrial ultrastructure and markers of dynamics in hepatocytes from aged, calorie restricted mice fed with different dietary fats.* Exp Gerontol, 2014. **56**: p. 77-88.
156. Jarnaess, E., et al., *Splicing factor arginine/serine-rich 17A (SFRS17A) is an A-kinase anchoring protein that targets protein kinase A to splicing factor compartments.* J Biol Chem, 2009. **284**(50): p. 35154-64.

157. Lignitto, L., et al., *Control of PKA stability and signalling by the RING ligase praja2.* Nat Cell Biol, 2011. **13**(4): p. 412-22.
158. Hanke, S.E., et al., *Cyclic nucleotides as affinity tools: phosphorothioate cAMP analogues address specific PKA subproteomes.* N Biotechnol, 2011. **28**(4): p. 294-301.
159. Bertinetti, D., et al., *Chemical tools selectively target components of the PKA system.* BMC Chem Biol, 2009. **9**: p. 3.
160. Boeshans, K.M., et al., *Structural characterization of the membrane-associated regulatory subunit of type I cAMP-dependent protein kinase by mass spectrometry: identification of Ser81 as the in vivo phosphorylation site of RIalpha.* Protein Sci, 1999. **8**(7): p. 1515-22.
161. Colledge, M. and J.D. Scott, *AKAPs: from structure to function.* Trends Cell Biol, 1999. **9**(6): p. 216-21.
162. Rodriguez-Vargas, J.M., et al., *ROS-induced DNA damage and PARP-1 are required for optimal induction of starvation-induced autophagy.* Cell Res, 2012. **22**(7): p. 1181-98.
163. Rahman, M., et al., *Reactive oxygen species regulation of autophagy in skeletal muscles.* Antioxid Redox Signal, 2014. **20**(3): p. 443-59.
164. Scherz-Shouval, R., E. Shvets, and Z. Elazar, *Oxidation as a post-translational modification that regulates autophagy.* Autophagy, 2007. **3**(4): p. 371-3.
165. Smirnova, E., et al., *A human dynamin-related protein controls the distribution of mitochondria.* J Cell Biol, 1998. **143**(2): p. 351-8.
166. Strack, S. and J.T. Cribbs, *Allosteric modulation of Drp1 mechanoenzyme assembly and mitochondrial fission by the variable domain.* J Biol Chem, 2012. **287**(14): p. 10990-1001.
167. Shirihai, O.S., M. Song, and G.W. Dorn, 2nd, *How mitochondrial dynamism orchestrates mitophagy.* Circ Res, 2015. **116**(11): p. 1835-49.
168. Lotz, C., et al., *Characterization, design, and function of the mitochondrial proteome: from organs to organisms.* J Proteome Res, 2014. **13**(2): p. 433-46.
169. Kinoshita, E., et al., *Phosphate-binding tag, a new tool to visualize phosphorylated proteins.* Mol Cell Proteomics, 2006. **5**(4): p. 749-57.
170. Backus, K.M., et al., *Proteome-wide covalent ligand discovery in native biological systems.* Nature, 2016. **534**(7608): p. 570-4.
171. Nelson, K.J., et al., *Use of dimedone-based chemical probes for sulfenic acid detection methods to visualize and identify labeled proteins.* Methods Enzymol, 2010. **473**: p. 95-115.
172. Zakhary, D.R., et al., *Protein kinase A (PKA)-dependent troponin-I phosphorylation and PKA regulatory subunits are decreased in human dilated cardiomyopathy.* Circulation, 1999. **99**(4): p. 505-10.
173. Han, Y.S., J. Arroyo, and O. Ogut, *Human heart failure is accompanied by altered protein kinase A subunit expression and post-translational state.* Arch Biochem Biophys, 2013. **538**(1): p. 25-33.
174. Hathaway, N., *Redox regulation of Type Ia PKA in the Heart* Kings College London, 2011.
175. Loilome, W., et al., *PRKAR1A is overexpressed and represents a possible therapeutic target in human cholangiocarcinoma.* Int J Cancer, 2011. **129**(1): p. 34-44.
176. Mantovani, G., et al., *High expression of PKA regulatory subunit 1A protein is related to proliferation of human melanoma cells.* Oncogene, 2008. **27**(13): p. 1834-43.
177. McDaid, H.M., et al., *Increased expression of the RIalpha subunit of the cAMP-dependent protein kinase A is associated with advanced stage ovarian cancer.* Br J Cancer, 1999. **79**(5-6): p. 933-9.
178. Bradbury, A.W., et al., *Protein kinase A (PK-A) regulatory subunit expression in colorectal cancer and related mucosa.* Br J Cancer, 1994. **69**(4): p. 738-42.
179. Bertherat, J., et al., *Mutations in regulatory subunit type 1A of cyclic adenosine 5'-monophosphate-dependent protein kinase (PRKAR1A): phenotype analysis in 353 patients and 80 different genotypes.* J Clin Endocrinol Metab, 2009. **94**(6): p. 2085-91.

180. Blackstone, C. and C.R. Chang, *Mitochondria unite to survive.* Nat Cell Biol, 2011. **13**(5): p. 521-2.
181. Hailey, D.W., et al., *Mitochondria supply membranes for autophagosome biogenesis during starvation.* Cell, 2010. **141**(4): p. 656-67.
182. Tanida, I., T. Ueno, and E. Kominami, *LC3 and Autophagy.* Methods Mol Biol, 2008. **445**: p. 77-88.
183. Mizushima, N. and T. Yoshimori, *How to interpret LC3 immunoblotting.* Autophagy, 2007. **3**(6): p. 542-5.
184. Cherra, S.J., 3rd, et al., *Regulation of the autophagy protein LC3 by phosphorylation.* J Cell Biol, 2010. **190**(4): p. 533-9.
185. Nath, K.A., et al., *alpha-Ketoacids scavenge H2O2 in vitro and in vivo and reduce menadione-induced DNA injury and cytotoxicity.* Am J Physiol, 1995. **268**(1 Pt 1): p. C227-36.
186. Lopalco, A., et al., *Mechanism of Decarboxylation of Pyruvic Acid in the Presence of Hydrogen Peroxide.* J Pharm Sci, 2016. **105**(2): p. 705-13.
187. Kolwicz, S.C., Jr. and R. Tian, *Glucose metabolism and cardiac hypertrophy.* Cardiovasc Res, 2011. **90**(2): p. 194-201.
188. Lopalco, A. and V.J. Stella, *Effect of Molecular Structure on the Relative Hydrogen Peroxide Scavenging Ability of Some alpha-Keto Carboxylic Acids.* J Pharm Sci, 2016.
189. Giandomenico, A.R., et al., *The importance of sodium pyruvate in assessing damage produced by hydrogen peroxide.* Free Radic Biol Med, 1997. **23**(3): p. 426-34.
190. Babich, H., et al., *Choice of DMEM, formulated with or without pyruvate, plays an important role in assessing the in vitro cytotoxicity of oxidants and prooxidant nutraceuticals.* In Vitro Cell Dev Biol Anim, 2009. **45**(5-6): p. 226-33.
191. Miwa, H., et al., *Pyruvate secreted by human lymphoid cell lines protects cells from hydrogen peroxide mediated cell death.* Free Radic Res, 2000. **33**(1): p. 45-56.
192. Long, L.H. and B. Halliwell, *The effects of oxaloacetate on hydrogen peroxide generation from ascorbate and epigallocatechin gallate in cell culture media: potential for altering cell metabolism.* Biochem Biophys Res Commun, 2012. **417**(1): p. 446-50.
193. Long, L.H. and B. Halliwell, *Artefacts in cell culture: pyruvate as a scavenger of hydrogen peroxide generated by ascorbate or epigallocatechin gallate in cell culture media.* Biochem Biophys Res Commun, 2009. **388**(4): p. 700-4.
194. Yanos, J., M.J. Patti, and R.T. Stanko, *Hemodynamic effects of intravenous pyruvate in the intact, anesthetized dog.* Crit Care Med, 1994. **22**(5): p. 844-50.
195. Dobsak, P., et al., *Antioxidative properties of pyruvate and protection of the ischemic rat heart during cardioplegia.* J Cardiovasc Pharmacol, 1999. **34**(5): p. 651-9.
196. Kobayashi, K. and J.R. Neely, *Effects of ischemia and reperfusion on pyruvate dehydrogenase activity in isolated rat hearts.* J Mol Cell Cardiol, 1983. **15**(6): p. 359-67.
197. Mentzer, R.M., Jr., et al., *Effect of pyruvate on regional ventricular function in normal and stunned myocardium.* Ann Surg, 1989. **209**(5): p. 629-33; discussion 633-4.
198. Hermann, H.P., et al., *Haemodynamic effects of intracoronary pyruvate in patients with congestive heart failure: an open study.* Lancet, 1999. **353**(9161): p. 1321-3.
199. Hermann, H.P., et al., *Improved systolic and diastolic myocardial function with intracoronary pyruvate in patients with congestive heart failure.* Eur J Heart Fail, 2004. **6**(2): p. 213-8.
200. Terrin, A., et al., *PGE(1) stimulation of HEK293 cells generates multiple contiguous domains with different [cAMP]: role of compartmentalized phosphodiesterases.* J Cell Biol, 2006. **175**(3): p. 441-51.
201. Zaccolo, M. and T. Pozzan, *Discrete microdomains with high concentration of cAMP in stimulated rat neonatal cardiac myocytes.* Science, 2002. **295**(5560): p. 1711-5.
202. Buxton, I.L. and L.L. Brunton, *Compartments of cyclic AMP and protein kinase in mammalian cardiomyocytes.* J Biol Chem, 1983. **258**(17): p. 10233-9.

203. Di Benedetto, G., et al., *Protein kinase A type I and type II define distinct intracellular signaling compartments.* Circ Res, 2008. **103**(8): p. 836-44.
204. Anand, G., S.S. Taylor, and D.A. Johnson, *Cyclic-AMP and pseudosubstrate effects on type-I A-kinase regulatory and catalytic subunit binding kinetics.* Biochemistry, 2007. **46**(32): p. 9283-91.
205. Oviosu, O., *Type Iα PKAas a co-incidence detector: Integration of cAMPand oxidant signals.* Kings College London 2016.
206. Pinto, A.R., et al., *Revisiting Cardiac Cellular Composition.* Circ Res, 2016. **118**(3): p. 400-9.
207. Humphries, K.M., C. Juliano, and S.S. Taylor, *Regulation of cAMP-dependent protein kinase activity by glutathionylation.* J Biol Chem, 2002. **277**(45): p. 43505-11.
208. Santos, C.X., et al., *Targeted redox inhibition of protein phosphatase 1 by Nox4 regulates eIF2alpha-mediated stress signaling.* Embo j, 2016. **35**(3): p. 319-34.
209. Sadayappan, S., et al., *A critical function for Ser-282 in cardiac Myosin binding protein-C phosphorylation and cardiac function.* Circ Res, 2011. **109**(2): p. 141-50.
210. Thoonen, R., et al., *Molecular Screen Identifies Cardiac Myosin-Binding Protein-C as a Protein Kinase G-Ialpha Substrate.* Circ Heart Fail, 2015. **8**(6): p. 1115-22.
211. Carruthers, N.J. and P.M. Stemmer, *Methionine oxidation in the calmodulin-binding domain of calcineurin disrupts calmodulin binding and calcineurin activation.* Biochemistry, 2008. **47**(10): p. 3085-95.
212. Persad, S., et al., *Modification of cardiac beta-adrenoceptor mechanisms by H2O2.* Am J Physiol, 1998. **274**(2 Pt 2): p. H416-23.
213. Persad, S., V. Panagia, and N.S. Dhalla, *Role of H2O2 in changing beta-adrenoceptor and adenylyl cyclase in ischemia-reperfused hearts.* Mol Cell Biochem, 1998. **186**(1-2): p. 99-106.
214. Van der Vliet, A. and A. Bast, *Hydrogen peroxide reduces beta-adrenoceptor function in the rat small intestine.* Eur J Pharmacol, 1991. **199**(2): p. 153-6.
215. Kramer, K., et al., *A disbalance between beta-adrenergic and muscarinic responses caused by hydrogen peroxide in rat airways in vitro.* Biochem Biophys Res Commun, 1987. **145**(1): p. 357-62.
216. Piechocki, J.T.T., K. , *Pharmaceutical Photostability and Stabilization Technology*. 2006: CRC Press.
217. Terland, O., et al., *One-electron oxidation of catecholamines generates free radicals with an in vitro toxicity correlating with their lifetime.* Free Radic Biol Med, 2006. **41**(8): p. 1266-71.
218. Haskova, P., et al., *Iron chelation with salicylaldehyde isonicotinoyl hydrazone protects against catecholamine autoxidation and cardiotoxicity.* Free Radic Biol Med, 2011. **50**(4): p. 537-49.
219. Remiao, F., et al., *Copper enhances isoproterenol toxicity in isolated rat cardiomyocytes: effects on oxidative stress.* Cardiovasc Toxicol, 2001. **1**(3): p. 195-204.
220. Burgoyne, J.R., et al., *Hydrogen peroxide sensing and signaling by protein kinases in the cardiovascular system.* Antioxid Redox Signal, 2013. **18**(9): p. 1042-52.

Appendix

A1. Supplementary data

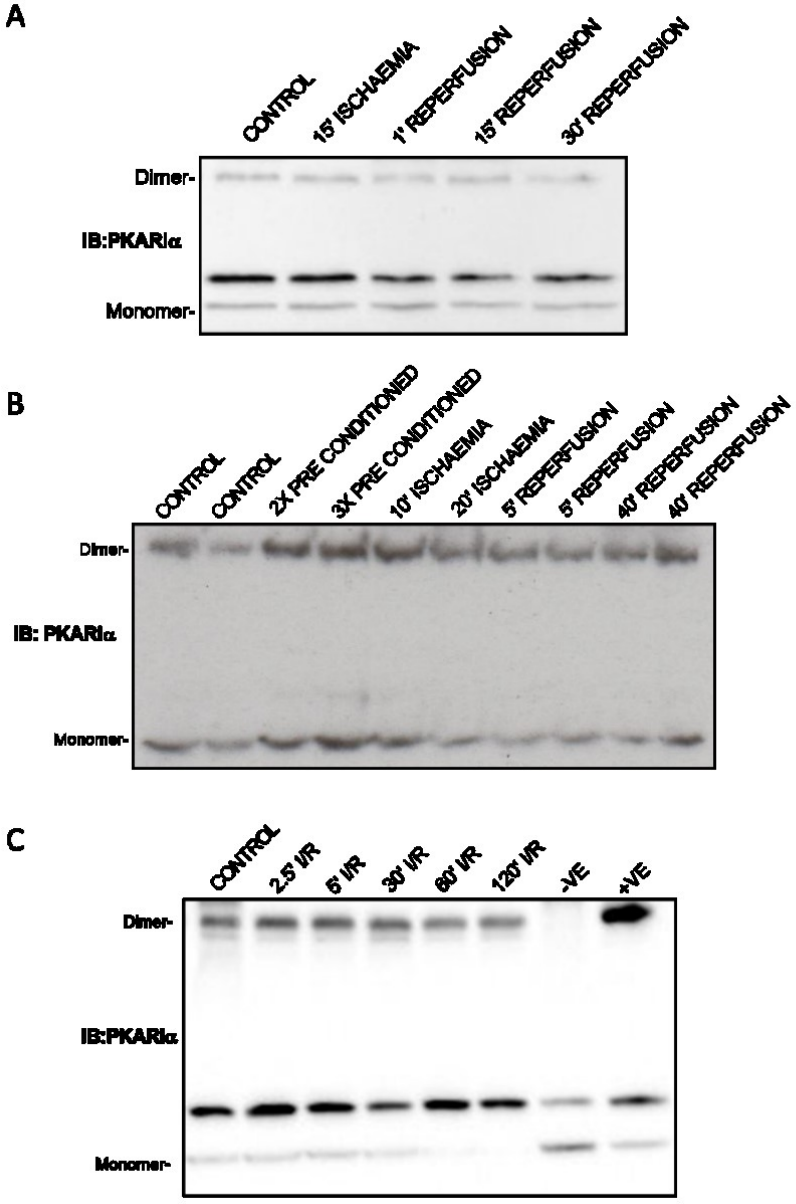

Figure S1. Ex-vivo ischaemia-reperfusion experiment does not induce disulfide PKARIα. Three separate experiments were undertaken using various periods of I/R. All interventions were preceded by a 20 minute stabilisation period. **(A)** Immunoblot of PKARIα from hearts subject to 15 minutes ischaemia, or 15 minutes of ischaemia followed by 1, 15 or 30 minutes of reperfusion. **(B)** Immunoblot of PKARIα from hearts subject to two and three bouts of pre-conditioning (1 minute ischaemia followed by 1 minute of reperfusion), 10 or 20 minutes of ischaemia, and 5 or 40 minutes of reperfusion following 20 minutes of ischaemia. **(C)** Immunoblot of PKARIα from hearts subject to 30 minutes of ischaemia followed by 2.5, 5, 30, 60 or 120 minutes of reperfusion. –ve, negative control (PKARIα C17S KI sample) and +ve, heart perfused with 100 μM H_2O_2. All controls were time matched.

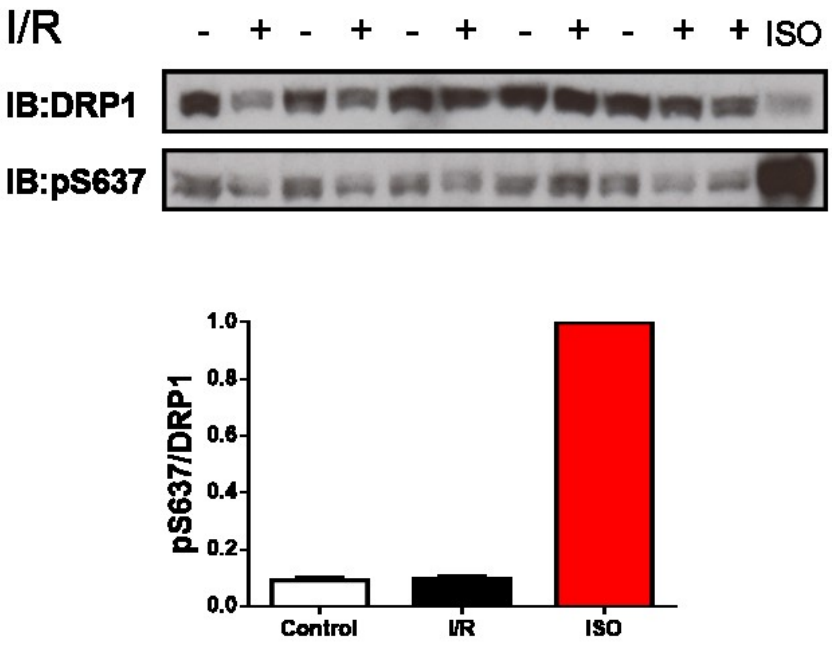

Figure S2. Ex-vivo ischaemia-reperfusion experiment does not alter pDRP1-S637. Immunoblot of DRP1 and pDRP1-S637 from mice hearts subjected to 30 minutes of ischaemia followed by 60 minutes of reperfusion. A mouse IP injected with isoprenaline served as a positive control for pDRP1-S637. (controls n=5, I/R n=6, ±SEM).

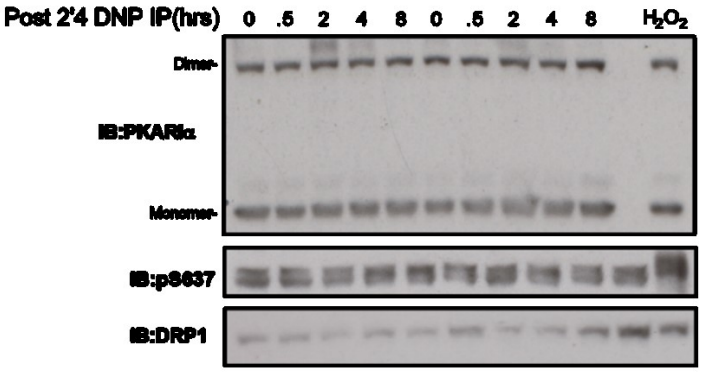

Figure S3. Mitochondrial uncoupling with DNP does not induce changes in disulfide PKARIα. Immunoblot of PKARIα and pDRP1-S637 in hearts from mice treated with DNP. Mice were injected with DNP (30 mg/kg) and hearts harvested 2, 4, and 8 hours post injection. Control mice received an equal volume of 0.9 % NaCl and were harvested 8 hours post IP. Hearts were immediately snap-frozen in liquid nitrogen.

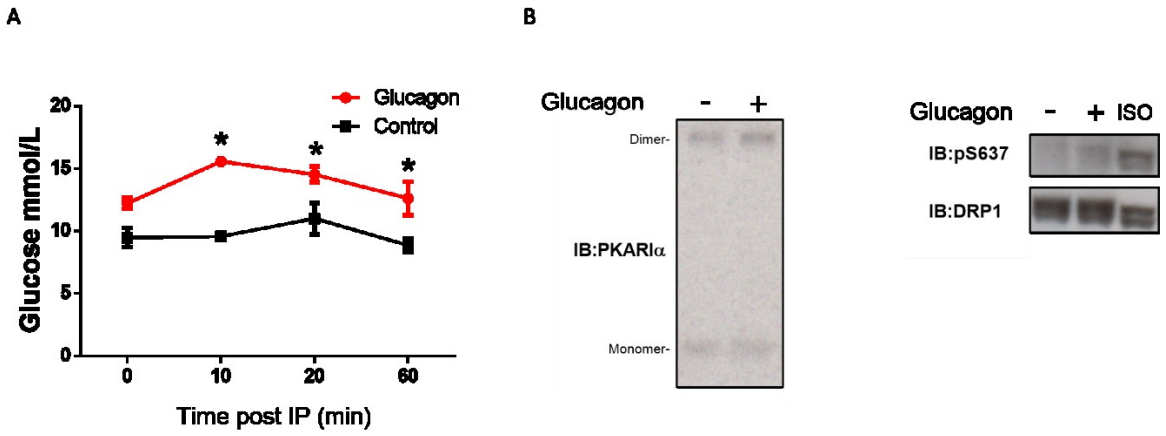

Figure S4. Glucagon elevates blood glucose but does not alter disulfide PKARIα formation or pDRP1-s637. Mice were fasted for 6 hours prior to glucagon (1 mg/kg) IP injection. Blood glucose measurements were taken 10, 30 and 60 minutes post-IP and assessed with an Akku Chek blood glucose monitor. Control animals had ab libitum chow access at all times. Hearts were harvested after the final blood glucose measurement and immediately snap-frozen in liquid nitrogen. **(A)** Blood glucose response to glucagon IP after 6 hours fasting. **(B)** Immunoblot of PKARIα and pDRP1-S637 in hearts from glucagon injected mice. * $p<0.05$ difference from Control group (Repeated measures Two way ANOVA, multiple comparison between groups).

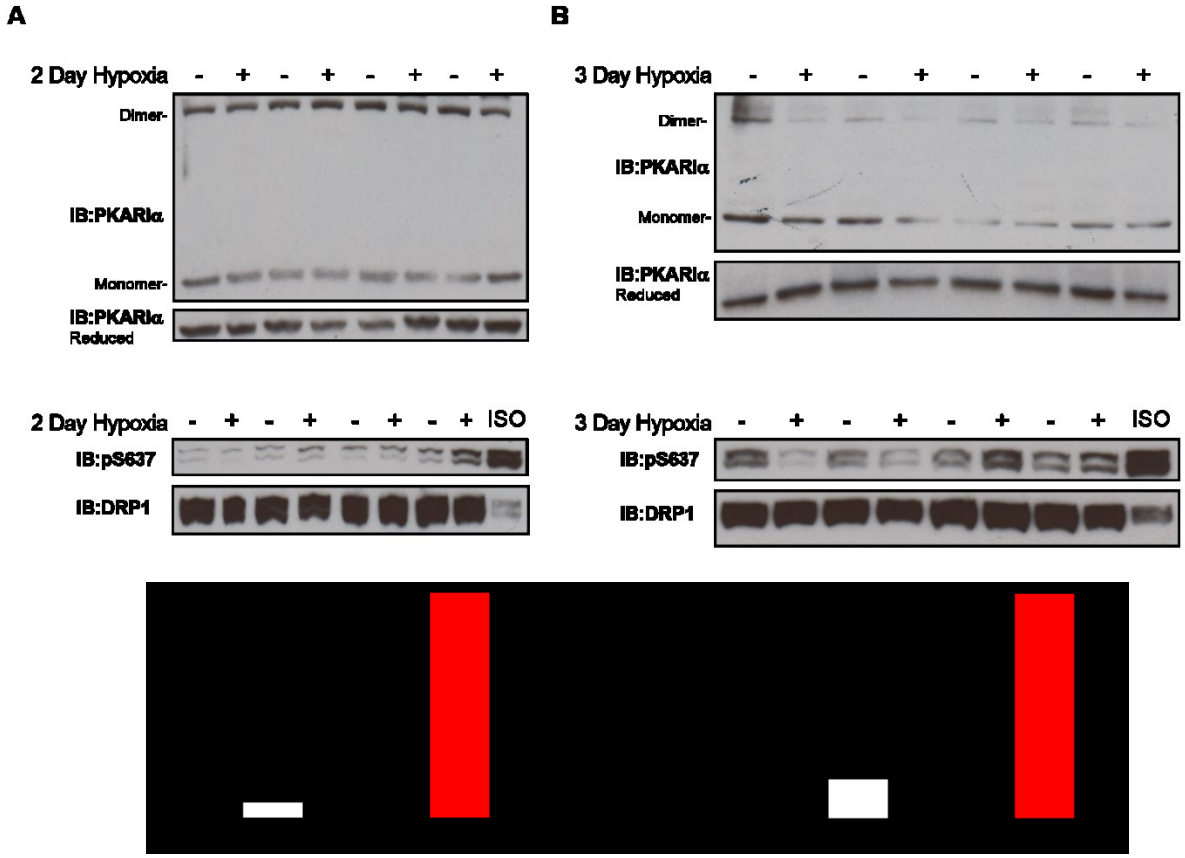

Figure S5. Two or three day hypoxia does not impact disulfide PKARIα or pDRP1-s637. Hypoxic animals were housed in the Proox P360 hypobaric chamber containing 10 % O_2 for two or three days. O_2 levels were monitored throughout the experiment with an in-chamber O_2 sensor. Control mice were kept in the same room and exposed to ambient O_2 (21%) for an equal duration of time. Upon cessation of the experiment hearts were immediately snap-frozen in liquid nitrogen. A mouse IP injected with isoprenaline was used as a positive control for pDRP1-S637. **(A)** Immunoblot of PKARIα and pDRP1-S637 in response to 2 day hypoxia. **(B)** Immunoblot of PKARIα and pDRP1-S637 in response to 3 day hypoxia.

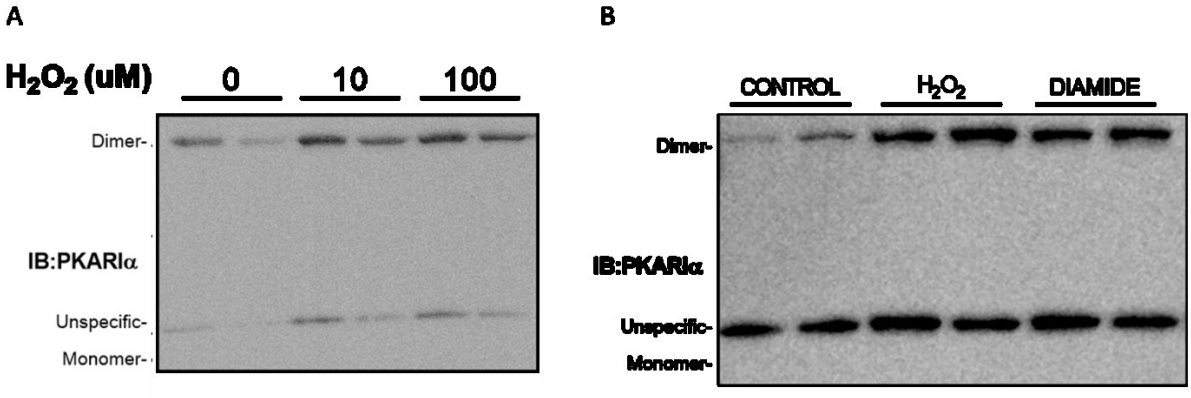

Figure S6. Freshly isolated cardiomyocytes show irregular disulfide PKARIα response to H_2O_2 and monomer protein is not visible. Freshly isolated cardiomyocytes were settled for 1 hour prior to treatment for 10 minutes with H_2O_2 (100µM, or as indicated), the thiol selective oxidant diamide (500 µM) or left as untreated controls. **(A)** Immunoblot of PKARIα in response to 0, 10 and 100 µM H_2O_2. **(B)** Immunoblot of PKARIα in response to 100 µM H_2O_2 and diamide.

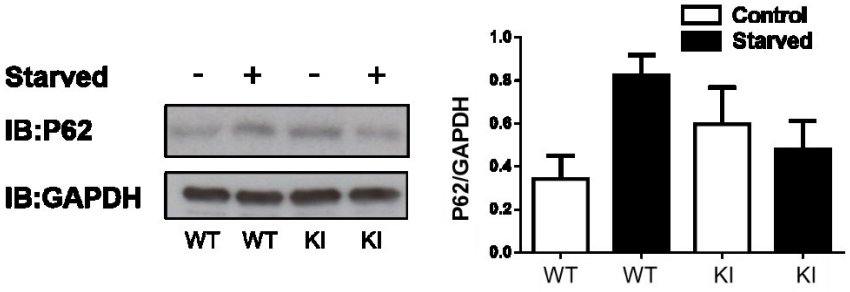

Figure S7. P62 is unchanged in PKARIα C17S KI mice. Food was removed from mice for 24 hours after which they were sacrificed. Left, immunoblot of P62 and GAPDH from WT and KI animals before and after starvation. Right, densitometry quantification of PKA substrate phosphorylation. KI: PKARIα C17S, WT: wildtype (n=3, ±SEM). Analysis: One-way ANOVA, $p<0.05$.

A2. Reagents and buffers

Krebs-Henseleit bicarbonate perfusate

$CaCl_2$	1.4 mM
NaCl	118.5 mM
Glucose	11 mM
$NaHCO_3$	25 mM
KCl	4.7 mM
KH_2PO_4	1.2 mM
$MgSO4 \cdot 7H_2O$	1.27 mM
Na-pyruvate	2 mM

The first four chemicals were added to ddH_2O and stirred until completely dissolved prior to the addition of the remaining chemicals. The buffer was freshly made on the day of its use and kept at 4 °C.

H_2O_2

10.2 µl of stock H_2O_2 (9.79 M) in 989.8 µl of ddH_2O gives 100 mM H_2O_2.

Insert 1 µl/ml of 100 mM H_2O_2 for final concentration of 100 µM

Make fresh on day of experiment. Pour stock solution into epindorff prior to pipetting to prevent contamination.

Isoprenaline

61.93 g of isoprenaline (MW 247.72) in 50ml ddH_2O gives 5 mM stock.

Dilute this 1:5 for 10 µM solution

Insert 1 µl/ml of 10 µM solution for final concentration of 10 nM.

Make fresh on day of experiment and shield from light.

For intraperitoneal injection

Stock: 30 mg of isoprenaline in 10 ml of 0.9 % NaCl

Stock is then diluted 1:10 in NaCl for a final concentration of 0.3 µg/µl

Mice are injected with 3.3 µl/g giving a dose of 1 mg isoprenaline per kg

Make fresh on day of experiment and shield from light.

2,4 dinitrophenol (DNP)

Stock: 90 mg of DNP in 10 ml of 0.9 % NaCl

Stock is then diluted 1:10 in NaCl for a final concentration of 9 µg/µl

Mice are injected with 3.3 µl/g giving a dose of 30 mg DNP/ kg

Make fresh on day of experiment and shield from light.

Glucagon

Stock: 30 mg of glucagon in 10 ml of 0.9 % NaCl

Stock is then diluted 1:10 in NaCl for a final concentration of 0.3 µg/µl

Mice are injected with 3.3 µl/g giving a dose of 1 mg glucagon per kg

Make fresh on day of experiment.

Cardiomyocyte isolation buffer

$NaHCO_3$	120.4 mM
KCl	14.7 mM
KH_2PO_4	0.6 mM
$Na_2HPO_4 \cdot 2\ H_2O$	0.6 mM
$MgSO_4 \cdot 7\ H_2O$	1.2 mM
HEPES	10 mM
$NaHCO_3$	4.6 mM
Taurin	30 mM
2,3-Butanedione monoxime	10 mM
Glucose	5.5 mM
pH 7.4 at 37 °C	

Tissue homogenisation buffer

Tric-HCL pH 7.4	100 mM
Maleimide	100 mM

1 x cOmplete mini EDTA-free tablet (Roche)
1:100 dilution of phosphatase inhibitor cocktail P5726 (Sigma Aldrich)

Homogenisation buffer was kept on ice at all times during homogenisation.

Sodium dodecyl sulfate (SDS) sample buffer

Tris-HCL pH 6.8	100 mM
SDS	4 %
Glycerol	20 %
Bromophenol blue	
Maleimide	100 mM

Reducing sample buffer was made by adding 5 % (v/v) β-mercaptoethanol.

Cell homogenisation buffer

HEPES	10 mM
Sucrose	300 mM
NaCl	1 mM
CaCl	2 mM
EGTA	1 mM
Triton X-100	1 %
PhoSTOP tablet (Roche)	1/10 ml
cOmplete mini EDTA-free tablet (Roche)	1/10 ml
pH 7.4	

All homogenisation is undertaken on ice.

PBS-Tween-20

PBS	1 L
Tween-20	1 ml

Coomassie Brilliant Blue

Coomassie Brilliant Blue R-250	0.2 %
Acetic acid	7.5 %
Ethanol	50 %

Destain	
Methanol	50 %
Acetic acid	1 %

Primary Antibodies: Western Blot			
Name	**Species**	**Manufacturer/Catalogue no.**	**Dilution**
PKARIα	Mouse	BD Transduction Laboratories (610165)	1:1000
Phospho-PKA substrate	Rabbit	Cell Signalling Technology (9624)	1:1000
PKARIIα	Mouse	BD Transduction Laboratories (612242)	1:1000
PKAcatα	Mouse	BD Transdcution Laboratories (610980)	1:1000
DRP1	Rabbit	Cell Signalling Technology (8570)	1:500
Mitofusion-1 (D6E2S)	Rabbit	Cell Signalling Technology (14739)	1:1000
Mitofusion-2 (D2D10)	Rabbit	Cell Signalling Technology (9482)	1:1000
LC3A/B XP	Rabbit	Cell Signalling Technology (12741)	1:1000
BRP44	Rabbit	Abcam (ab 111380)	1:1000
DRP1	Rabbit	Santa Cruz Biotechnology(sc-32898)	1:1000
pDRP1-s637	Rabbit	Cell Signalling Technology (6319)	1:500
pDRP1-s637	Rabbit	Cell Signalling Technology (4867)	1:500
D-AKAP1	Rabbit	Proteintech Europe (15618-1-AP)	1:1000
PKGα	Goat	Santa Cruz Biotechnology (sc-10338, E-17)	1:1000
GAPDH (V-18)	Goat	Santa Cruz Biotechnology (20357)	1:1000
NaKATPase-α1	Mouse	Developmental Studies Hybridoma Bank (α6F)	1:1000
Cardiac Troponin I	Rabbit	Abcam (ab47003)	1:1000

Secondary Antibodies: Western Blot		
Name	**Manufacturer/Catalogue no.**	**Dilution**
Anti-mouse IgG HRP	Cell Signalling Technology (7076)	1:1000
Anti-rabbit IgG HRP	Cell Signalling Technology (9624)	1:1000
Anti-goat IgG HRP	BD Transduction Laboratories (612242)	1:1000

Primary Antibodies: Immunofluorescence			
Name	**Species**	**Manufacturer/Catalogue no.**	**Dilution**
PKARIα	Mouse	BD Transduction Laboratories (610165)	1:500
RYR2	Mouse	Piece Antibodies via Thermo (MA3-916)	1:500
Cav3	Rabbit	Abcam, (Ab 2912)	1:500

Secondary Antibodies: Immunofluorescence		
Name	**Manufacturer/Catalogue no.**	**Dilution**
AlexaFluor 514 goat anti-mouse	Molecular Probes, Life Technologies (A31555)	1:1000
AlexaFluor 633goat anti-rabbit	Molecular Probes, Life Technologies (A21071)	1:1000

Prkar1 polymerase chain reaction master-mix for one reaction

5 x green GoTaq flexi buffer (Promega)	-	10 µl
$MgCl_2$ (Promega)	25 mM	4 µl
dNTPs (Promega)	10 mM	1 µl
PKA primer 1 (Invitrogen)	5 µM	1 µl
GCT TTC CTT TAC CAA GCA GG		
PKA primer 2 (Invitrogen)	5 µM	1 µl
GTC TGT GAG TCA CAC TGA CC		
Tas (5 U/ µl)(Promega)	-	0.4 µl
Nucleotide free H_2O	-	35.6 µl
DNA elute	-	4 µl

Master-mix is first made on ice and then 36 µl added to every 4 µl DNA sample

Polymerase chain reaction thermocycler program

95 °C	5 minutes	
95 °C	30 seconds	35 cycles
60 °C	30 seconds	
72 °C	1 minute	
72°C	10 minute	

TAE buffer

Tris-Base	40 mM
Glasical acetic acid	20 mM
EDTA	1 mM
pH 8.3	

2 % Agarose gel

2 g of agarose powder (Applichem) is dissolved in 100 ml of TAE buffer and heated in a microwave until dissolved. Once cooled, 0.01 % (v/v) gelRed Nucleid Acid Gel Stain (Biotium) is added. The solution is then poured into a casting tray, combs added and allowed to set.

PBS lysis buffer

PBS	50 ml
Triton X-100	1 ml
1 x protease inhibitor tablet	

2-AHA-cAMP

On arrival beads were centrifuged (1,000 g, 5 minutes), the supernatant removed and beads re-suspended in 10 ml of PBS containing 0.1 % sodium azide. Beads are stored at 4 °C until needed.